ABSTRACT

Title of Document: INVESTIGATION OF THE AFFECT OF OXYGEN CONCENTRATION ON THE PYROLYTIC DECOMPOSITION OF POLYPROPYLENE

Brent Allen Turner III, M.S., 2018

Directed by: Professor Stanislav Stoliarov
Department of Fire Protection Engineering

Limited research exists on the effect of oxygen on the species production during the pyrolytic decomposition of polypropylene. In this study, the pyrolytic decomposition of polypropylene was conducted in 0% O_2, 5% O_2, and 15% O_2. The gaseous product of this pyrolysis, or the pyrolyzate, was analyzed using three methods. First, a custom tube-furnace reactor and auto-sampling system were developed to pyrolyze, collect samples, and analyze samples using gas chromatography to identify and quantify present species. Data collected were converted to rates of production and mass evolved for individual species identified. Second, using the same tube-furnace reactor pyrolyzate was sent directly to a stack of IR and FID analyzers to measure O_2, CO, CO_2, and total hydrocarbon production. This data was converted and used to compare with and verify the data from the gas chromatography analyses. Thermogravimetric analysis was used as a third technique to measure the mass loss of the polypropylene under the three O_2 scenarios. For all three analytical methods, the effect of O_2 was studied and was found to have a profound effect on assumed reaction rates and species production.

INVESTIGATION OF THE AFFECT OF OXYGEN CONCENTRATION ON THE PYROLYTIC DECOMPOSITION OF POLYPROPYLENE

By

Brent Allen Turner III

Thesis submitted to the Faculty of the Graduate School of the
University of Maryland, College Park, in partial fulfillment
of the requirements for the degree of
Master of Science
2018

Advisory Committee:
Professor Stanislav Stoliarov
Professor Arnaud Trouvé
Professor Peter Sunderland

© Copyright by
Brent Allen Turner III
2018

Acknowledgements

This research has been primarily supported and funded by Combustion Science & Engineering, Inc.

The author would like to thank Casey Fuller, Dr. P. (Gokul) Gokulakrishnan, Dr. Michael Klassen, Dr. Richard Joklik, and Dr. Richard Roby for their technical assistance and guidance. The author would also like to acknowledge Maclain Holton for his assistance in the programming of the experimental apparatus.

The author would like to thank Professor Stanislav Stoliarov for his continued patience and guidance throughout the duration of this extended and ever-changing attempt. The author would also like to acknowledge Yan Ding for her help in producing TGA data for this research.

The author would like to thank Professor Arnaud Trouvé, Professor Stoliarov, and Nicole Hollywood for their assistance in navigating difficult and unusual circumstances due to a 10-year long endeavor.

Most importantly, the author would like to thank his wife, Talia, and children (Elliott and Simon) for allowing him time to work on this project.

Table of Contents

LIST OF FIGURES

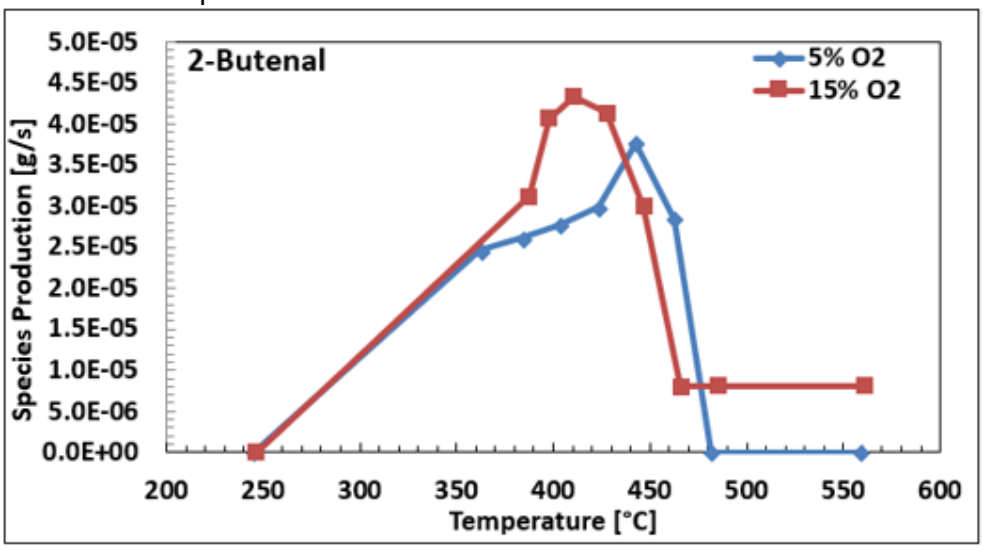

Chapter 1: Introduction

1.1 Problem Definition

The word pyrolysis is derived of the Greek elements *pyro* and *lysis* standing for "fire" and "separating", respectively. Technically, pyrolysis is a thermal decomposition process occurring at elevated temperatures. During pyrolysis, a material is decomposed via changes in chemical composition and structure. The effects are irreversible. A general understanding of pyrolysis is that the high-temperature reactions intrinsic to the process take place in an inert atmosphere [1]; however, this is not always the case. Pyrolysis is applied frequently in the study of organic materials, textiles, chemicals, and plastics to garner an understanding of how these materials decompose under the extreme conditions. The current study focuses on plastics, primarily Polypropylene.

Large scale production of plastics can be traced as far back as 1950. While plastics were manufactured earlier in the 20th century, they were not widely used as a consumer product until after World War II. In 1950, 2 million metric tons (Mt) of virgin plastics were produced globally. From 1950-2015, this production has increased by a compound annual growth rate of 8.6% leading to the manufacture of ~322 Mt of plastic in 2015. This production has put a rough total of 7800 Mt of plastics into the consumer marketplace since the beginning of manufacture. Plastics are omnipresent, finding wide-scale usage in construction, transportation, clothing, manufactured goods, and general goods packaging among many other uses [2]. While plastics are considered a

global success story and have allowed for many advancements in technology, growth in production rates have also lead to an increase in the generation of municipal solid waste (MSW). The EPA reported that in 2014 plastics comprised 13% of gross MSW in the United States. Of this 36.6 Mt of plastic waste, 76% ended up in landfills, 15% was incinerated for energy recovery, and 9% was recycled [3].

The numbers discussed, both in manufacture and disposal rates, provide evidence for why there might exist a large interest in the decomposition of plastics. For decades now, there have been two main groups interested in the pyrolytic decomposition of plastics. As plastics continue to fill our homes, offices, automobiles, and airplanes there are those seeking to make the products safer for the consumer. From the fire protection standpoint, the pyrolysis of plastics provides key information on burning rate and potential products of combustion; information that can be used to enhance decomposition models and enable the development of better, flame-retardant materials. As plastics continue to fill landfills and add to non-biodegradable environmental pollution, there are those seeking out means for more efficient disposal and recycling of the materials. In a similar fashion, the results of pyrolysis provide specific information on pathways to decomposition, temperature dependent species generation, effects of gas composition on decomposition, and much more. This information can be used to establish techniques for hydrocarbon recovery, of both liquids and gases, which can be used in more efficient ways to produce clean energy.

The objective of this effort is to investigate the role that oxygen plays on the decomposition of Polypropylene. The results of the analysis will be useful for both the fire

protection and waste-management segments. Ultimately, oxygen has a drastic effect on the decomposition rate and speciation of products produced during the pyrolysis and gasification of the material. The production of these gases defines the process of ignition and the ensuing burning rate dynamics directly through increases in ignition characteristics and decomposition reaction rates. Acceleration of these characteristics has a direct connection to the rate of fire growth. The hope was to study the surface effects of the presence of oxygen on gaseous pyrolyzate for several materials; but the method, pyrolysis apparatus, sampling apparatus, as well as analysis techniques were all designed and built specifically for this research thus limiting the scope.

Polyolefins encompass more than 55% of the global plastics demand. Low-density and high-density polyethylene are the most used, accounting for 32% of the total plastic demand. Polyethylene has a large share in the construction market where it is used in the manufacture of water and sewer piping, conduit, plastic sheeting, and water-proof coatings. While it has the largest demand in the global market, it was decidedly not the focus of this investigation due to the more long-term or "permanent" nature of its usage. Polypropylene, on the other hand, finds large use in consumer products including furniture, technical components (e.g. vehicle bumpers), textiles (e.g. carpeting), and packaging for food and other items making it a more applicable material for the focus if this study. Globally, polypropylene has the 2nd-largest demand among manufactured plastics at 23% [4].

1.2 Literature Review

As discussed in the previous sections, there are two main segments interested in the study of thermal decomposition of polypropylene: fire safety of materials and waste management and recycling. Significant research has been conducted and published on the topic of pyrolysis and the effect of oxygen as it relates to both areas of interest. The earliest interest seems to focus on the pyrolysis of polypropylene as it related to its use as a solid fuel for propulsion and for material fire safety. There were investigations into the perceived effect of O_2 on the pyrolysis as well as research into the speciation during pyrolysis, whose results were used in the development of mechanistic models to predict decomposition modes. Understanding the global behavior of a material and learning how to crudely model it were paramount endeavors and natural channels of investigation. It also makes sense as the management of plastic waste and investigation into its repurpose didn't become a focal point until later, when its use became more and more prevalent and dealing with the waste started to become an area of concern. Several papers have been reviewed for this study; a summary of these papers follows.

In 1973, Kashiwagi et al. [5] investigated the effect that hot oxidizing gas had on the ignition delay time of solid fuels, fuels used for rocket propulsion and in industrial processes. The experiments were conducted in a 1.6" ID by 9' long stainless-steel shock tube apparatus. Samples of the polymers, flush mounted at the end wall, were suddenly exposed to 47 atm of 1800°K gas whose oxygen concentration varied from 18 to 100%. The results of the research showed that the partial pressure of oxygen had an obvious effect on the ignition of the fuels and that the ignition

phenomenon is quite sensitive to the partial pressure. It was concluded in general that the ignition delay increased sharply as the partial pressure of O_2 was reduced and that ambient oxygen had a more profound effect than imbedded oxidizers. The results uncovered some inadequacies in their mechanism for modeling ignition.

In 1976 and 1982, Kiran et. al. [6] and Amorim et. al. [7], respectively, used GC-MS analysis of gases produced during the pyrolysis of polypropylene to aid in understanding the mechanism of degradation. Kiran's pyrolysis system consisted of a programmable pyrolyzer, thermal conductivity cell, and mass chromatograph coupled in series to compare the degradation of three polyolefins. 10mg samples of polypropylene were heated at 20°C/min to 800°C. The gases produced were carried to the GC through 300°C transfer lines. Products volatilized between 300°C and 600°C were collected for analysis in the GC. Four major, relevant peaks discovered during the analysis were propylene, isobutylene, pentane, and 2-methyl-1-pentene.

Amorim [7] used three forms of pyrolysis to collect and analyze gas samples from polypropylenes with varying isotacicity. Gas produced during flash pyrolysis at 700°C for 1s, liquid pyrolyzate produced through thermolysis at 470°C, and samples directly heated by the GC to 300°C were analyzed with GC-MS. Thermogravimetry was also used to investigate the kinetics of the decomposition. Low molecular-weight compounds were not identified due to experimental conditions and GC setup.

Both Kiran and Sousa concluded that evolution of products during decomposition can be mainly explained by intramolecular radical transfer. Chain scission initiation results in the

formation of primary and secondary radicals. Next, depolymerization leads to further radical and monomer formation. Intramolecular radical transfer leads to the formation of the alkanes and alkenes discovered during analysis.

In 1994, Kashiwagi [8] published further research investigating the effect of oxygen concentration on polymer pyrolysis. The investigation focused on the effect of O_2 on the condensed phase as the gas phase had already been heavily explored. The viscosity of a melting polymer is lower at its outer surface and higher toward the cooler, inner surface. This high (inner surface) to low (outer surface) viscosity gradient promotes the transport of higher viscosity molecules to the surface, resulting in an inside-out gasification of the higher viscosity molecules. Subsurface gasification is important to understanding the condensed phase phenomena. Ambient oxygen plays a part in the decomposition and increases this rate of gasification. In the work reviewed, the effect of O_2 appeared to be more powerful in low heating rate instances where evolved gases don't buffer the diffusion of the surrounding oxygen. Kashiwagi notes that a near endless number of polymer products are examined in many tests to assess their flammability. Unfortunately, the results of these tests do not always agree with each other or reflect how a material might behave in a real fire. He discusses an overall lack of understanding by researchers of the chemical and physical mechanisms in the condensed phase. He concludes that further investigation into the condensed phase is needed, including the effect of oxygen on the condensed phase.

In 2006, Chen et al. [9] used TGA analysis to investigate the effect of flame retardants on the degradation kinetics of polypropylene during oxidative pyrolysis. Activation energies, pre-

exponential factors, and reaction orders were developed using the results of the experimentation. In air, 8mg samples various polypropylenes were pyrolyzed at 5°C/min, 10°C/min, 20°C/min, and 30°C/min from ambient up to 600°C. Kissenger and Flynn-Wall-Ozawa Methods were used to determine apparent activation energies for the three materials. Chen concluded that the flame-retardant composites were more difficult to degrade.

In 1992, Hayashi et al. [10] investigated the effect of oxygen on the pyrolysis of polypropylene as it relates to the conversion of the polyolefin into high-grade transportation fuels and other chemicals. Oxygen, a chain-breaking agent, was stated to efficiently depolymerize polypropylene. The focus of the research was on the decomposition of peroxides into hydroxy and carbonyl groups. Hayashi et. al. used TGA to conduct his experimentation. Polypropylene sheets were processed and adhered to alumina resulting in varying micron diameter particles to increase surface area and decrease agglomeration. 20mg of the particles were heated to 600°C in a Shimadzu TGA at 5, 10, 15, and 20°C/min heating rates. The TGA was purged with a helium-oxygen mixture of differing concentrations of roughly 4%, 11%, 17%, and 28.5%. Hayashi et. al. observed a significant change in the rate of mass loss when oxygen was present. At 17% O_2, half of the mass was consumed by the time the sample reached 280°C. In pure Helium, the mass loss didn't reach 50% until 450°C. The research shows that the formation of peroxide seems to be the rate determining step in the decomposition of polypropylene and the rate coefficient, K, is a function of O_2 concentration. Hayashi concluded that the presence of oxygen promoted mass release in the early stages of decomposition, dramatically in the 200-300°C range, and suppressed

mass release at higher temperatures due to the formation of refractory solids, which are resistant to decomposition. The formation of the refractory solids led to a more gradual decomposition. The solids eventually volatilize at higher temperatures.

In 1999, Bockhorn et al. [11] studied the degradation of polyolefins via pyrolysis in pure Helium and subsequent GC-MS analysis. Two methods of pyrolysis and sample delivery were used in this study. The first method focused on decomposition occurring within a specific temperature range. This was accomplished by creating a thin liquid film in a gradient-free reactor. 40 mg of polypropylene was quickly pre-heated and then pyrolyzed between 410°C and 460°C for 15 minutes to 6 hours. The products were sent directly to a mass spectrometer. Due to the difficulty investigating gas evolved over the course of 6-hour test, additional pyrolysis was performed to fractionate the products over a longer period of time. A quartz tube, furnace, and cold traps were used to pyrolyze ~100 mg samples of polypropylene and collect gas over five specified temperature ranges. Thermogravimetric analysis was conducted to establish five sampling ranges of 20-369°C, 370-388°C, 389-399°C, 400-406°C, and >406°C. The analysis identified species up to C31 made up of approximately 7.6% dienes, 7.6% alkanes, 84.8% alkenes. The data was used to determine kinetic rate parameters and compare these findings with existing mechanistic models. It was concluded that the data agreed with existing data and a more detailed investigation into the reaction mechanism can take place.

A study published in 2002 by Ballice, and Reimert [12] found similar results. The research detected dienes, alkanes, and alkenes up to C31 in the same proportion and complexity as

Bockhorn [11]. The authors again focused on the temperature range of 410-460°C, conducted pyrolysis experiments that ranged from 20 minutes to 5 hours in length, and used two test methods to collect sample for GC-MS analysis. Initially, TGA was performed in 100% N_2 at 5, 10, and 15 °C/min up to 600°C. Secondly, a fixed bed reactor was used to pyrolyze the sample in a 400 mm long, 10mm ID Duran glass reactor tube. 250 mg was mixed with 5ml of quartz sand and loaded into the reactor. A thermocouple was inserted into the middle of the bed. Pyrolysis was carried out at 2°C/min under a 90 ml/min flow of Argon gas. The pyrolyzate was collected in ampules at different moments for analysis. Transfer lines were maintained at 380°C to prevent condensation. Molecules in the C1-C6 range accounted for roughly 30% of the total mass collected. The author describes similar pathways of degradation as described in research previously reviewed in this section. Global kinetic parameters were determined but no quantitative model was presented. It was concluded that a kinetic model is critical to the efficient development of an economically feasible conversion of waste plastic into hydrocarbon fuel.

In 2003, Kruse et al. [13] reported that the pyrolysis of waste plastics is an attractive means of resource recovery but that there remained a lack of understanding of the complex, underlying reaction pathways and high difficulty in predicting a full product distribution from the degradation. In previous work, the results of pyrolysis testing on polypropylene was limited to more general development of reaction rate parameters and the development of rate constants based on mass loss. In Kruse's study, the authors captured the formation of all low molecular weight products C1-C15 and used them to develop a model that tracked 27 products, 24000 reactions, and 213 species.

Kruse concludes that the model worked relatively well, predicting values within 1.5 times of what was found experimentally. The research is a step towards a more thorough understanding of the degradation phenomena.

Hajekova and Bajus [14] investigated the possibility of recycling polypropylene, in 2005, via thermal decomposition using steam cracking techniques already in place on existing ethylene units. BP Chemicals has a plant in the UK that thermally decomposes plastic waste at 500°C, in the absence of air. The authors used a stainless-steel batch reactor heated at ~11.25°C/min to decompose PP up to 450°C. Wax, oil, and gas analysis was collected for analysis under a nitrogen purge. The outlet of the reactor was heated and maintained at 70°C to prevent condensation and build-up in the tubing. It was confirmed that the yields or ethane, propane, propene, methyl-propene, 1-butene, pentane, and a 2-methyl-1-pentene confirm the possibility of polyalkenes recycling using existing steam cracking facilities.

In 2006, Sojak et al. [15] also pyrolyzed polypropylene in a batch reactor at 450°C to investigate the feasibility of recycling waste into petrochemical feedstock. Again, the conclusion was that the resulting oils and waxes were favorable to the development of reusable feedstock. The authors noted that the identification of the separated analytes was usually the most difficult step of the analysis and results in a demanding exercise due to a complex reaction product.

Hujuri et al. [16] completed a study of the degradation of polypropylene using TGA to develop a mechanistic model to predict the formation of low-molecular weight species, C1-C15. The research monitored molecules ranging from C5-C44 over 6 different temperature ranges:

200°C, 300°C, 400°C, 446°C, 500°C, 600°C. The results showed that C5-C8 production below 300°C was negligible but above 300°C became significant. The product yield reached its maximum at 446°C, at which point hydrocarbon cracking reactions became vigorous. The authors' concluded that intramolecular reactions were the cause for the wide range of hydrocarbons produced in the free radical mechanism that they developed. They view multi-component polymer mixture pyrolysis as the next logical step in the pursuit of achieving a targeted product profile.

In 2012, Park et al. [17] conducted a study using a tube furnace apparatus and a TGA to pyrolyze refuse plastic fuel (RPF) and analyze the resulting gas. RPF is explained as a mixture of low-density polyethylene, poly vinyl chloride, polyethylene, and polypropylene. A tube furnace with a stainless-steel reactor, 800mm in length and 40mm in diameter, was used to pyrolyze powderized RPF in an inert, N_2, atmosphere. 2-3 grams of the powder was loaded into a sample boat and placed into the furnace. A flow of nitrogen was established at 1.5 l/min while the furnace was heated at 30°C/min up to 400°C, 600°C, or 800°C to characterize the effect of temperature on product yield. Once at temperature the pyrolysis continued for 10 minutes. The resulting gas was cooled to separate the shorter chain volatiles from the oils and waxes. These volatiles were collected and analyzed by a GC-MS. The results found major compositions of CO, H_2, CH_4, C_2H_4, C_2H_6, and C_3H_8. A larger volume of gaseous product was evolved at higher temperatures where it is easier to breakdown longer chained hydrocarbons. TGA was also conducted on the individual components of RPF, pyrolyzing them in 1.5 l/min of N_2 at 10, 20, 30 and 40°C/min. Mass loss was first noticed between 360-450°C and total mass loss was reached between 360-450°C. Activation

energies and pre-exponential factors were calculated for the individual polymers.

A very thorough study on thermal cracking of waste plastics (PP) was conducted by Jing and Wen [18] in 2015. GC, FTIR, H NMR, and GCMS analyses were used to differentiate evolved products between virgin plastic and waste plastic while TGA was used to determine kinetic parameters. In both case, pyrolysis was conducted in an inert atmosphere of N_2. Roughly 5-15 mg of pelletized polypropylene was pyrolyzed under 40 ml/min N_2 flow at a heating rate of 10, 20, 30, and 50°C/min from 20°C to 600°C. Kinetic parameters were developed using the results of the TGA and implementing the modified Coats-Redfern model. A batch reactor was used to pyrolyze 30 g samples of polypropylene under 150 l/min of N_2 at 10-15°C/min from 25 to 460°C. To separate the volatile products from the oil fraction, the pyrolyzate was passed through a holding furnace at 200°C before being cooled with water. Yields of propylene, 41.01%, suggest that β-scission of the end-chain radicals is the major reaction, potentially followed by intramolecular hydrogen transfer. n-pentane yielded 25.46% which is surely β-scission followed by intramolecular hydrogen transfer. The chain scission reactions are confirmed as being the predominant degradation mechanisms in the thermal cracking process.

Overall the literature describes the pyrolysis of polypropylene in a zero-oxygen atmosphere well with many investigations into the decomposition for the development of kinetic models. In this case the degradation is well understood. There are investigations into the oxidative pyrolysis of polypropylene but most them focus on a more global effect of oxygen and how it effects the outcome of a decomposition or process of decomposition. There is little research into a more local

investigation of how oxygen effects a decomposition on a level of species production and conversion. It is suspected that the presence of oxygen at a materials surface during pyrolysis in a turbulent flow regime could be significant.

It is known that oxygen has an accelerating effect on decomposition rates, ignition characteristics, and fire growth. A better understanding of species evolution during oxidative pyrolysis could help in the development of more advanced kinetic models and in determining when and why it is necessary to consider the effects of oxygen. A first step to accomplishing this is to develop pyrolysis experiments designed to specifically collect and precisely analyze pyrolyzate.

It is hypothesized that the reaction of oxygen with the polymer and evolved hydrocarbons at its surface is important to the global decomposition of the material during pyrolysis. It is also hypothesized that controlling the surface area of the testing sample during pyrolysis is important in effectively analyzing the process.

1.3 Motivation, Objectives, and Summary

The goal of this study is to investigate the effect of oxidation on the controlled surface area pyrolytic decomposition of polypropylene by monitoring the production of gases and identifying hydrocarbon species produced throughout. To accomplish this task, a custom reactor and sampling system were developed to pyrolyze, collect, and analyze the gases produced. Additionally, a unique sample holder was developed to control the surface area of the solid throughout the experimentation. Unlike in many previous studies, controlling the surface area of the solid is paramount due to the nature of the reaction between the oxygen and the solid taking place at its surface.

Multiple methods of analysis were used to characterize the role that oxygen plays in the pyrolysis of plastics, specifically reaction rates and species generation throughout the process. This effort focuses on polypropylene as the subject material due in part to its prominence in consumer goods. Pyrolyzate was collected for gas-chromatographic analysis, infrared O_2, CO, and CO_2 analysis, and total hydrocarbon analysis via flame ionization detection. The polypropylene material was pyrolyzed under three oxygen scenarios: in pure nitrogen with no oxygen, in 5% oxygen balanced with nitrogen, and in 15% oxygen balanced with nitrogen.

This thesis has been divided into several chapters that provide a detailed explanation of the apparatus, analysis, and results. Chapter 2 is divided into several sections that describe the experimental setup, design, and method. The section on the experimental apparatus describes the pyrolysis reactor in detail. The gas collection section describes the auto-sampler that was

developed to precisely collect the products of the pyrolysis reactor and to work in conjunction with a gas-chromatograph equipped with a barrier discharge-ionization detector (BID) to analyze them. The method section describes the procedure that was used to pyrolyze the polypropylene and the several methods used to analyze the gas samples.

Chapter 3 presents the results of the GC-BID, IR and FID analyzer, and thermogravimetric analysis. Data is converted in rates of production or mass-loss and compared to data from the literature. The effect of oxygen on the data set is observed and discussed.

Chapter 4 summarizes the data as presented in Chapter 3, concludes the thesis, and provides a brief discussion on avenues for future investigation.

Chapter 2: Experimental Setup and Design

2.1 Experimental Apparatus

2.1.1 Overview of Apparatus

To produce and collect the pyrolyzate to the degree required for this analysis, a careful design approach and tactful commissioning process were undertaken to ensure the quality of the method being developed. A process flow diagram of the apparatus is found below in **Figure 2-1**. The apparatus consists of six main components: a tube furnace (D), a reactor tube (E), an inlet flow panel (C), an inlet manifold (unlabeled), an outlet flow manifold (unlabeled), and an automated sampling system (K).

The Carbolite HST tube furnace has a 600mm heated length, two heating zones, and a main controller allowing for temperature programming. The reactor tube is made from 316 stainless steel and measures 36” in length (914 mm), 2” in outer diameter (44.7 mm), and 0.145” in wall thickness (3.7mm). Stainless steel was chosen over quartz or ceramic for the tube material due to its tensile strength. The tube is sealed with gaskets and a clamping mechanism thus it needs to withstand the tensile pressure associated with the sealing method. Several quartz tubes were broken during the early commissioning of the reactor in attempts to seal them sufficiently.

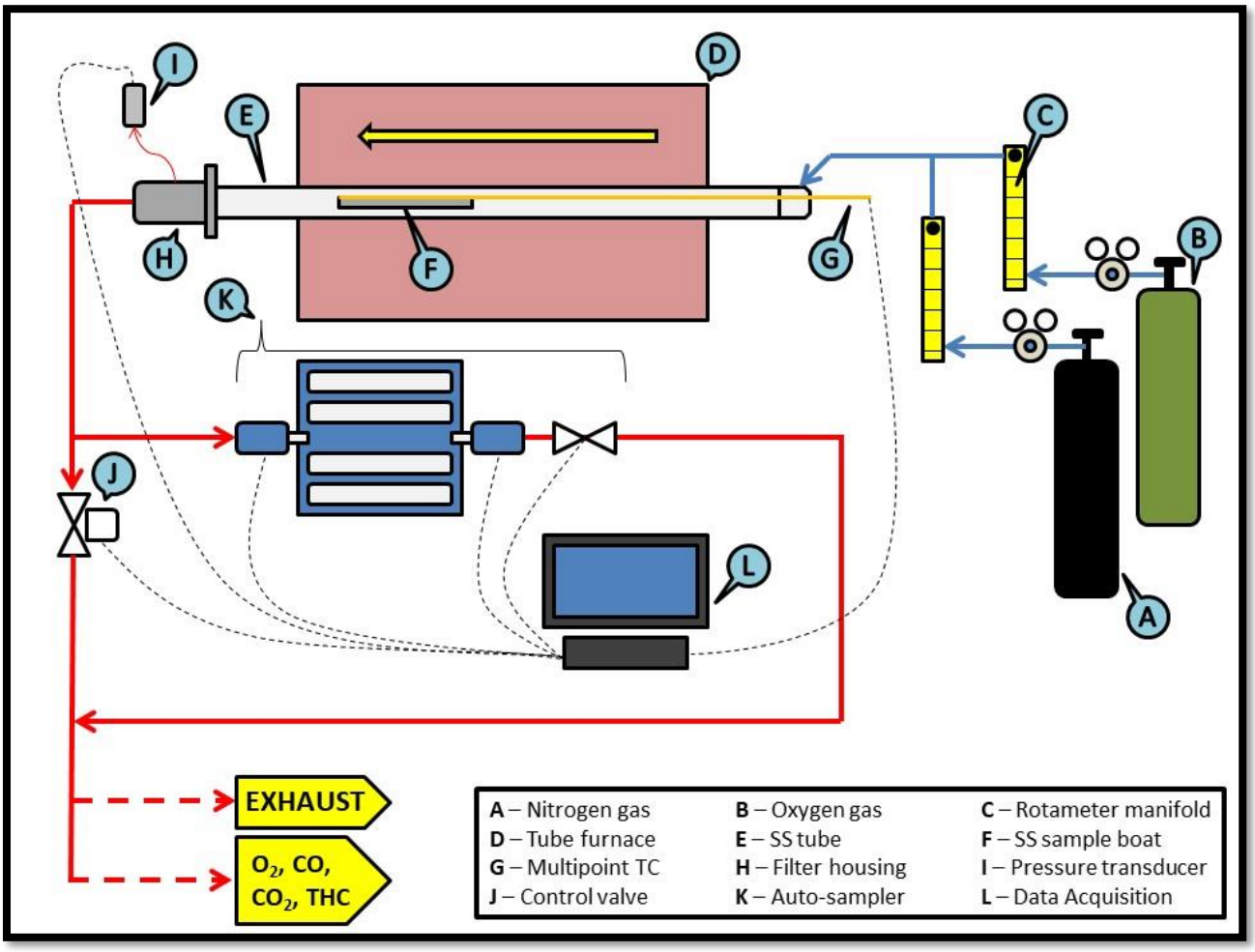

Figure 2-1: A process flow diagram for the pyrolysis apparatus.

Mounting tabs welded to an inlet manifold are used to compress a silicone gasket to the inlet end of the reactor tube to provide a proper seal. The manifold, constructed from 316 stainless steel, has two ports: a ¼" compression-fitting port for inlet gas flow and an 1/8" compression-fitting port to secure and seal a multi-point thermocouple (G).

Compressed cylinders are used to supply nitrogen (A) and oxygen (B) to the system. The

gases are regulated to 50psi prior to feeding the flow control panel. The flow control panel (C) consists of two calibrated Matheson rotameters. These rotameters regulate the oxygen and nitrogen flow to the reactor via ¼" ports in the inlet manifold. Prior to testing, the rotameters underwent 5-point calibrations using a NIST-traceable Bubble-O-Meter.

A two-piece stainless-steel boat assembly (F) is used to hold and position the material sample during the pyrolysis tests. For this study large sheets of polypropylene were cut down into testing units measuring 30mm wide x 195mm long x 0.8mm (0.03125") thick and weighing ~5g each. Testing units are loaded into the base of the boat and a multi-point thermocouple probe is place along the center of the sample boat, resting on the top of the testing unit, and then clamped between the boat's base and lid to hold it in place. The thermocouple probe is positioned on the surface of the plastic to record temperature data from two locations during testing. Temperatures are recorded by thermocouple points at the center of each "window". **Figure 2-2** below shows the boat assembly complete with the multi-point thermocouple probe. The tips of the black arrows in the figure also represent the locations of the thermocouples used to collect surface temperature data. More information on the boat design and thermocouple locations can be found in section 2.3 of this chapter**.**

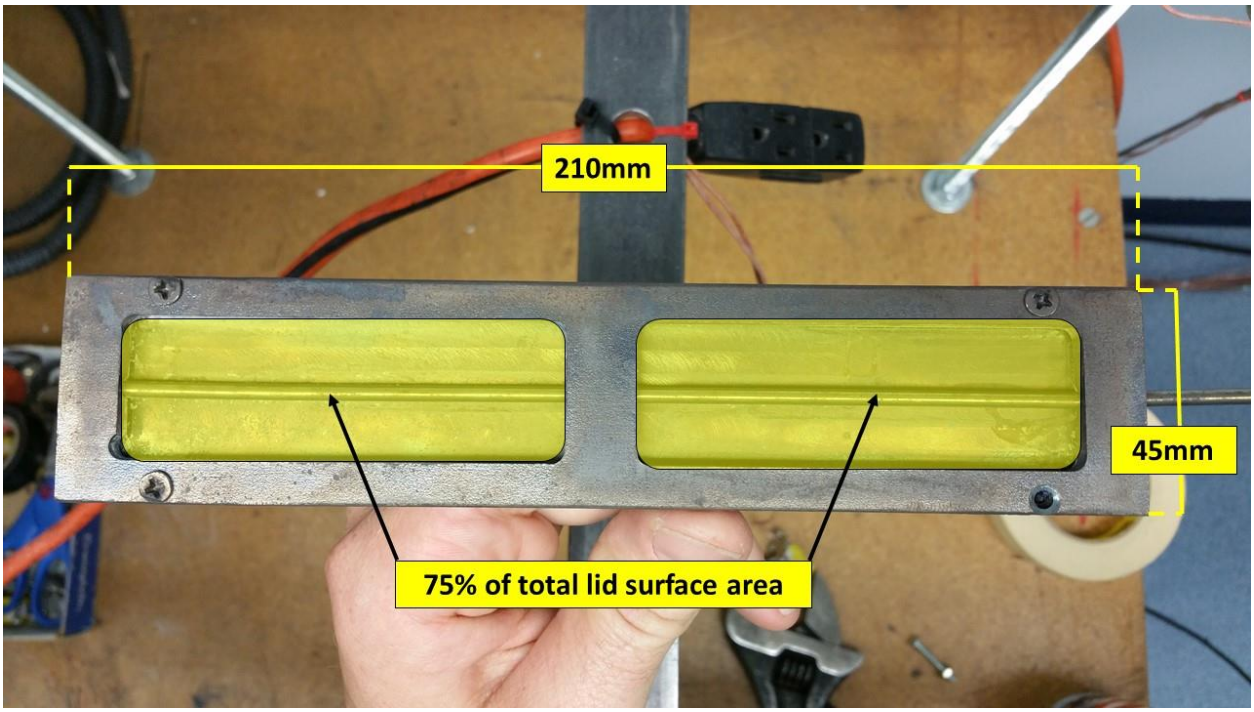

Figure 2-2: The sample boat is loaded with a sample of polypropylene sheet and fit with a multi-point thermocouple. The sample boat measures 230mm long x 32mm wide x 6.35mm thick. The machined "windows" in the lid account for 75% of the total lid surface area. The tips of the black arrows also represent the two locations of temperature measurement.

An outlet manifold, constructed of stainless steel, is attached to the end of the furnace tube to handle the pyrolyzate gas and seal the downstream end of the reactor. Mounting tabs welded to the manifold compress a graphite gasket to the reactor tube end to provide a proper seal. The manifold contains two outlet ports. One port consists of a ¼" butt-weld, compression fitting that is fit with a pressure transducer (I) to provide pressure feedback to a control system (L) programmed to maintain a reactor pressure of 7psig, roughly1.5 atm. The pressure setting has been established to provide enough gas as required by the multiple sampling and analysis systems, as

discussed later in this chapter. The positive pressure (7 psig) of the system also protects it from entraining outside air due potential leaks that would alter the carefully controlled reactor oxygen concentrations. The 2nd port directs the outlet flow of pyrolyzate, through a coalescing filtering assembly (H), to the sampling system (K) or to a path that bypasses the pyrolyzate to exhaust. The bypass path is fit with a control valve (J) that works in conjunction with the aforementioned pressure transducer to relieve and maintain pressure in the reactor throughout the duration of the pyrolysis test. All components of the outlet assembly are heat-traced and maintained at 170℃ to avoid the condensation of longer-chain hydrocarbons. The outlet assembly of the apparatus is seen in **Figure 2-3** below.

Figure 2-3: The outlet assembly of the apparatus maintains reactor pressure and manages the delivery of the pyrolyzate to the sampling systems.

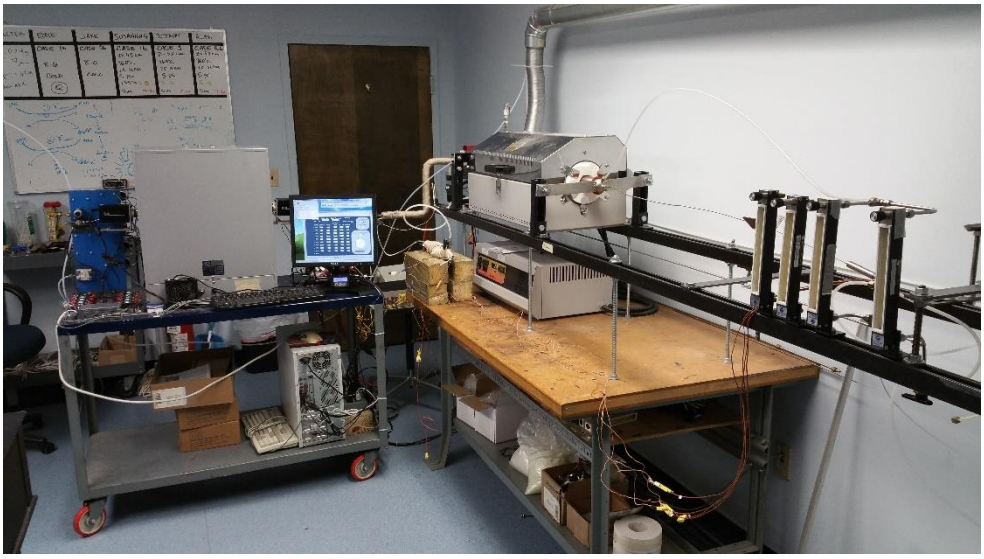

Figure 2-4: The auto-sampler, on the cart to the left, is connected to the outlet manifold of the pyrolysis reactor and collects gas samples for analysis.

Pyrolyzate is directed to an auto-sampler (K), seen in **Figure 2-4**, for collection and species analysis or to a stack of IR analyzers for compositional analysis. During pyrolysis, a computer with LabView system-design software (L) was used to collect real-time temperature data from the multi-point thermocouple as well as provide the control logic to maintain a set reactor pressure throughout the duration of the temperature-controlled pyrolysis.

2.2 Gas Collection - Auto-Sampler and GC-BID/GC-MS Analysis

An auto-sampler was developed to collect samples of the pyrolyzate at user specified times over the course of the experiment. **Figure 2-5** below provides a process flow diagram for the auto-sampler. The system consists of six major components: a convection furnace (B), an inlet multi-port selector valve (C), nine stainless steel sampling cylinders (D), a flow-through multi-port selector valve (F), an outlet containment and exhaust manifold (G/H), and a computer with LabView software to control the sampling system.

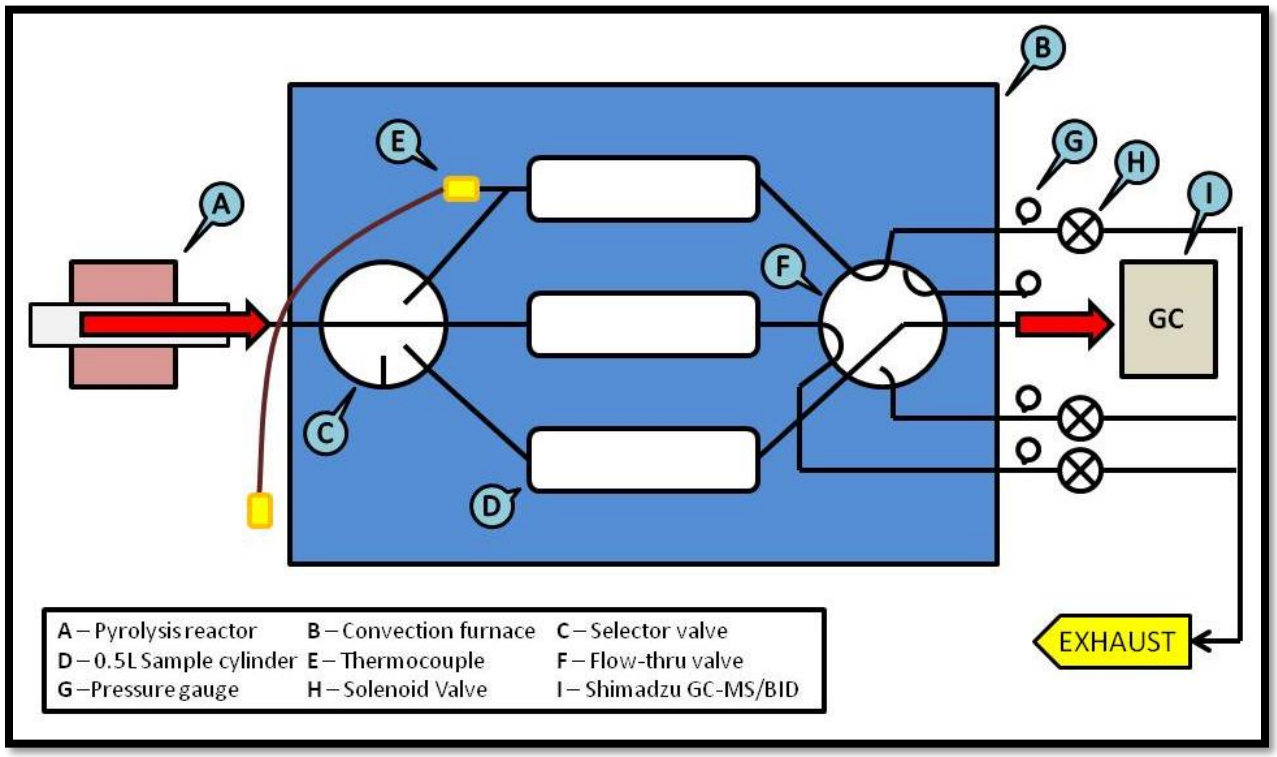

Figure 2-5: A simplified process flow diagram for the pyrolysis apparatus. The control system, and 6 of 9 sample cylinders are not shown.

Prior to a pyrolysis experiment and subsequent sample collection, the researcher inputs time criteria for a desired collection schedule based on the assumed gas production into the system control software. When an initial time criterion is met, the control system signals the valve maintaining the reactor pressure to close, directing all the flow and pyrolyzate through the sampling system. The multi-port selector valve (C) directs this flow to one of nine sample cylinders (D) contained within the convection furnace (B). Downstream of the selected cylinder a flow-through multi-port valve (F) allows the pyrolyzate to flow through the sample cylinder and purge all its contents to exhaust.

When a secondary time criterion is met, the control system triggers a normally-open solenoid valve (H) downstream of the multi-port selector valve (F) to close. This closure blocks the outlet of the selected sample cylinder, trapping the pyrolyzate inside. After a set amount of time (10s), ~10 psig has built in the incident sample cylinder and the inlet and outlet multi-port selector valves are signaled to change position, directing flow to the next sample cylinder and trapping a pressurized sample of pyrolyzate in the cylinder. Pyrolysis gas is purged through the subsequent sample cylinder until the next collection sequence is initiated. The reaction time is affected by the set oxygen concentration which in turn determines the timing of the sample collection, discussed in more detail later. Purge and pressurization timing were established to prevent the sample cylinders from becoming contaminated or diluted and to ensure sufficient sample was retained for thorough analyses. During the pyrolysis, each sample cylinder was purged with pyrolyzate for 5 minutes prior to being filled and pressurized for 10s.

Table 2-1 provides the times and temperatures at which pyrolyzate samples were collected for the varying oxygen concentrations.

Table 2-1 – Sample Collection Timing

Sample Collection Times and Temperatures						
Cylinder	**0% O_2**		**5% O_2**		**15% O_2**	
	Time [min]	**Temp [°C]**	**Time [min]**	**Temp [°C]**	**Time [min]**	**Temp [°C]**
1	100	308	85	245	85	247
2	125	416	110	362	110	388
3	130	436	115	384	115	398
4	135	457	120	403	120	411
5	140	479	125	423	125	428
6	145	499	130	443	130	447
7	150	519	135	462	135	466
8	155	538	140	482	140	485
9	175	612	160	559	160	561

*Heating rate and temperature programming of the pyrolysis are discussed in section 2.3

The convection furnace is set to maintain a sample temperature of 170°C. Three of the nine sample cylinders were specifically selected for constant temperature monitoring. Type-K thermocouples (E) are mounted in each of those three of the sample cylinders and the temperature was monitored throughout the collection and analysis process to ensure an even temperature distribution across all nine cylinders. Each cylinder also has a pressure gauge (G) to provide an indication of cylinder pressure. The inside of the convection furnace containing the nine sample cylinders is seen in **Figure 2-6.**

Figure 2-6: Nine sample cylinders are stacked in a 3x3 orientation inside of a convection furnace. The furnace is sealed and maintained at 170°C

The computer software used to control the collection of the gas samples is also used to deliver the gas samples for analysis. Once a pyrolysis experiment is completed the inlet to the auto-sampler is disconnected from the reactor outlet. The portable auto-sampler is immediately moved and connected to a Shimadzu GC-2010 Plus Gas Chromatograph. This gas chromatograph (GC) is equipped with a dielectric barrier discharge ionization detector (BID) to ionize and sort chemical species for quantification. The BID provides lower detection limits and more sensitivity than its counterpart, the flame ionization detector (FID). The BID cannot be used to identify species thus mass spectrometry (MS) is employed to identify the chemical components within a gas sample. Results from the GC-BID and GC-MS analyses are used together to identify and quantify concentrations of chemical components within a gas sample.

Calibration of the equipped detector is paramount in ensuring accuracy of its results. The BID detector was calibrated using several mixtures of a 20-component calibration gas balanced with nitrogen to provide a 5-point, linear relationship between the standard qualitative output and mole-fraction for each component. A Shimadzu QBOND column was used in both the MS and BID analyses allowing for the precise identification and quantification of C1-C6 hydrocarbons. Shimadzu batch processing is used in conjunction with LabView software to coordinate the analysis of the gas in all nine cylinders. **Table 2-2** provides specifications for the QBOND-BID column. **Table 2-3** provides details on the GC-BID temperature program used to sort and quantify species within the gas samples. **Table 2-4** provides details on the GC-MS temperature program used to identify species within the gas samples.

Table 2-2 – GC-BID Column Information

Manufacturer	Shimadzu
Type	QBOND
Serial Number	1133340
Length	30 in
Inner Diameter	0.25 mm
Film Thickness	8 μm
Max Temperature	300°C

Table 2-3 – GC-BID Temperature Programming

Steps	Process	Hold Time
1	heat to 40°C	4 min
2	ramp at 10°C/min to 100°C	4 min
3	ramp at 10°C/min to 200°C	4 min

Table 2-4 - GC-MS Temperature Programming

Steps	Process	Hold Time
1	heat to 40°C	2 min
2	ramp at 15°C/min to 250°C	8 min

2.3 Method

In preparation for testing, the stainless-steel sample boat is lightly cleaned with acetone to remove residual from previous tests. The weight of the boat is then measured and recorded for the upcoming test. A precut sample of polypropylene is separately weighed and recorded. The sample is placed in the base of the boat. The multipoint thermocouple probe is then placed on top of the polypropylene sample and positioned so that the thermocouple located at the tip of the probe is flush with the front plane of the sample boat. A top plate is then added and used to clamp the entire assembly in place. A schematic of the boat, sample, thermocouple probe, and cap assembly are shown in **Figure 2-7**.

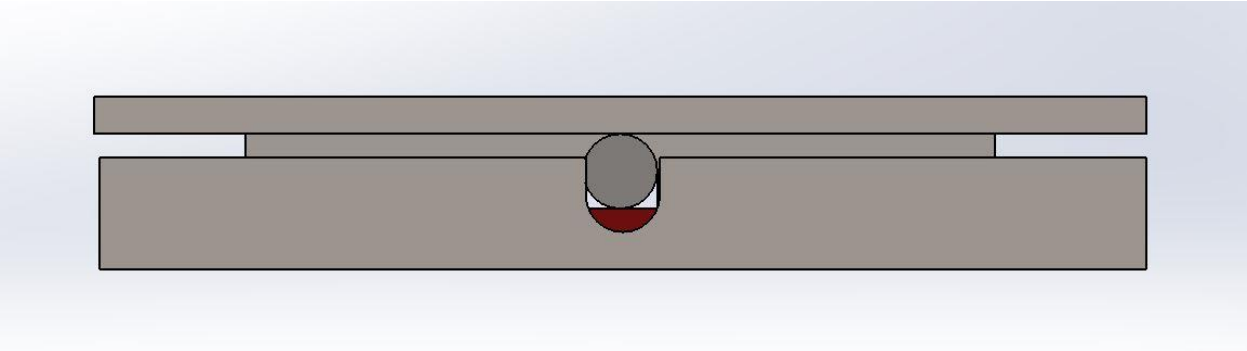

Figure 2-7: A front view of the loaded sample boat. The red represents the material seated in the base of the boat and the circular cross-section represents the tip of the thermocouple.

The sample boat assembly is then loaded into the stainless-steel reactor tube and positioned ¾ of the way down the heated section of the tube. The center of the boat sits 450 mm from the front edge of the 600 mm long heated section of the tube. This position was determined after thorough temperature profiling discussed in Appendix 5.1.1; a linear temperature profile is important to the pyrolysis. Once the boat is positioned, the inlet flange assembly is tightened down to seal the reactor.

Immediately following the sealing of the reactor is sealed, a flow of 10 SLPM of nitrogen is initiated to purge the reactor of air for five minutes. After the purge period is complete, the composition of the flow is adjusted (i.e. 0%, 5% or 15% O_2 balanced with N_2) while the overall flow rate is maintained at 10 SLPM. **Table 2-5** provides flow characteristics of the reactor for given test points. In the table, Residence Time 1 corresponds to the time required for the gas to move from the inlet of the reactor and reach the outlet of the reactor and Residence Time 2 corresponds to the time required for the pyrolysis gas to leave the outlet of the reactor and reach the inlet of the auto-sampler.

Table 2-5 - Reactor Flow Characteristics

Reactor Flow Characteristics	
Flow Rate	10 SLPM
Bulk Flow	0.49 m/s
Reynold's Number	209.5
Residence Time 1	4.28 s
Residence Time 2	1.35 s

The initiation of the pyrolysis test is the point at which the purge is complete and the test flow composition is initiated. Simultaneously, the pre-programmed tube furnace is turned on, temperature recording software is initiated to record temperature information from the multi-point thermocouple, and a LabView virtual instrument is initiated to control the pressure of the reactor to 7 psig and to control the sample collection via the auto-sampler. The tube furnace temperature increases at a rate of 4°C/min from 25°C to a steady state set point of 700°C. There is a period of non-linearity for the first 50 minutes of the program. This resulted in a slower rate of temperature increase from 25°C to about 100°C that did not affect the overall pyrolysis. The set-point temperature (700°C) is set this high to ensure the capture of the full picture of the pyrolysis, fully understanding that the mass-loss of the polypropylene reaches 99% well before this temperature. Because of the slow heating rate, the duration of a single test under these conditions is nearly 4 hours. Throughout the duration of the test the auto-sampler collects nine samples as described in the previous section.

Completion of a test results in the shutdown of the furnace, the termination of data

collection, and the deactivation of the LabView VI. The auto-sampler is disconnected from the tube furnace and connected to the Shimadzu GC. Control signals and heat-traced tubing link the auto-sampler to the GC. Batch processing, a function of the Shimadzu analysis software, allows for the automated analysis of several gas samples. The Shimadzu software works in conjunction with a separate, custom LabView VI to control the selection of sample cylinders from the auto-sampler. The program works with the timing of the GC to purge the sample column and provide sufficient sample volume for an analysis. Each of the nine samples is analyzed twice providing 18 total analyses for each pyrolysis test. This analysis takes approximately 18 hours to complete.

In this study, polypropylene was pyrolyzed in gas mixtures containing 0%, 5%, and 15% O_2 balanced with N_2. For the 0% and 15% O_2 cases, tests were replicated to provide a total of three (3) tests per O_2 concentration. For the 5% O_2 case, a single test was performed. Many additional tests were conducted early in the development of the test-method to commission the reactor and sampling system. These earlier tests were also used to develop the bounds for the timing of the sample collection by the auto-sampler. Significant efforts were allocated to the development of the pyrolytic reactor and auto-sampling system; the results of the commissioning tests were critical to resolving many of the foreseen and unforeseen complications associated with the development of a test method.

Between pyrolysis tests, the hot auto-sampler is purged with hot air for 5 minutes per 0.5 L of sample cylinder volume. The purpose of the purge is to oxidize and remove any lingering hydrocarbons that would affect subsequent testing. After the air purge, the cylinders are purged

for 2 minutes each with nitrogen to remove all oxygen.

In addition to the testing and collection for GC analysis several tests were conducted for real time analyses by a stack of IR gas analyzers. Four analyzers were used to collect carbon monoxide (CO), carbon dioxide (CO_2), and total hydrocarbon (THC) production data as well as oxygen (O_2) depletion. Information on the make and model of these analyzers can be found in **Table 2-6** below.

Table 2-6 – Analyzers

Gas	Analyzer
O_2	Siemens Oxymat
CO	Rosemont 880 IR – CO
CO_2	Rosemont 880 IR - CO2
THC	CAI 301FID HC Analyzer

Prior to pyrolysis, the tubing that had been installed to direct gas into the auto-sampler was removed and replaced with a tubing system to direct the pyrolysis gas to the analyzer stack in an adjacent lab. **Figure 2-8** below provides a process flow diagram for the reactor, configured to send the pyrolyzate to the stack of gas analyzers. The only difference is the removal of the autosampler and the implementation of a heat exchanger to cool the pyrolyzate. Directly downstream of the reactor, the gas is sent through a coil-and-bath heat exchanger (K) to lower the temperature to below 90℃, the maximum temperature limitation of the analyzers. Concentration data from these tests are recorded simultaneously with the sample boat temperature data.

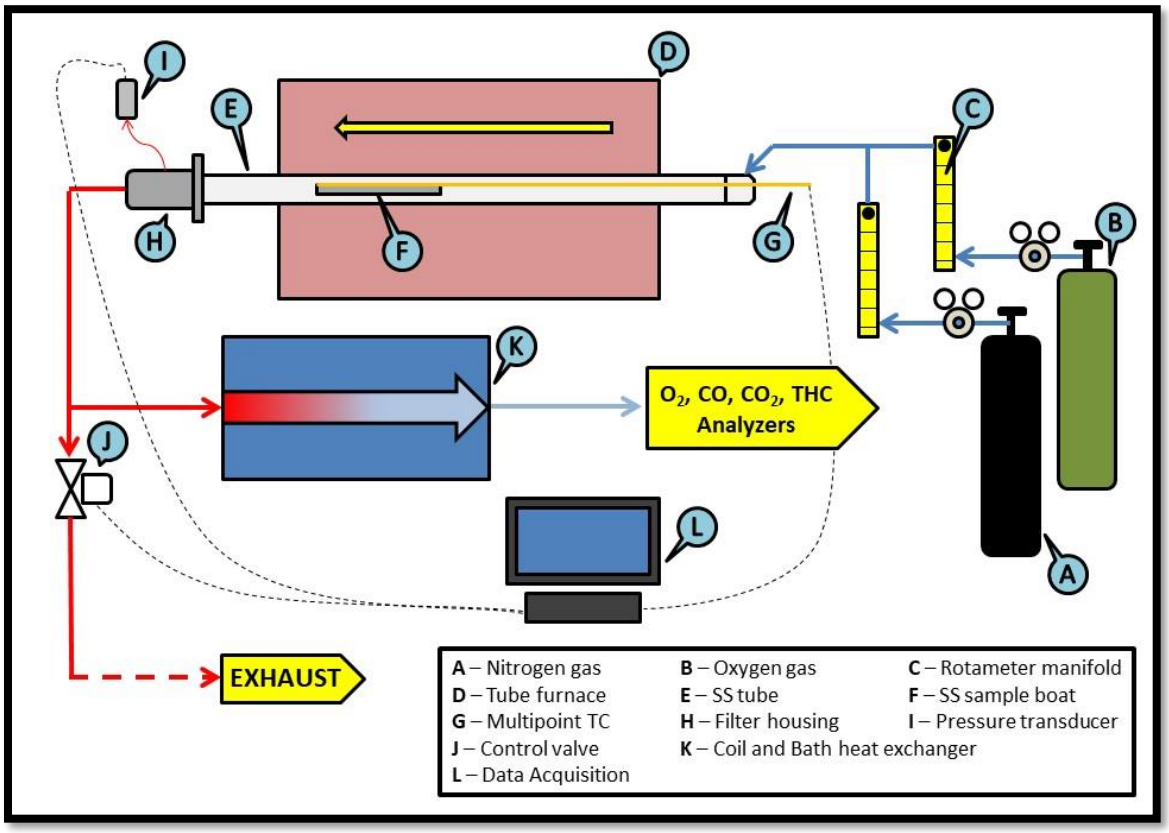

Figure 2-8: Pyrolyzate leaving the reactor is cooled prior to an analysis for O_2, CO, CO_2, and THC concentration.

A set of initial scoping tests using the apparatus as described in **Figure 2-8** were used to determine and program the sample timing of the autosampler for the GC-BID testing. The red data set in **Figure 2-9** represents the total hydrocarbon data collected using the FID analyzer. The green points along the plot represent the nine sampling times that were chosen for a given O_2 concentration to collect data with the autosampler for the GC-BID analysis. The purpose was to map out the collection of the data so that the data collected using both methods (FID and BID) could be compared.

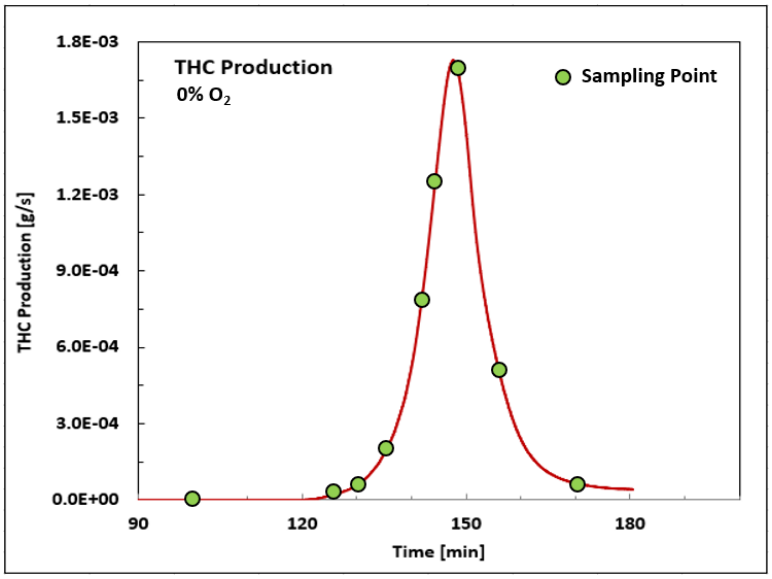

Figure 2-9: Data from an initial scoping test was used to determine the sample collection timing of the auto-sampler for comparative analysis by the GC-BID.

A third method of testing was conducted using the TGA apparatus. This testing was conducted by Yan Ding of the University of Maryland on behalf of the author and the advisor. The TGA apparatus provides a much smaller, yet reputable means of pyrolysis and analysis.

Data from the GC-BID and the GC-MS analyses are used to quantify gas production at nine points throughout the pyrolysis experiment. Data from the IR gas analysis is used to quantify continuous oxygen depletion and provide data for the completion of a carbon balance. Data from the TGA analysis is used to verify the quality of the decomposition of the focus reactor through a much smaller scale comparison. This combined data set is presented and discussed in totality in the following chapters

Chapter 3: Experimental Results

3.1 GC-BID – Results

Gases produced during pyrolysis are captured by the auto-sampler in nine sampling cylinders. The auto-sampler is connected to a GC-BID for automated batch processing of the nine cylinders to produce 18 data sets for each pyrolysis experiment, two from each cylinder. The gas present in each cylinder is representative of the time and temperature of when it was collected, thus each data set produced provides a snap-shot of decomposition at a specific time and temperature. The calibrated GC-BID produces a chromatograph for each gas analysis that provides retention time and area count data. Analyses of the same gases using a GC-MS allow for the identification of the previously quantified hydrocarbon species by identifying them with respect to their retention times. Calibration data is used to convert area count data into mole fractions. In this investigation a single column, QBOND, was used to analyze the pyrolysis gas, which limited the analysis to lower molecular weight species (C1-C6). **Figure 3-1**, below provides three chromatographs, each representing the moment of maximum production for 0%, 5%, and 15% O_2 pyrolysis respectively.

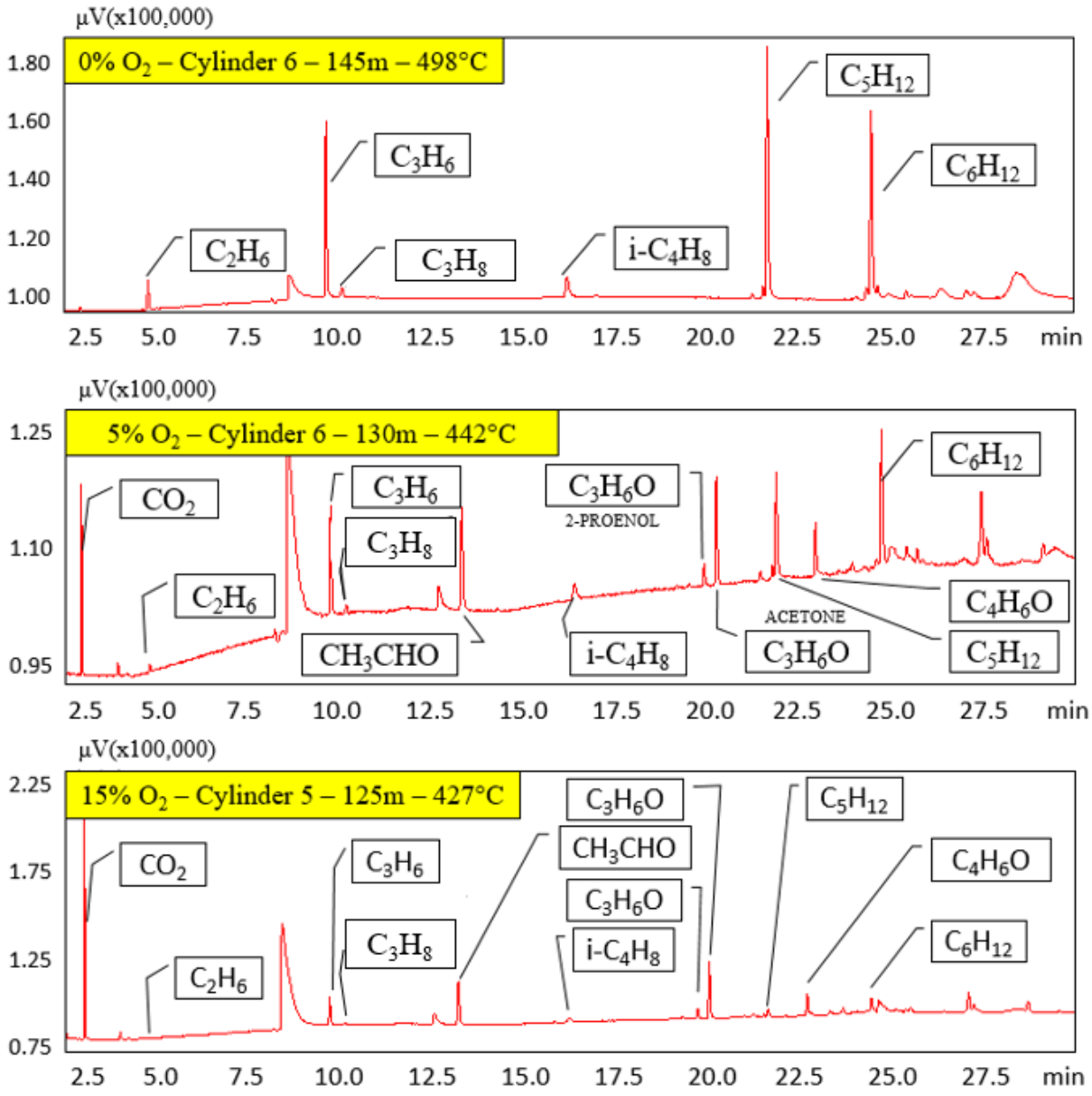

Figure 3-1: These chromatographs represent the production maxima from polypropylene pyrolysis in 0%, 5%, and 15% O_2. The samples were collected at 498°C, 442°C, and 427°C respectively.

Six main species are produced and effectively quantified from the 0%-oxygen experimentation: ethane, propylene, propane, i-butene, n-pentane, and 2-methyl-1-pentene. Several authors have encountered these results in similar research [19, 18, 7, 13]. When oxygen is introduced, the number of identifiable species is nearly doubled with the inclusion of CO_2. Production of these species is also expedited. While production of some species decreases with increasing O_2 concentration there are several that experience and increase in production. It should be noted that the presence and prevalence of CO_2 nearly doubles the y-scale for the 15% O_2 plot. The scaling might lead one to believe that the species mole fractions are reducing with the increased O_2, while several are increasing.

Area count data are produced, converted, and compiled for each chromatograph from a pyrolysis test. These data sets are used to develop time or temperature dependent production curves. The following sections will investigate, more closely, the production of individual species at differing oxygen concentrations.

3.1.1 Temperature dependent species production

A multi-point thermocouple was used to gather temperature data in real time during all pyrolysis experiments. This time-dependent temperature data was used to link the time-dependent species concentration data and to allow for the presentation of temperature-dependent species concentration data. **Figure 3-2** below provides the average surface temperature data for pyrolysis for 0%, 5%, and 15% O_2. Temperature measurements from the two thermocouples centered inside the windows of the sample boat, as seen in **Figure 2-2**, are averaged across all tests at a given O_2 concentration. The standard deviations for these measurements are 4.93˚C for 0% O_2, 5.84˚C for 5% O_2, and 8.96˚C for 15% O_2. The average standard deviations for these measurements are 3.67˚C for 0% O_2, 3.10˚C for 5% O_2, and 1.31˚C for 15% O_2.

An increasing concentration of oxygen enhances the heating rate of the pyrolysis through the addition of heat to the reactor. This provides evidence of an exothermic process likely due to an increase in species decomposition reaction rates. This is also likely the reason for the increasing maximum standard error with increasing O_2 concentration. It is important to note the early, non-linearity in heating rate. This is unpreventable and characteristic to the operation of the temperature programming of the tube-furnace. This non-linearity does not affect the results of the pyrolysis, as the temperature ramp enters a linear heating-rate regime around 50°C.

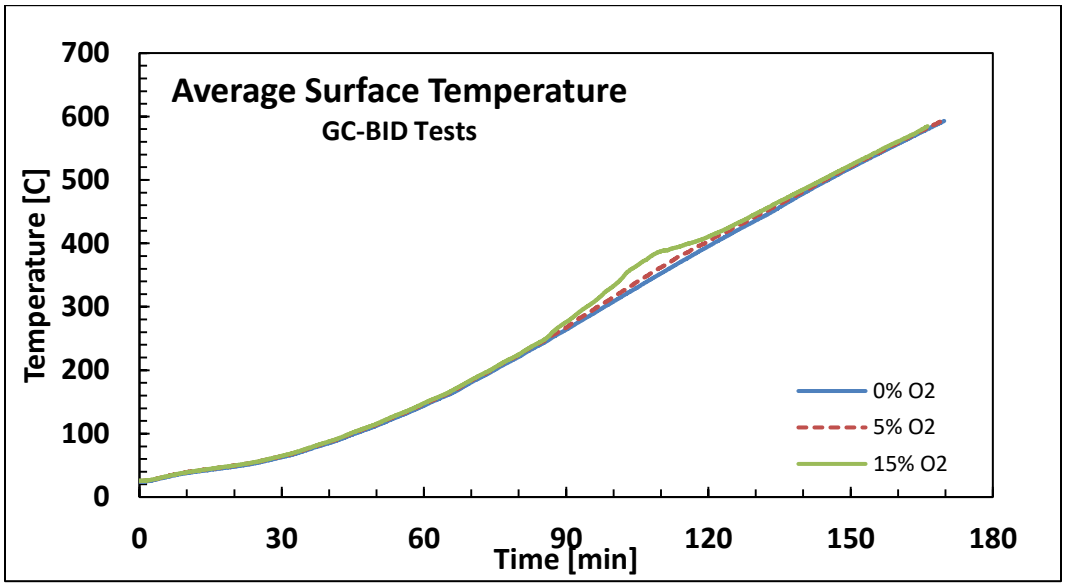

Figure 3-2: Average Surface Temperature of Polypropylene During Pyrolysis in 0%, 5%, and 15% O_2

3.1.2 Polypropylene pyrolyzed in 100% N_2

To effectively investigate the effect of oxygen on the pyrolysis of polypropylene, a baseline investigation into the oxygen-free decomposition of the polymer needed to take place first.

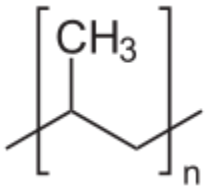

Figure 3-3: Structural formula for polypropylene

The analysis of gases evolved during the pyrolysis of polypropylene revealed a mix of alkanes and alkenes: ethane, propylene, propane, i-butene, n-pentane, and 2-methyl-1-pentene. The structural formulas for these six major species evolved in the oxygen-free pyrolysis of polypropylene can be seen below in **Figure 3-4**.

Using linear relationships developed through a calibration of the BID detector and column, area count data is converted to mole fraction data for individual species, X_i. **Figure 3-5** below provides an example of a calibration curve developed during the column calibration exercise. The figure represents the calibration for only one of 20 calibrated species, 19 additional curves exist.

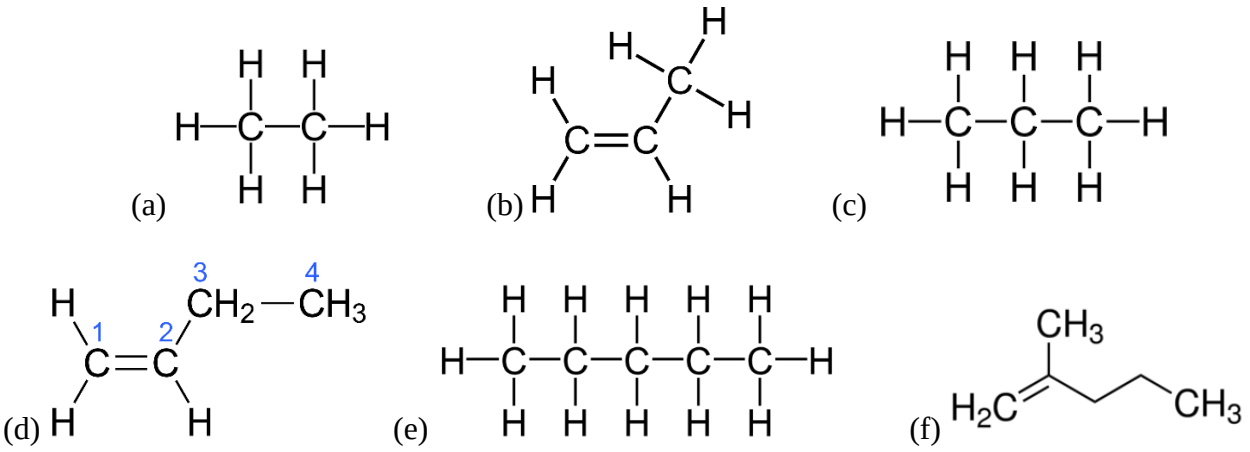

Figure 3-4: Structural formulas for (a) ethane, (b) propylene, (c) propane, (d) i-butene, (e) pentane, and (f) 2-methyl-1-pentene

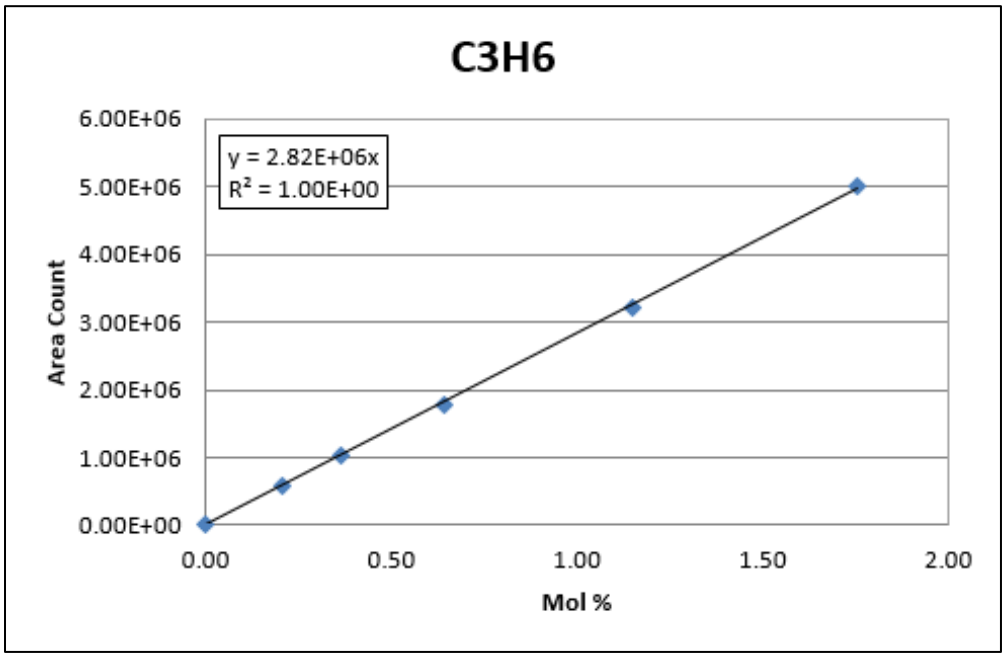

Figure 3-5: BID calibration curve for polyproplyene displaying linear relationship between area count and mole fraction.

The ideal gas law, (1), was used to calculate a molar volume for a gas at normal temperature and pressure. NTP was used because these values more closely resemble the initial state of the reactor.

$$(1) \qquad V_m = \frac{nRT}{P}$$

$$P = 1\ atm \qquad T = 293K \qquad n = 1\ mol \qquad R = 8.21x10^5\ \ m^3 * atm * K^{-1} * mol^{-1}$$

$$V = 0.024\ m^3$$

A mass flow is then calculated using the mole fraction converted from the measured area count, calculated molar volume, established reactor volumetric flow rate, and species molecular weight.

$$(2) \qquad \dot{m}_i = \frac{X_i}{V_m} \times \dot{V}_R \times MW_i$$

$$\dot{V}_R = 10\ SLPM\ or\ 1.67x10^{-4}\ \frac{m^3}{s}$$

These temperature specific mass flow rates are plotted using a straight-line scatter plot and presented as rates of mass-loss. This mass flow data is then integrated using the trapezoidal method and summed to provide a mass of recovered hydrocarbons.

The data is provided via the decomposition and mass-loss of the polypropylene sheet. Production of these six species roughly occurs between 400°C and 550°C with the maximum production occurring at around 500°C. The 500°C point also marks the moment of maximum decomposition of the polypropylene. Pentane, propylene, and 2-methyl-1-pentene are the three most highly produced species.

Three pyrolysis experiments were conducted with polypropylene in 100% N_2, producing three sets of data. These data sets were used to develop an average set of data and standard deviations. The six figures that follow provide an individual plot for the temperature dependent evolution of each species, including a shade of error bars that represent two times the standard deviation for a given data point. The boundaries provide an idea of minimum and maximum evolution potential for each species.

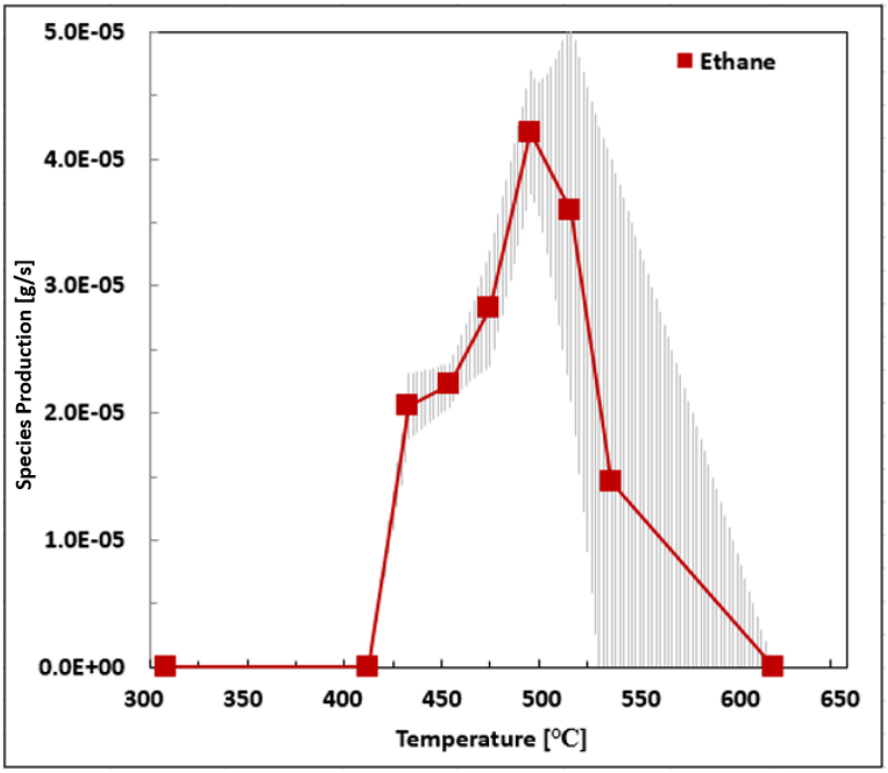

Figure 3-6: Ethane production in 100% N_2

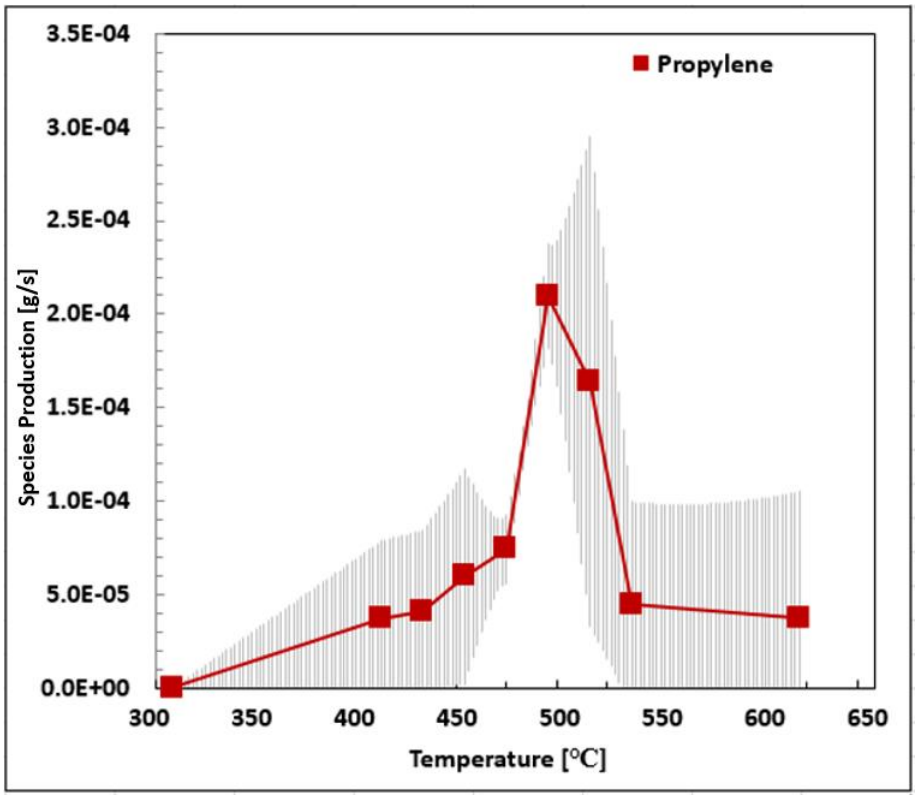

Figure 3-7: Propylene production in 100% N_2

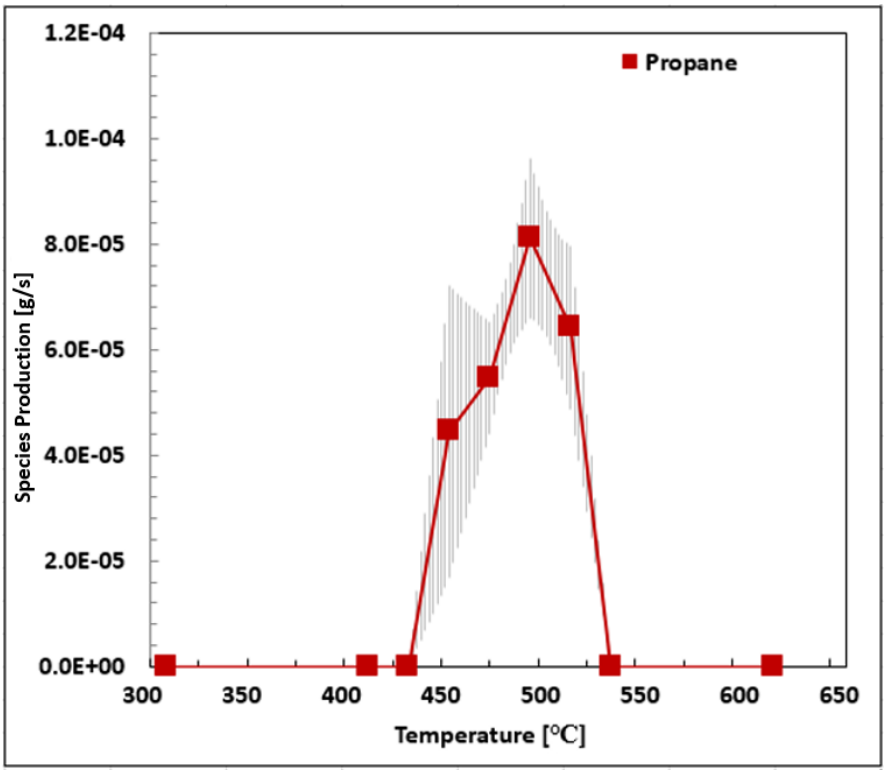

Figure 3-8: Propane production in 100% N_2

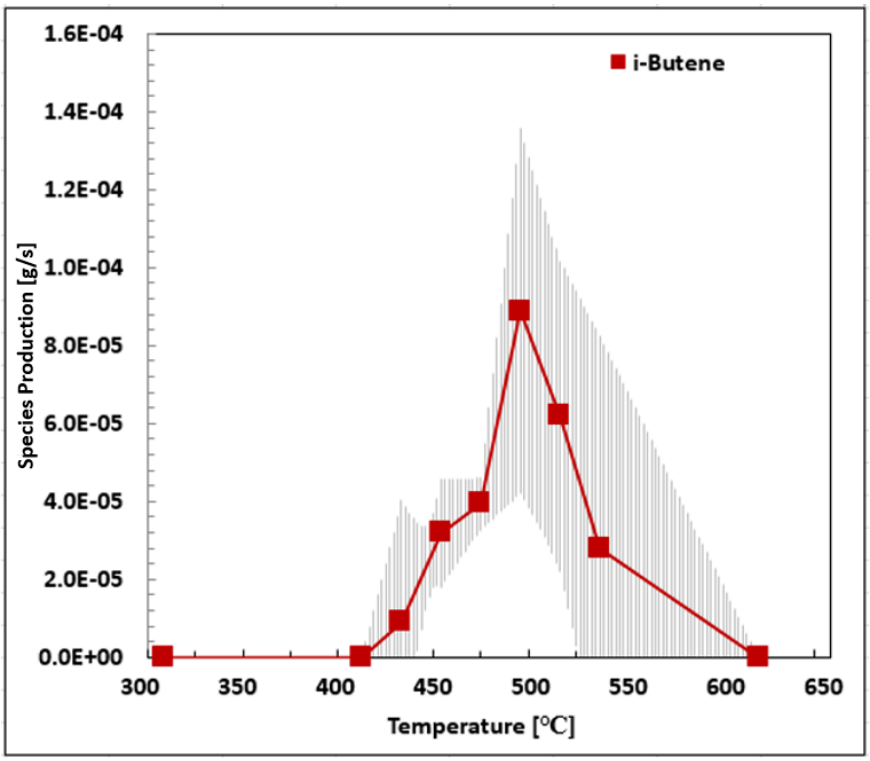

Figure 3-9: i-Butene production in 100% N_2

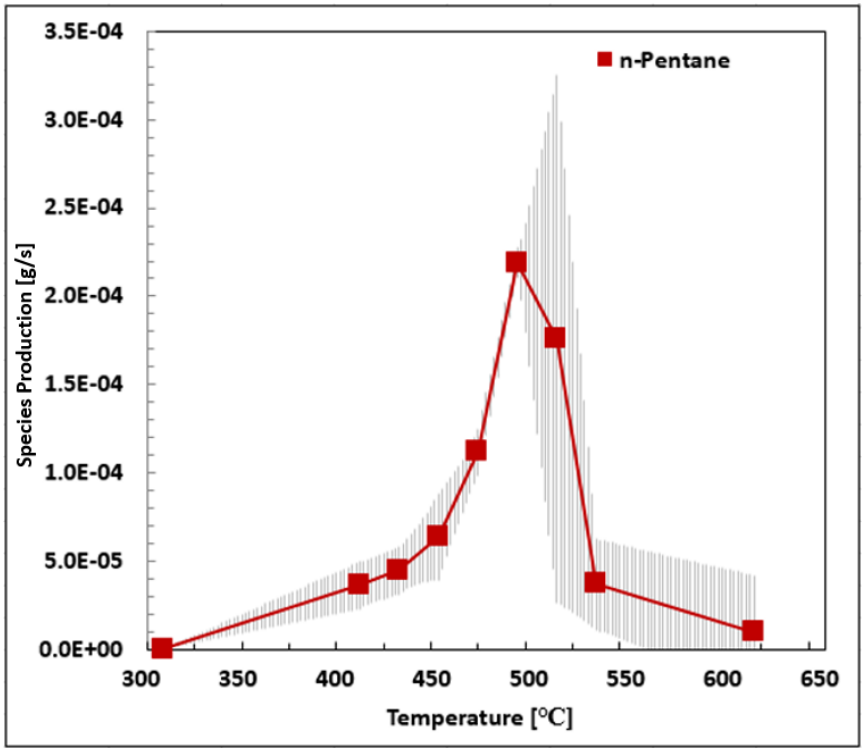

Figure 3-10: n-Pentane production in 100% N_2

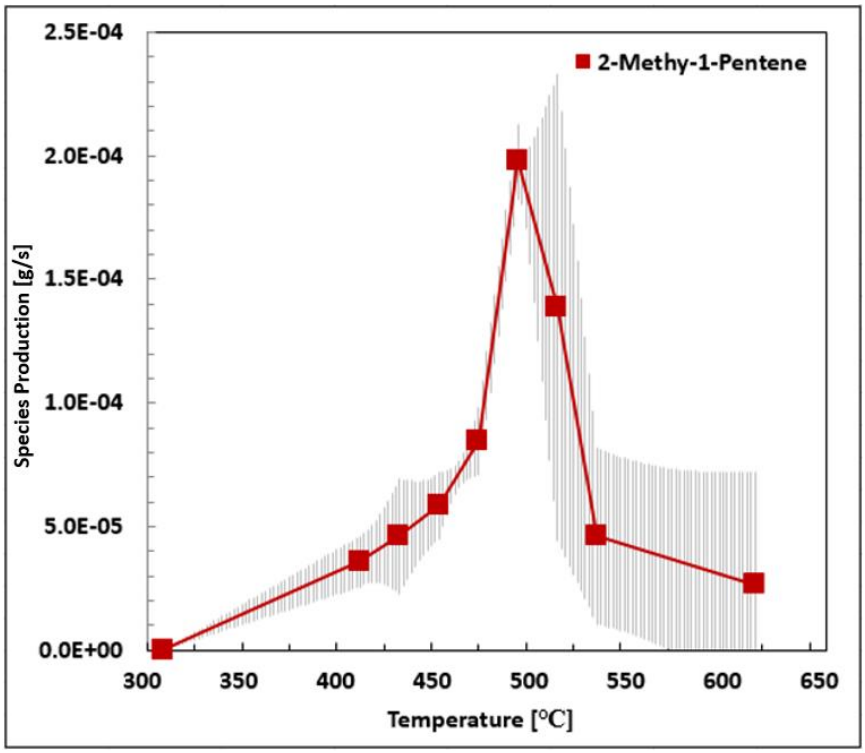

Figure 3-11: 2-Methyl-1-Pentene production in 100% N_2

Figure 3-6 through **Figure 3-11** showcase a relatively repeatable data set for the pyrolysis of polypropylene in 100% N_2. The error bars are at their largest in the periods after maximum species production. After production maxima, the liquid polymer bed is likely non-uniform, if existing at all. The large errors could be due to a non-uniform bed or areas of trapped liquid or oil that have not completely volatilized. The shapes of the ethane and propane curves may suggest that their evolution is not a first-order reaction. The shapes of these curves could also be affected by low production rates relative to the other evolved species.

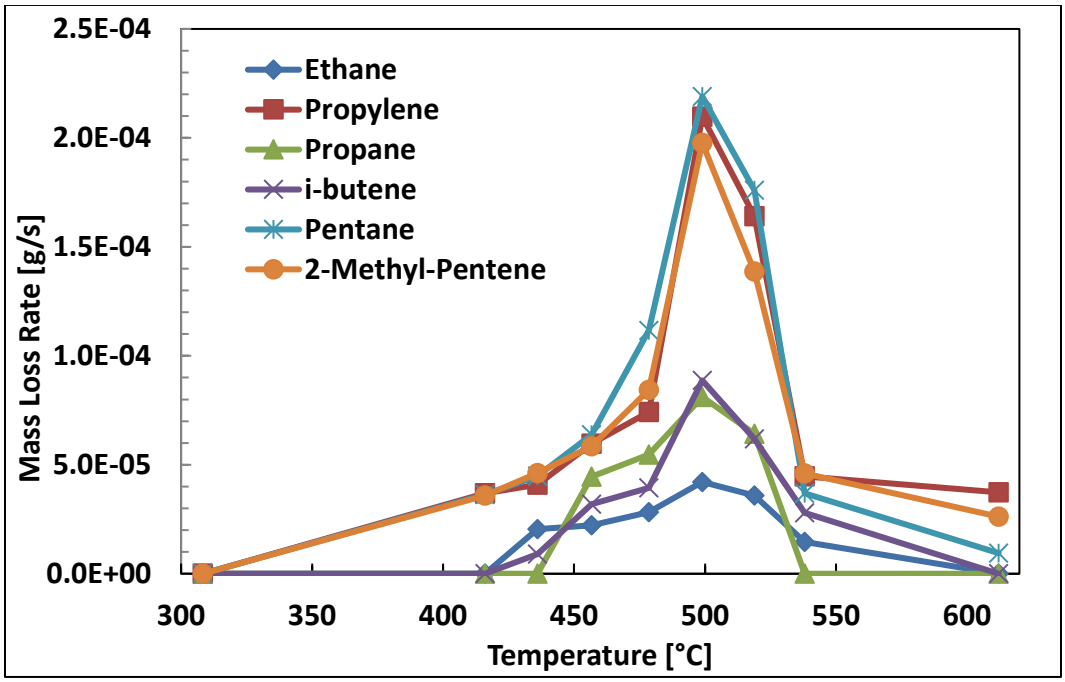

Figure 3-12: Curves representing average values for evolution of C1-C6 species during pyrolysis in an oxygen-free atmosphere.

Figure 3-12 above represents the average set of data for all six of the evolved species. Evolution of the gases was not noticed until after 415℃; however, it is possible the species were evolving earlier and were not captured due to the sampling method that was employed. All six of the species experienced maximum evolution around 500℃ after which there was a sharp drop off in production. Propylene, pentane, and 2-methyl-1-pentene were the largest contributors to the total mass recovery. Combined, these three species accounted for 77% of the total mass recovered in the current research.

Anaerobic decomposition is very well known and can be used to better understand the evolution of the species found in this testing. Polypropylene decomposes following a free radical mechanism. The decomposition is initiated by chain scission, breaking the polymer into a primary and a secondary radical. Depolymerization of the primary and secondary radicals leads to the production of the monomer, propylene. Intramolecular hydrogen transfer then leads to the formation of tertiary radicals. Finally, Beta-scission of the tertiary radicals leads to the formation of alkenes (propylene, i-butene, 2-methyl-1-pentene) and alkanes (ethane, propane, pentane).

As discussed in the literature review, researching the pyrolysis of polypropylene is not a new endeavor. **Table 3-1** below provides a compilation of data extracted from previously existing research into the pyrolysis of polypropylene as well as the data resolved from the current investigation.

Table 3-1 – Evolved Species Comparison

Species	**Turner** **400-550°C**	[18] **420-460°C**	[7] **700°C**	[19] **438°C**	[13] **380°C**
	Weight %				
ethane	6%	6%		3%	3%
propylene	26%	44%	67%	27%	14%
propane	8%	4%		0%	1%
i-butene	9%	14%		6%	7%
n-pentane	26%	28%	22%	38%**	34.2%
2-methyl-1-pentene	25%	4%*	11%	25%	41%

* labeled as Hexane ** labeled as 2-methyl-1-butene
In some cases, low wt% species were removed from the data set to correct for a 6-component data set

The analysis of the pyrolyzate collected under 100% N_2 in this research identified six major components as listed in **Table 3-1**. The mass data for these six species was converted into % mass yield by dividing individual mass yields by the total mass recovered for all six species. The total mass recovered only represents a fraction of the total mass lost during the pyrolysis. The column used in the GC-BID apparatus limited the analysis to species with molecular structures ranging from C1-C6. This data is compared with mass yield data produced in similar research focused on the oxygen-free pyrolysis of polypropylene.

Kruse et. al. pyrolyzed 20mg samples of polypropylene in the absence of O_2 in a small-scale batch reactor under isothermal conditions. The comparison data represents that collected at 380°C over 180 minutes. Mass yields for 27 major components were observed in their research [13]. For comparison purposes, data for the six similar species were normalized as if they were the only six species evolved and measured in the analysis. The six species being compared only

accounted for 5.2% by mass of all the products they quantified. All the evolved species C1-C15 only accounted for roughly 22% by mass of the total products [13].

Jing and Wen conducted research using a small batch reactor with a large, 30g sample size, and a heating rate of 10-15°C/min [18]. They identified 16 species in the C1-C6 range. The six species being compared in Table 3-1 accounted for 92% of the total mass yield that they observed. Again, this data was normalized to provide for better comparison. The inclusion of the dissimilar species would only skew the comparison.

The data produced by Amorim was collected through flash pyrolysis for 1s at 700°C. The analysis identified 27 species ranging from C2-C17 [7]. Only three species were identified as being like what has been identified in this research. The similar components were normalized for comparison. The lack of low-molecular weight species is likely an effect of the high temperature flash pyrolysis or detection limits of their GC-MS.

Lastly, Chien and Kiang used rapid heating rate, iso-thermal pyrolysis of 1mg samples of polypropylene to identify 14 species ranging from C1-C13 [19]. Their work identified five similar species to those identified in the current research, which have been normalized for comparison in Table 3-1. These five species account for 40% of the total mass recovered through their analysis.

Data from the current research agrees well with the results of Jing and Kruse who conducted their research in 2015 and 2003 respectively. The data produced by Amorim and Chien follow the same production trends, but their data sets did not identify all the low-molecular weight species or have misidentified species [7, 19]. These authors methods were small scale and relied

on rapid evolution of pyrolyzate for real time detection. Their research was published in 1982 and 1978 respectively so it's reasonable that there were limitations and inconsistencies in the measurement techniques as well.

In most cases propylene, pentane, and 2-methyl-1-pentene were the most prominent species. The agreement of the current data with previously existing data supports the effectiveness of the subject reactor, auto-sampler, and GC analysis techniques, which are still very much in their infancy. The effect of oxygen on the pyrolysis of polypropylene will be investigated in the following section.

3.1.3 Polypropylene pyrolyzed in 5% and 15% O_2, balanced with N_2

Using the same testing, collection, and sampling techniques, polypropylene was pyrolyzed in atmospheres of 5% and 15% O_2. Nine species were identified and quantified during the analysis: propylene, propane, 1-butene, n-pentane, and 2-methyl-1-pentene, acetaldehyde, 2-propenol, acetone, and 2-butenal. Out of these nine species, five were evolved under all three oxygen conditions, 0%, 5%, 15% concentration. These were propylene, propane, 1-butene, n-pentane, and 2-methyl-1-pentene whose production in 0% O_2 was discussed in the previous section.

The following five figures provide a good portrayal of how oxygen effects the evolution of like species produced during the pyrolysis of polypropylene under varying oxygen concentrations.

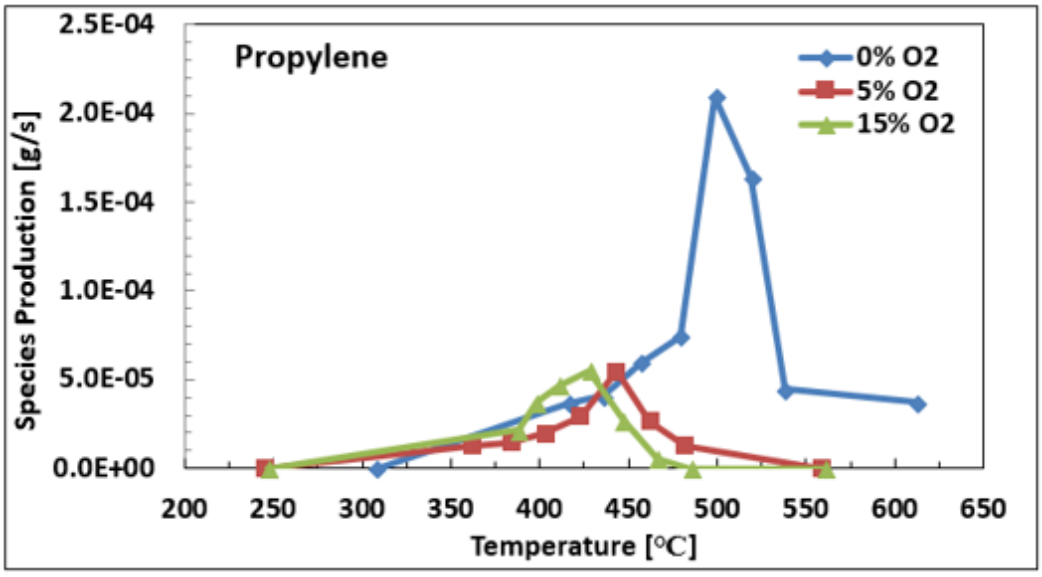

Figure 3-13: Propylene production in 0%, 5%, and 15% O_2

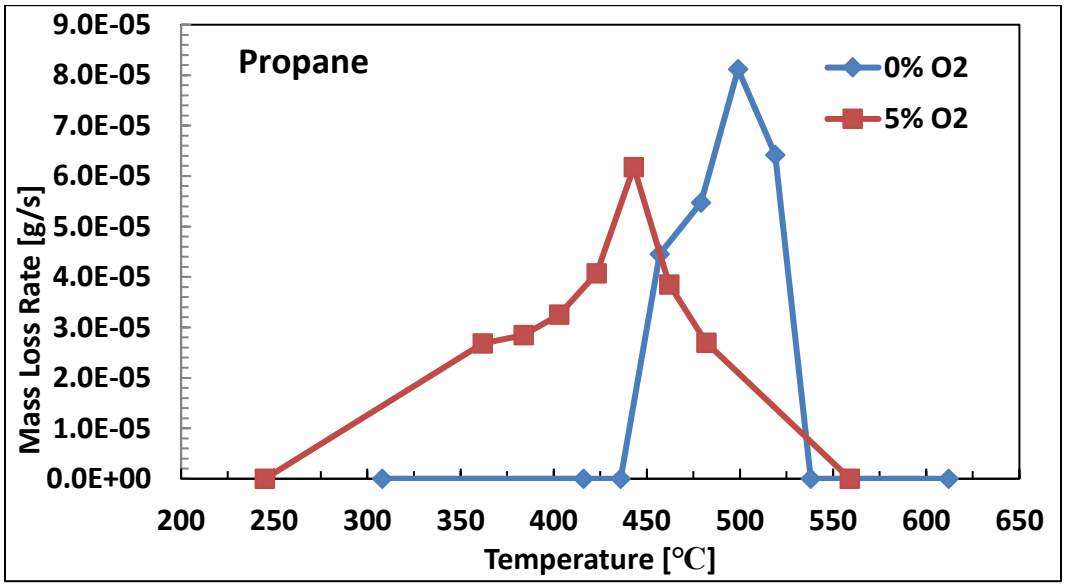

Figure 3-14: Propane production in 0% and 5% O_2. No propane was recovered from the 15% O_2 test case.

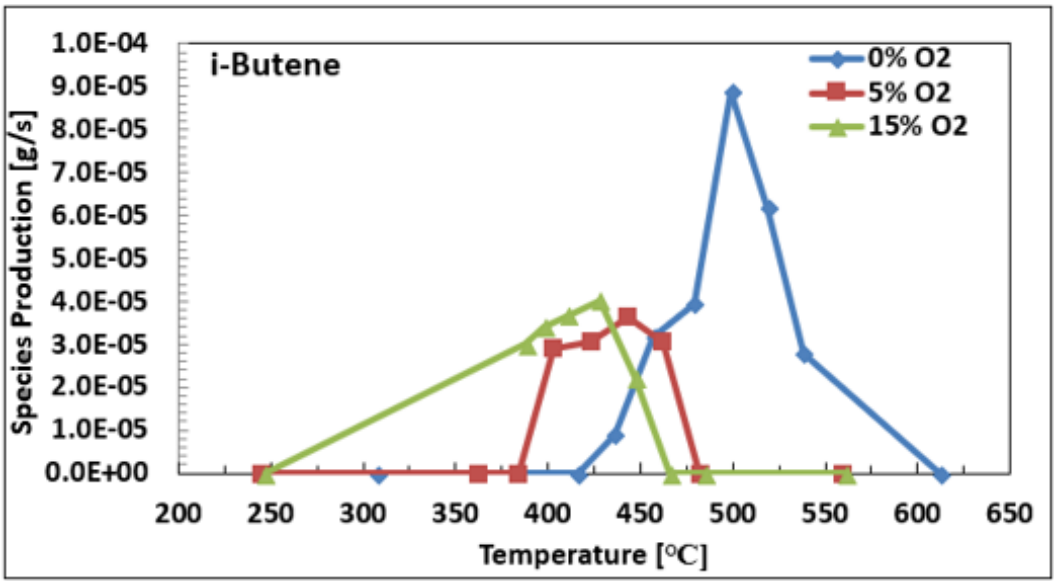

Figure 3-15: i-Butene production in 0%, 5%, and 15% O_2.

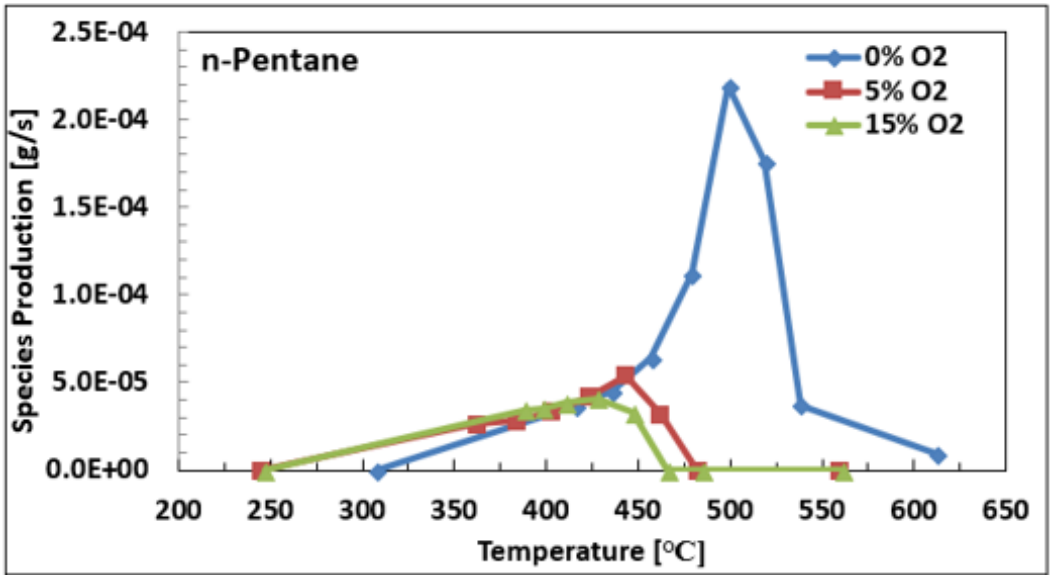

Figure 3-16: n-Pentane production in 0%, 5%, 15% O_2

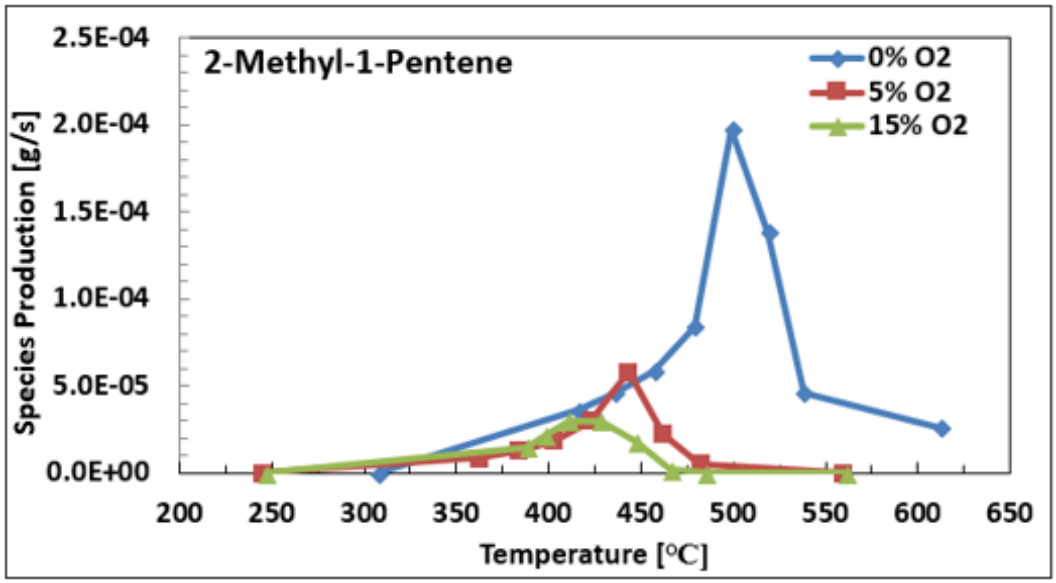

Figure 3-17: 2-Methyl-1-Pentene production in 0%, 5%, 15% O_2

Two obvious effects of the presence of oxygen on pyrolysis are the evolution of species at lower temperatures and the reduction in the total recovered mass of the hydrocarbon species. **Table 3-2** below provides the time and temperature of maximum species evolution from pyrolysis in 0%, 5%, and 15% O_2. With the addition of 5% O_2, it is seen that species are evolved at a temperature more than 50°C lower than that which they are evolved during pyrolysis in the absence of O_2. With the addition of 15% O2, it is seen that species are evolved at a temperature more than 70°C lower than that at which they are evolved during pyrolysis in the absence of O_2. In both cases, the decrease in the temperature of evolution correlates to a decrease in time to the initiation and completion of species evolution.

Table 3-2 – Time and Temperature for Maximum Species Production in 0%, 5%, 15% O_2

$[O_2]$	Time	Temperature
%	min	℃
0	145	499
5	130	443
15	125	428

Table 3-3 below compares the mass yield data recovered from the 5% and 15% O_2 cases by presenting them as fractions of the mass yield recovered from the 0% O_2 case. The mass yields recovered from the 0% O_2 case are being considered the initial and maximum mass yields for the overall experimentation. The numbers in the table represent the reduction in mass yield from the

"initial mass" and are presented in this way to provide a trend for the effect of O_2 on species evolution. For example, in 5% and 15% O_2 the recovered mass yield of propylene represents 26% of the mass evolved during 0% O_2 case. The decrease in evolution of these hydrocarbon species provides evidence of their further decomposition and conversion to the identified oxygenated hydrocarbons or to CO and CO_2.

Table 3-3 –Mass Yield for 5% and 15% O_2 Compared to 100% N_2

Species	0% O_2	5% O_2	15% O_2
Ethane	100%	0%	0%
Propylene	100%	26%	26%
Propane	100%	76%	0%
i-Butene	100%	41%	45%
n-Pentane	100%	25%	19%
2-Methyl-1-Pentene	100%	29%	15%

When discussing the effect of O_2 on the decomposition, it is important to note that 5 of 6 species identified in the baseline, 0% O_2 case were also identified in the 5% and 15% O_2 cases. The only species that wasn't identified from the results of the oxygenated case was ethane. Ethane was not recovered in either oxygenated case. Additionally, the mass yield of propane dropped to 0% in 15% O_2. The diminishment of these species is likely due to lower initial concentrations. The lack of apparent decomposition of some of the alkenes could represent the production of these species because of the decomposition of the lower molecular weight alkanes. The formation of new molecules with increasing oxygen concentration explains the exothermic reaction and

increase in apparent heating rate of the temperature profiles.

An increase in O_2 concentration lead to an increased rate of decomposition of the polypropylene. This increase caused the faster evolution of previously existing species and at lower temperature. Though they evolved more quickly and at lower temperature, the species that were identified and quantified for all O_2 concentrations experienced a reduction in mass yield with an increase in O_2 concentration. Some species going completely undetected with the addition of O_2. While the rate of production of alkanes and alkenes was being reduced, several new oxygenated species were detected and the concentration of oxygen had the reverse effect on their production. Figure 3-1 shows this combined effect. Acetaldehyde, 2-propenol, acetone, and 2-butenal are the four oxygenated species identified through the GC-BID analysis of the oxygenated cases. The chemical structures of these species are found below in **Figure 3-18**.

Hayashi et al. identified acetaldehyde and acetone through their investigation into the formation of peroxides during oxidative pyrolysis [10]. Of the four oxygenated hydrocarbons, acetaldehyde experienced the sharpest increase in its rate of evolution with the increase in O_2 concentration. Acetone and 2-propenol had the highest rates of evolution. Figures of the four species are seen below. The data presented for 15% O_2 represents an average of three pyrolysis experiments. Figures of all nine species evolved in 15% O_2 can be found in the appendices. The curves for 2-butenal and 2-propenol provide very good repeatability. Acetaldehyde and acetone data provide good repeatability at the maxima but disagreement at the beginning of the evolution.

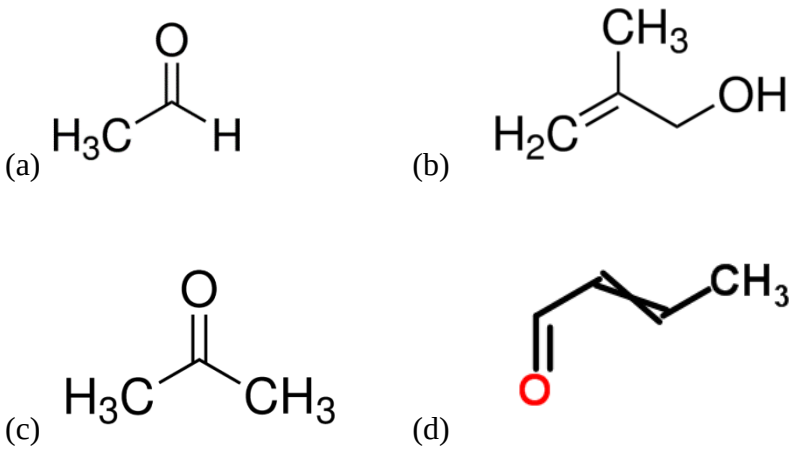

Figure 3-18: Structural formulas for (a) acetaldehyde, (b) 2-propenol, (c) acetone, (d) 2-butenal

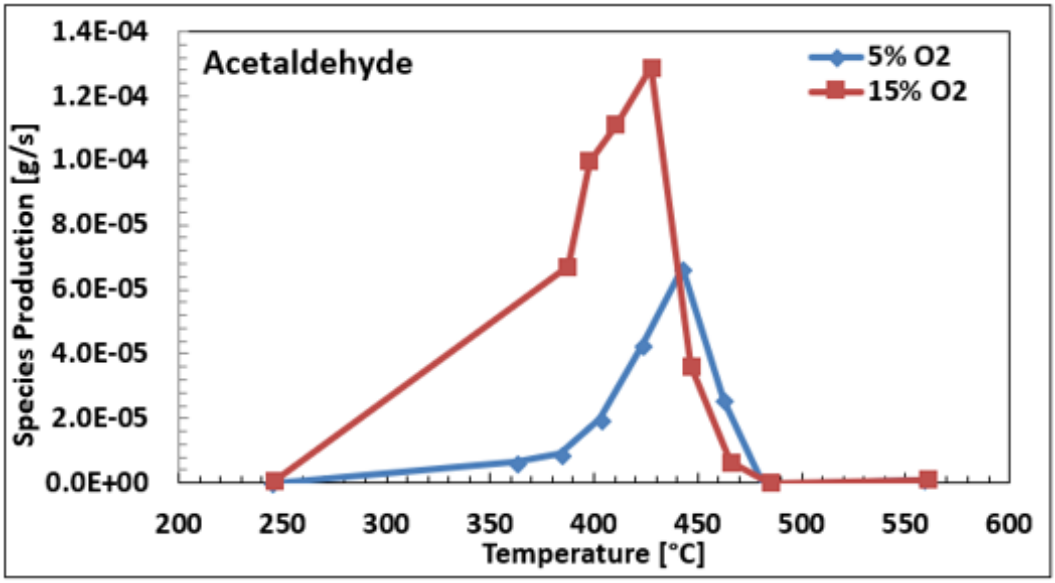

Figure 3-19: Acetaldehyde production in 5% and 15% O_2

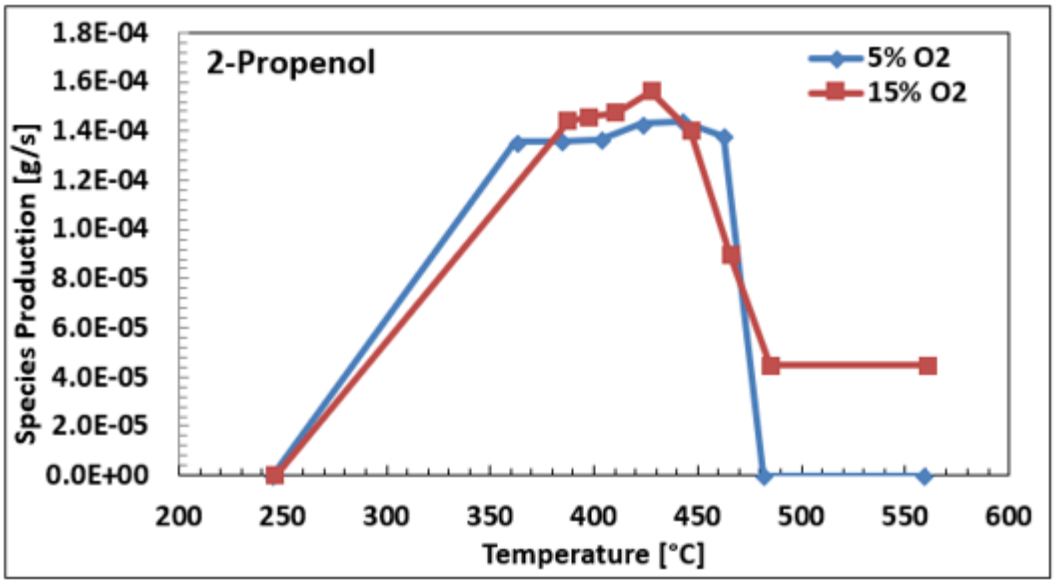

Figure 3-20: Propenol production in 5% and 15% O_2

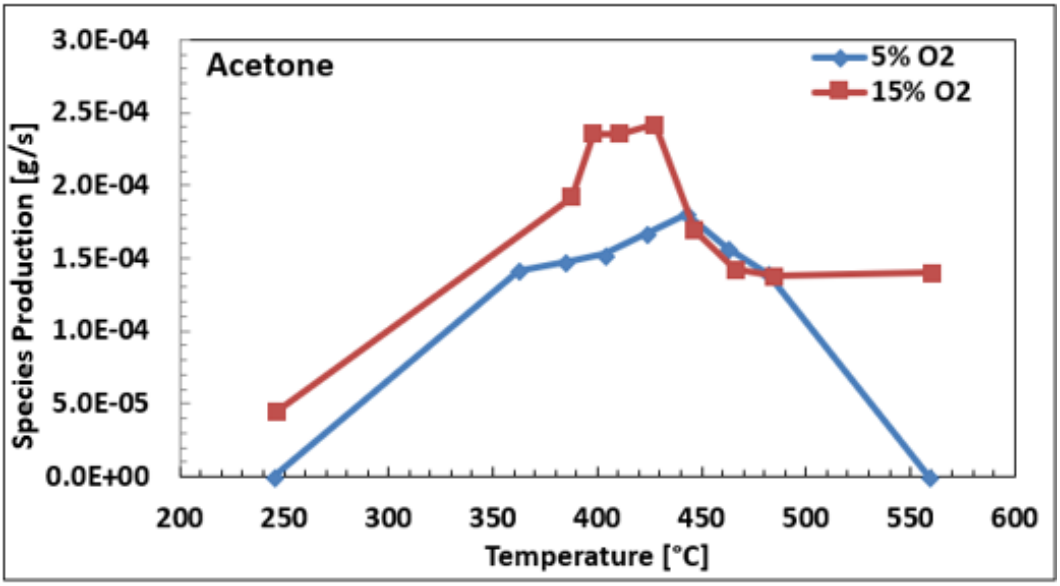

Figure 3-21: Acetone production in 5% and 15% O_2

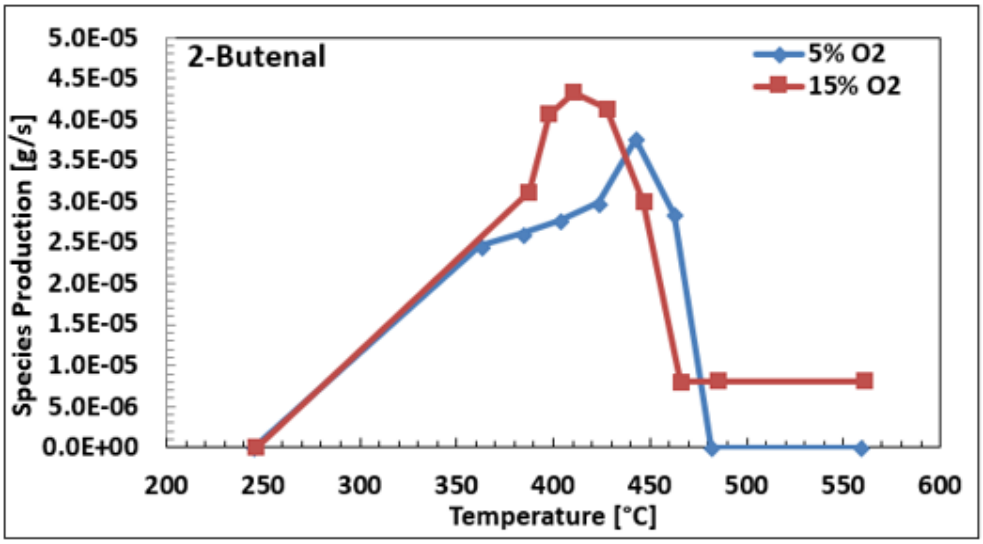

Figure 3-22: 2-Butenal production in 5% and 15% O_2

The 20-component gas mixture used to calibrate the GC-BID column did not include any oxygenated species therefore the curves in **Figure 3-19, Figure 3-20, Figure 3-21, and Figure 3-22** were approximated using existing calibration curves for species that had similar retention times and molecular weights. This provides a good approximation of species production.

For all concentrations of O_2, the mass loss curves for all species were integrated, using the trapezoidal rule, to calculate a total mass evolved in grams. These values were then used to calculate the mass recovered through the GC-BID analysis and compare it to the mass of the starting sample. This calculation is discussed in more detail in section 3.1.2 of this chapter. The average starting sample mass for all seven tests (three at 0% O_2, one at 5% O_2, and three at 15% O_2), was 4.9 ± 0.1 grams.

Table 3-4 – Mass of Carbon and Hydrogen from Evolved Species (oxygen removed)

Species		Mass, fraction of total recovered		
		0% O_2	5% O_2	15% O_2
Ethane	C_2H_6	5.8%	0.0%	0.0%
Propylene	C_3H_6	26.3%	6.4%	5.8%
Propane	C_3H_8	7.6%	10.4%	0.0%
Acetaldehyde	CH_3CH_O	0.0%	3.5%	9.3%
i-Butene	i-C_4H_8	9.3%	3.8%	5.5%
2-Propenol	C_3H_6O	0.0%	23.7%	23.4%
Acetone	C_3H_6O	0.0%	33.8%	41.6%
n-Pentane	C_5H_{12}	26.0%	7.9%	5.2%
2-Butenal	C_4H_6O	0.0%	5.2%	5.6%
2-Methyl-1-pentene	C_6H_{12}	24.9%	5.4%	3.5%
Recovered Mass Fraction of Initial		**19.8%**	**20.7%**	**24.9%**

Table 3-4 above provides that 19.8% of the initial sample mass was recovered during the pyrolysis of polypropylene in 100% N_2, 20.7% was recovered in 5% of O_2 and 24.9% was recovered in 15% O_2. With the increase in O_2 concentration there was an increase in recovered mass due mostly to the hydrocarbon content of the evolved oxygenated species. The mass recovered in 100% N_2 represents ~20% of the starting mass. This is feasible based on hydrocarbon recovery as reported by Ballice and Rainer who identified a carbon distribution up to C31, Bockhorn et al. who also identified species up to C31, and Jing and Wen who identified species up to C22 [12, 11, 18]. Ballice and Ranier report that in the temperature range of 400-450˚C that volatile species ranging C1-C6 account for ~30% of the total volatilized product. Jing and Wen report that gas makes up only 13.67% of the total product yield from the cracking of virgin

polypropylene. ~19% fits inside of this range. The data produce by Kruse et. al. provided that the mass recovered from species raging C1-C6 accounted for 5.2% of the total mass, while species ranging C1-C15 accounted for 20% of the total mass recovered. These results do not agree with the results presented in the current research. Differences in scale and scope of the pyrolysis and analysis could account for the differences in recovered mass. The pyrolysis experiments were conducted in different reactors and at different temperatures. These factors can affect the evolution of these hydrocarbon species. There are also opportunities for error in the current pyrolysis and analysis procedures.

3.1.4 Comments on Arrhenius Rate Expression

The rate of disappearance of a chemical species is proportional to the product of the concentration of the chemical species reacting. The Arrhenius rate expression contains a constant, k, called the reaction rate coefficient. This coefficient is dependent on temperature alone and is independent of species concentration. The Arrhenius expression is used for the development of plots which plot the logarithm of K as a function of T^{-1}. Slope data from these plots are used to determine activation energies of reactions [20]. This is important information when considering the role that oxygen plays in the decomposition of polypropylene. Increasing oxygen concentration shifts the time at which decomposition begins, peaks, and concludes. The reactions occurring during pyrolysis with increased oxygen concentration also seem to be exothermic, adding heat to the reactor.

3.2 IR Analyzer Results

As a secondary method of measurement and to verify the outcome of the GC testing and analysis, pyrolysis tests were conducted with real-time analysis using IR and FID analyzers. The pyrolysis was conducted using the same process as it was for the GC-BID only rather than collect the gas with the auto-sampler, the gas was sent to a stack of analyzers. IR analyzers measured O_2 depletion, CO production, and CO_2 production. A FID analyzer was used to measure total hydrocarbons (THC). A single test was conducted for each oxygen concentration, 0%, 5%, and 15%. Figures for each analysis are found below.

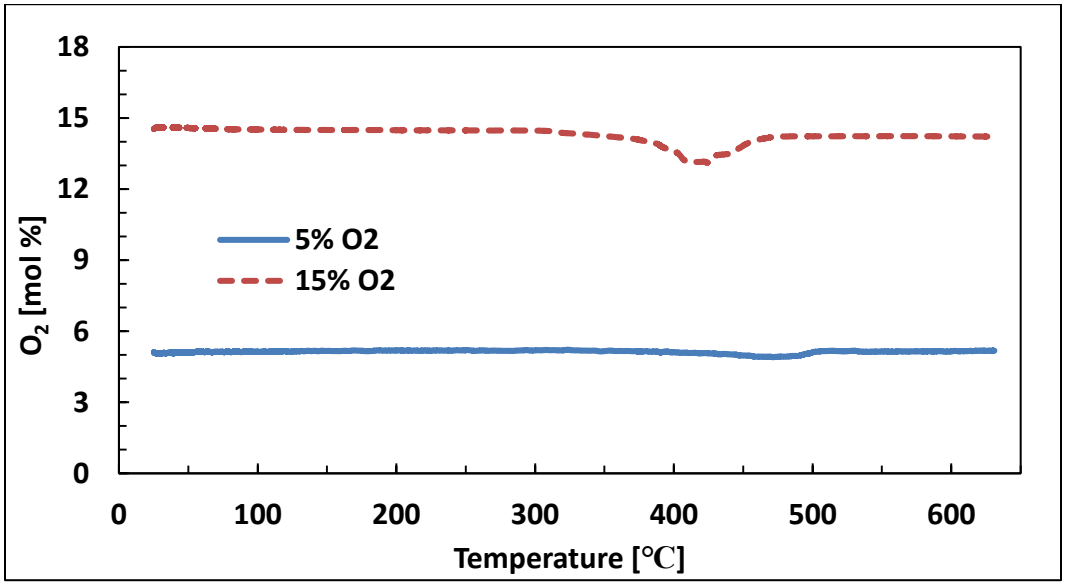

Figure 3-23: Oxygen Depletion

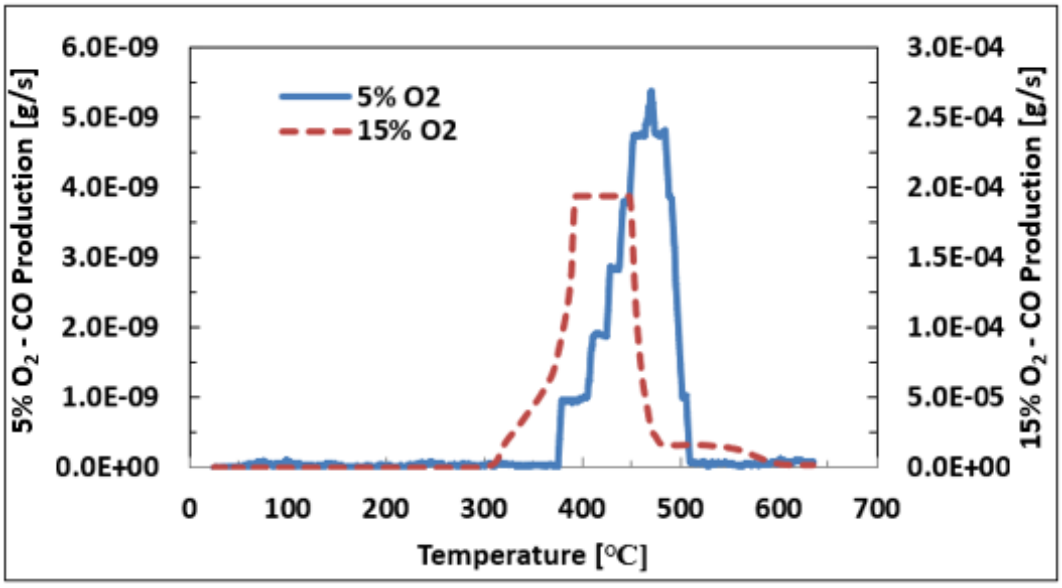

Figure 3-24: CO Production – [CO] for 15% O2 exceeded the upper limit of the detector.

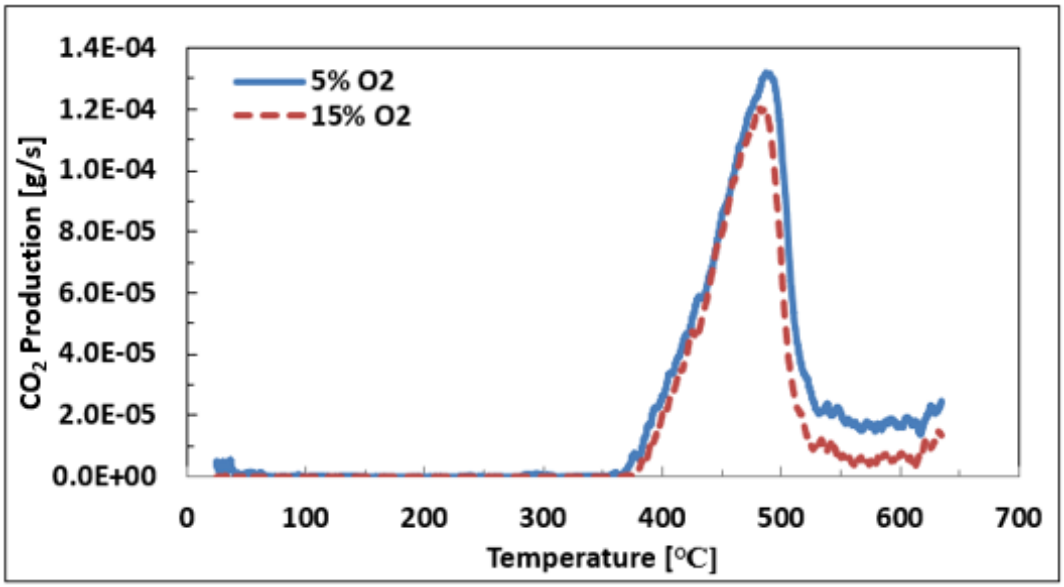

Figure 3-25: CO_2 Production

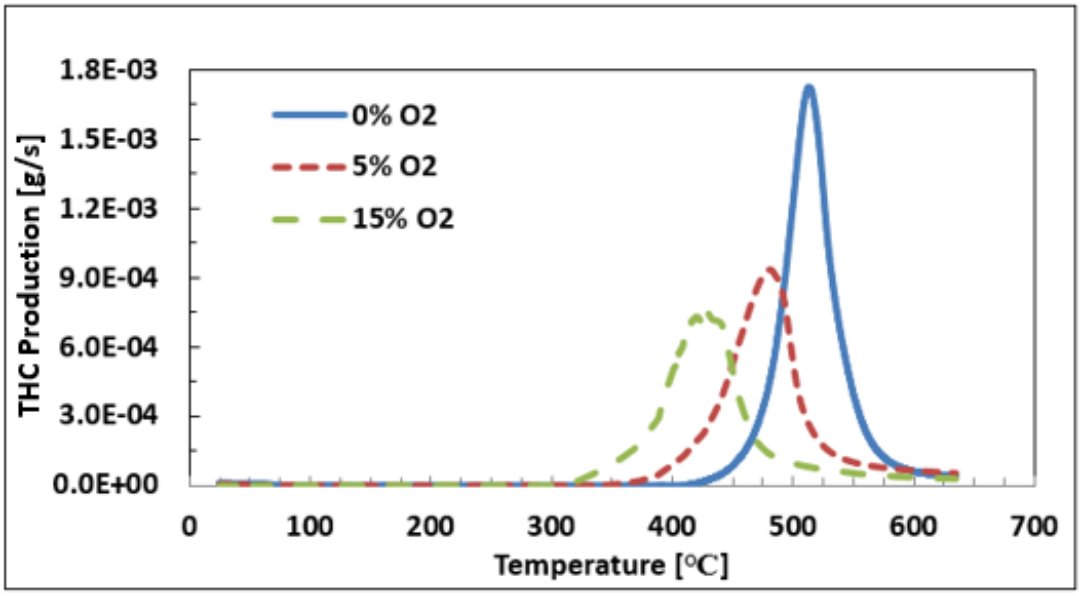

Figure 3-26: Total Hydrocarbon Production

Figure 3-23 above is a plot of the oxygen depletion for the pyrolysis experiments with 5% and 15% O_2. The valleys in the O_2 data sets correspond with the peaks in the CO, CO_2, and THC. These peaks represent the moment that the gas evolution began to wane. The presence of the oxygen enhanced the rate of reaction and is then consumed by converting the alkenes and alkanes into oxygenated hydrocarbons.

Figure 3-24 is a plot of CO production. In 5% O_2 very little CO is produced which explains the step appearance of the curve corresponding with that data set. A significantly larger amount of CO was produced during the 15% O_2 experiment. Unfortunately, the sensor became saturated close to the peak and cut-off the top portion of the data set. A large portion of the curve was still captured.

Figure 3-25 is a plot of CO_2 production for 5% and 15% O_2. The curves are nearly identical but show a decrease in production coinciding with an increase in O_2 concentration. O_2 concentration does not seem to have an enhancing effect on the timing of the CO_2 production like it does on CO and THC production. The decrease in CO2 could be an effect of the oxygen being consumed prior to the kinetics taking place.

Figure 3-26 above is a plot of total hydrocarbon production for all three oxygen concentrations, 0%, 5%, and 15%. The presence of oxygen clearly enhances the evolution of hydrocarbons. Gas analysis by the GC-BID showed the same effects. Increasing O_2 concentration lead to a slight decrease in total hydrocarbon production. The timing of the peak THC evolution was used to establish the sampling criteria for the collection of pyrolyzate by the auto-sampler for the gas analysis in the GC-BID/MS. The goal was to collect nine samples along this production curve and retain a similar form of evolution with the results of the analysis.

To calculate the mass of total hydrocarbons recovered by the analyzers, concentration data was first converted to volumetric flow data by using the system flow of 10 SLPM. This volumetric flow was converted a volume of evolved gas per timestep of the data logged. The data logger recorded data every 1s. Using the density of the given gas being analyzed, the volume per timestep was converted to a mass per timestep. This mass data was then used to calculate a total evolution of mass for a given gas over the course of an analysis. The mass was also used with the known timestep of the data logger to compute the corresponding mass-flow rates, which are presented as mass-loss. Mass-loss data from the THC analysis was combined with the carbon-specific mass

loss data from the CO and CO_2 analyses to compute a broader total hydrocarbon mass-loss. These sets of data for 0%, 5%, and 15% O_2 were normalized by the total mass of recovered hydrocarbons for each case and plotted versus time, seen in **Figure 3-28** of the following section.

Table 3-5 – Recovered Mass Comparison

Recovered Mass, Fraction of Initial Mass			
Gas	0% O_2	5% O_2	15% O_2
CO/CO_2	0.0%	1.1%	3.9%
$THC_{FID} + CO/CO_2$	29.1%	23.3%	24.1%
$THC_{BID} + CO/CO_2$	19.8%	21.7%	28.8%

Table 3-5 contains the mass data recovered from the BID analysis discussed in section 3-1 of this chapter and the mass data recovered from the IR and FID analysis discussed in this section. CO and CO_2 mass data collected by the IR analyzers were included in both mass calculations to give a more complete analysis of the total recovered hydrocarbon mass from each technique. Considering that two different analysis methods were used to obtain the data and different techniques were used to calculate the values for recovered mass, they are in good agreement with each other. A finer integration of the BID data would likely bring the data closer in agreement.

3.3 TGA Results

As a third method of analysis, ~10mg samples of the polypropylene were pyrolyzed using thermogravimetric analysis (TGA) under 100% N_2, 5% O_2, and 15% O_2 at a total flowrate of 50 ml/min ± 2 ml/min. The plot of the TGA experiments is found below in **Figure 3-27**. The presence of O_2 had a profound effect on the reaction rate of the decomposition. The higher the concentration of O_2, the earlier the polymer begins to degrade. Mass data recovered from the CO, CO_2, and THC analysis from the previous section were organized into a mass-loss dataset and normalized. This data is plotted in **Figure 3-28** and resembles the results of the TGA with a few major differences; mainly the temperatures at which decomposition is initiated.

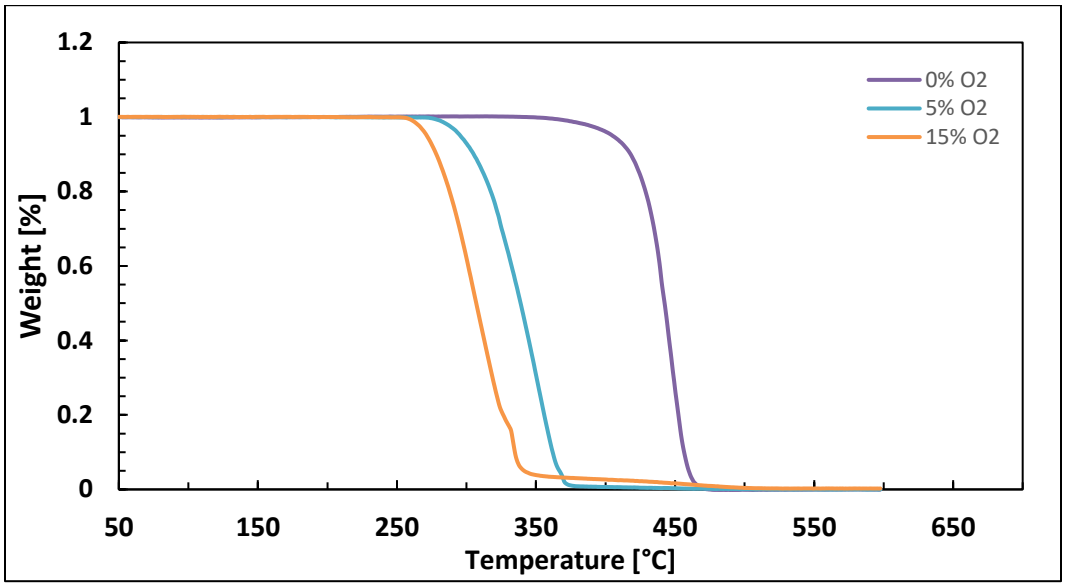

Figure 3-27: TGA Mass Loss

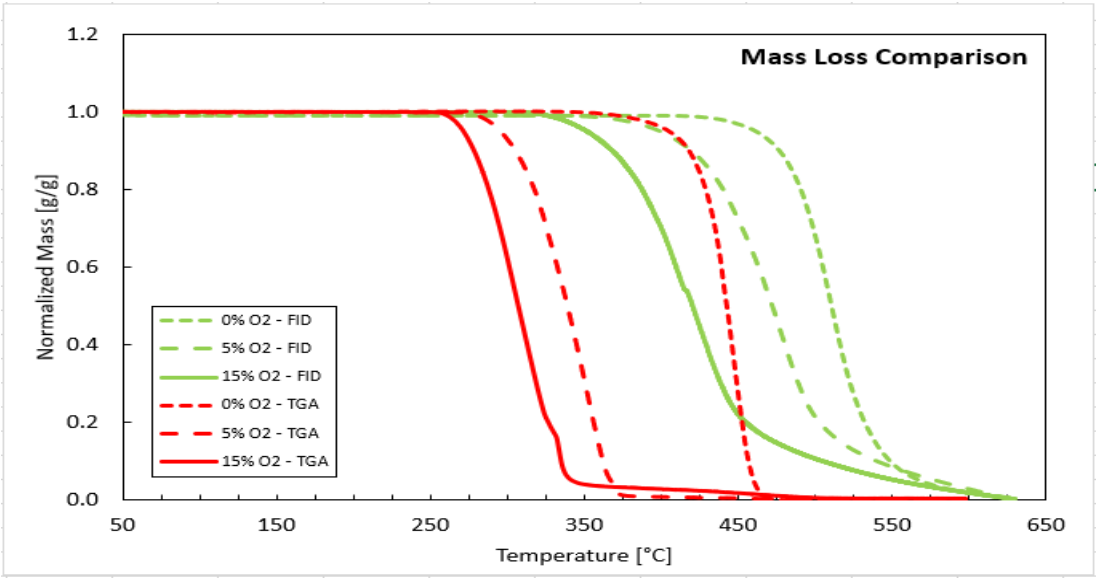

Figure 3-28: TGA and FID Mass Loss Comparison

Table 3-6 – TGA Data Comparison

Mass Loss Fraction	Temperature [°C]							
	0% O_2			5% O_2		15% O_2		21% O_2
	TGA	TGA [1]	FID	TGA	FID	TGA	FID	TGA [8]
5%	400	396*	461	296	400	272	352	248
20%	428		490	317	440	288	387	278
50%	442	441	510	339	472	307	420	307
95%	459	459	566	367	576	341	551	
* data point corresponds to2% mass loss								

In **Table 3-6** the TGA data produced for this investigation is compared to two sets of similar TGA data found in the literature as well as the normalized mass-loss data produced from the IR and FID analysis (ANA). Temperatures correlating to 5%, 20%, 50%, and 95% mass loss are listed in the table for comparison.

The TGA data produced for this investigation at 0% compares almost identically to the data published by Jing and Wen [18]. The low value in their data set was established at 2% mass loss and is compared to a low value of 5% mass loss from the current TGA pyrolysis. The TGA data produced for this investigation at 15% O_2 also compares favorably with the TGA dataset published by Chen et al. for polypropylene pyrolyzed in air [9]. A higher concentration of O_2, 21%, enhances the temperature at which decomposition begins but the rate of decomposition is slower and at 50% the data is identical.

The TGA data produced for this investigation compares favorably to previously published data; however, it does not compare well to the data converted from the IR and FID analyzers. The differences are visibly defined in **Figure 3-28** above. At 0% O_2 there is an average difference of

~80˚C and at 5% and 15% O_2 there is an average difference of 140˚C. This difference isn't unexpected. The pyrolysis experiments were also conducted at different pressures, 1atm for the TGA and ~1.5 atm for the IR/FID. There is no means for direct measurement of mass loss in the pyrolysis conducted in this investigation. Data is converted into a rate of mass-loss, which includes several potential areas for error, mainly that the data only accounts for roughly 20% of the total mass pyrolyzed. Additionally, the mass of the pyrolysis is 500 times larger than the mass of the TGA and the flow of the pyrolysis is 200 times larger than that of the flow of the TGA. When dealing with a new apparatus and method of testing, scale of the experiment is always a factor. Ideally, two experiments of differing scale will produce equivalent data, but it is not always a correct assumption.

Chapter 4: Summary, Conclusions, and Future Work

4.1 Summary of Results

Three methods of pyrolysis and analysis were conducted to gain a better understanding of how oxygen effects the pyrolysis of polypropylene. Gases produced during pyrolysis of polypropylene were collected and analyzed with a GC-BID or sent directly to a stack of IR and FID analyzers. Additionally, polypropylene was pyrolyzed in a TGA apparatus. In all methods of testing and analysis, the effect of oxygen was profound and followed the same trends with increasing concentration.

4.1.1 GC-BID Analysis

In a custom configured flow-reactor, pyrolysis of polypropylene was conducted at three concentrations of O_2: 0%, 5%, and 15%. Three experiments were conducted at 0% O_2, one experiment was conducted at 5% O_2, and three experiments were conducted at 15% O_2. For each experiment nine sample cylinders were filled automatically at specified times with the end purpose of mapping out species evolution during polypropylene degradation. The gas in the nine cylinders was analyzed in a calibrated GC-BID to get mole fractions for all species present. Time and temperature data, also collected during the pyrolysis, were used to convert the data into mass-loss rate for each of the species evolved and eventually a total recovered mass.

At 0% O_2, ethane, propylene, propane, i-butene, n-pentane, and 2-methyl-1-pentene were

identified and quantified. Alkenes and alkanes were the main hydrocarbon groups evolved during the decomposition at 0% O_2 which is consistent with known anaerobic decomposition mechanisms. At 5% and 15% O_2, propylene, propane, i-butene, n-pentane, 2-methyl-1-pentene, acetaldehyde, 2-propenol, acetone, and 2-butenal were identified and quantified. Plots of species mass loss rate vs time and temperature were provided. The creation of new molecules with the addition of oxygen is an exothermic process, one that is observed in the temperature data.

Table 3-1 compares mass fractions of the produced data with several sets of published data. The overall agreement with data from the literature was good. **Table 3-4** is used to calculate the total average recovered mass for all three concentrations of O_2. The resulting mass is feasible based on published data regarding the total mass fraction of hydrocarbons in the range C1-C6. A significant amount of the pyrolyzate went unmeasured do to the measurement range constraint of the column used in the GC-BID analysis. For 0%, 5% and 15% O_2, 19.8%, 21.7%, and 28.8% of the initial sample mass was recovered, respectively. These values are in line with published data discussing the mass fraction of volatile hydrocarbons C1-C6 as part of large product distributions up to C31. The results show that there is a significant amount of chemical reaction taking place.

Oxygen had a profound effect on the time, temperature, and concentration of maximum species production. The temperature at which decomposition initiated and peaked was lower with increasing O_2 concentration. The temperatures of maximum production were 499°C, 443°C, and 428°C respectively for 0%, 5%, and 15% O_2. Concentrations of the originally evolved alkane and alkene species reduced with increasing O_2 concentration.

The pyrolysis reactor and autosampler that were developed specifically for this research performed well. They allowed for the effective creation and collection of pyrolyzate for analysis. The results of the testing did not match very well with the data from the literature, which supports the hypothesis previously stated. The results of the experimentation provide support for the importance of controlling the surface area of the material during pyrolysis. This had not been emphasized in previously published work. In a related manner, the results also provide support for the belief that the interaction between oxygen and the material at the material's surface is significant and important to the overall decomposition of the material.

4.1.2 IR and FID Analysis

Using the same pyrolysis apparatus and technique, polypropylene was pyrolyzed and the resultant gas sent to a stack of IR and FID analyzers for O_2, CO, CO_2, and THC determination. One test was conducted at each O_2 concentration for a total of three tests. Again, the data was converted to mass-loss rate and mass for each species. A total recovered mass was calculated and compared to the findings of the GC-BID analysis for an accuracy check. The two sets of mass data were in reasonable agreement with each other. For all tests, the GC-BID recovered an average of 23.4% of the initial sample mass and the IR/FID recovered an average of 25.5% of the initial sample mass. Again, the results didn't match well with the data from the literature which supports the hypothesis.

4.1.3 Thermogravimetric Analysis

As a third analysis technique, TGA was used to pyrolyze polypropylene and collect mass-loss data. The pyrolysis reactor designed for the subject pyrolysis was not capable of directly measuring the mass-loss, therefore it was calculated. Results from the TGA experiments were compared with two sets of published TGA data and met with great agreement. The results of the TGA were also compared to the calculated results of the IR and FID analysis and had significant differences. At 0% O_2 there was an average difference of ~80˚C for differing levels of percent mass-loss and at 5% and 15% O_2 there was an average difference of 140˚C over the same range of percent mass-loss. There are several explanations for the discrepancy.

The two sets of data were developed in pyrolysis apparatuses of different scale and at different pressures, 1 atm for the TGA and ~1.5 atm for the IR/FID. The mass of the polypropylene is 500 times larger than in the TGA and the flow-rate is 200 times larger than in the TGA. TGA also tracks the mass loss of the total starting polymer mass whereas the subject analysis calculates mass-loss using a fraction of the total mass. Unknown systematic errors do the scale and immaturity of the pyrolysis reactor, sampling system, and analysis techniques could have also contributed.

Most importantly, the surface area is not controlled in thermogravimetric analysis. There is an enormous surface area to volume ratio in TGA and the process of oxidation competes strongly with the process of pyrolysis. As hypothesized in this research, controlling the surface area is very important when studying the pyrolytic decomposition of a material, especially when oxygen is

involved. This is very important and the comparison of the results from the TGA is perhaps the most reinforcing exercise in proving this hypothesis.

4.2 Conclusions

The objective of this thesis was to investigate the role oxygen plays on the pyrolytic decomposition of polypropylene while also observing the effect of a controlled surface area on the pyrolysis. Several methods of analysis were applied and verified with published data to accomplish this objective. The pyrolysis and auto-sampler apparatus that were designed to produce, collect, and deliver pyrolyzate for analysis worked very well.

Oxygen has a profound effect on the pyrolysis of polypropylene. In the results from all three testing and analysis methods, the decrease in the temperature for reaction with increasing oxygen concentration was obvious. In the GC-BID analysis, timing of maximum species production (or polypropylene degradation) was shifted with increasing O_2 concentration because the reactions were initiating at lower temperature (earlier times). The analysis also identified oxygenated hydrocarbons that replaced, through conversion, originally present alkanes and alkenes. Similar results were discovered through the IR and FID analyzers. Again, the temperature at which pyrolyzate production was initiated decreased with increasing O_2 concentration. CO and CO_2 measurements increased with increasing O_2 concentration. In the TGA data, there was a clear increase in the rate of decomposition as the temperature for 5% mass-loss decreased by more than 100˚C from 0% O_2 to 5% O_2.

The information discovered in this research is important to the understanding the effect oxygen had on pyrolysis of polypropylene and polymers in general. Controlling the surface area of a material during pyrolysis appears to have a critical effect on the overall decomposition. Oxygen cannot always be ignored in modeling and the reaction of the oxygen at the surface is important to consider. The surface reaction may be more important than previously thought by the research community.

Knowledge gained can be used to further develop the subject test method that, on a larger scale, can track the production and conversion of species as they change with oxygen concentration. This information can also be used to enhance kinetic models used to predict polymer degradation and gas evolution on a molecular level. The data produced highlights potential deficiencies in current understanding of oxygen on pyrolytic decomposition. The research shows a potentially important phenomena taking place. A precise model could improve efficiencies in the development of fire retardants, modeling of fires, and methods for recycling polymers or converting them to fuels.

4.3 Future Work

The findings of this study only identified a portion of the total products evolved and because of this had a limited, but useful, view into the effect of oxygen on the pyrolysis of polypropylene. Equipment, temperature, and time constraints limited the scope of the work to focus on a smaller portion of the evolved products of the pyrolysis. With more time, a more

thorough investigation into all hydrocarbon products evolved during the pyrolysis is feasible, the equipment exists.

Conducting multiple pyrolysis experiments at a given oxygen concentration and varying the sampling time would allow for a more complete species evolution curve. A curve like this would allow for better fitting, more accurate integration, and thus more accurate measurement of recovered mass. Knowledge of anticipated species would allow for the targeted calibration of a GC column, allowing for more accurate conversion of area counts into mole fractions. Very low concentrations of calibration gases should be used for a future calibration of a system attempting to resolve species on the scale described in this research.

A more thorough investigation into how species evolution data can be applied to the development or improvement of an analytical model to better model fire growth would be beneficial to the research community. Determining the deficiencies in existing models and targeting future research to improve these deficiencies would be an efficient path to improvement.

The apparatus can be investigated for improvements and optimized to make the ~3hr long pyrolysis test more efficient. A method for collecting oils and waxes, which obviously weren't accounted for in this study, would promote a more complete analysis of all species produced during the pyrolysis. Obviously, this research can be extended to additional polymers with the data being compared to published data in literature to continue the validation of the apparatus and method.

The difference in the results of the FID data and the TGA data should be further investigated. With a more well-defined scope for the testing and analysis, a lot could be learned

about the two methods. It is possible that TGA is not the best method for researching the effect of oxygen on pyrolytic decomposition due to the large surface to volume ratio.

Chapter 5: Appendix

5.1 Boat Characterization

5.1.1 Temperature

Nine thermocouples (TCs) were welded at different locations along the length of the machined stainless-steel boat. These TCs were used the collect temperature data to characterize the temperature distribution along the surface of the boat during a test.

Two trials were conducted with the TCs welded in different configurations to provide a more thorough analysis. In the first trial, the TCs were all welded with even spacing down the centerline of the boat. In the second trial, the TCs we welded in a lateral configuration, providing temperature data closer to the outer edges of the boat windows.

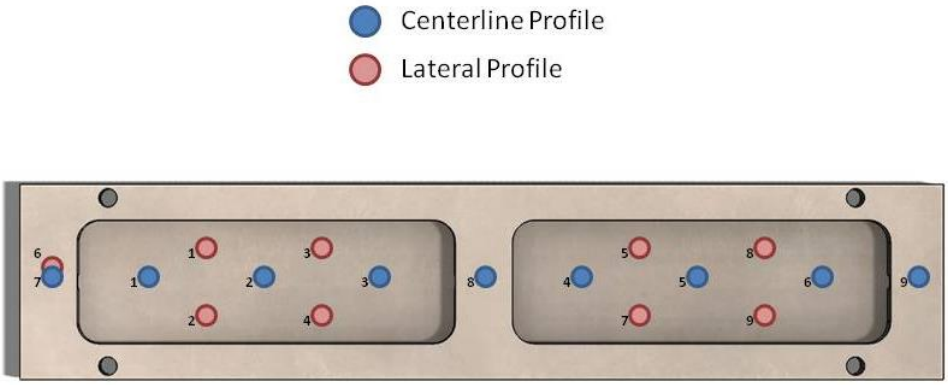

Figure 5-1: Locations of Welded TCs for Temperature Characterization

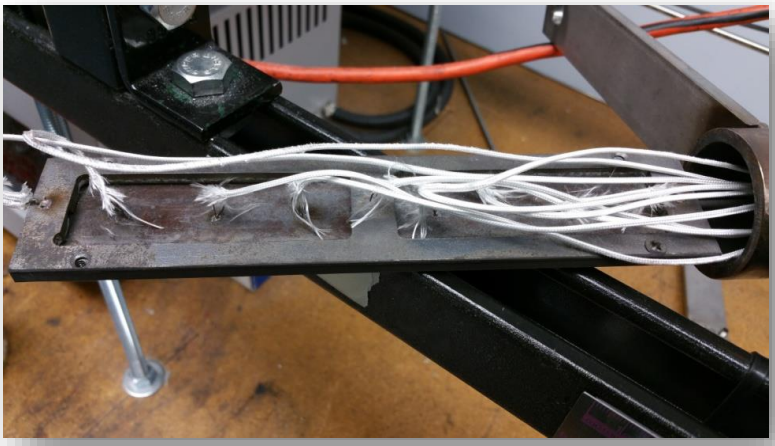

Figure 5-2: Image of Centerline Arrangements

Figure 5-3: Image of Lateral Arrangement

The boat was inserted into the furnace and sealed. A flow of 10 SLPM of air was established. The temperature controller on the furnace was set to ramp at 3℃/min up to 700℃. Temperature data that was collected was isolated and averaged for each test. Table 5-1 and Table 5-2 below provide the standard deviation results from the two trials.

Table 5-1 - Avg and Max Standard Deviations from the Centerline Trial

Centerline Arrangement				
All	Front Window	Read Window	Cover Plate	
(TC1-TC9)	(TC1-TC3)	(TC4-TC6)	(TC7-TC9)	
5.39	1.43	3.53	8.26	Avg. Std. Dev. [°C]
8.07	3.55	5.11	12.30	Max. Std. Dev. [°C]

Table 5-2 - Avg and Max Standard Deviations from the Lateral Trial

Lateral Arrangement			
All	Front Window	Rear Window	
(TC1-TC9)	(TC1-TC4)	(TC5, TC7-TC9)	
3.08	1.65	4.42	Avg. Std. Dev. [°C]
6.23	3.09	9.30	Max. Std. Dev. [°C]

The data provides that the average standard deviation in temperature measurement for both boat windows is <5℃, the desired limit of characterization.

Two main effects could have resulted in error in these data sets. The wires from the TCs provided disruption in the flow and could have caused turbulence in an otherwise laminar flow. The TCs were individually hand welded to the stainless-steel surface. Differences in weld quality could have led to differences in temperature data.

5.1.2 Uniform Melt

A uniform melt of the polypropylene inside the sample boat is important to a controlled surface area analysis. It is important that during pyrolysis the material decomposes evenly with a controlled and constant surface area for incident gases to react.

The sample boat was loaded with a sheet of polypropylene and sealed inside the furnace. A flow was set to 10 SLPM and the temperature controller on the furnace was set to heat at 10℃/min up to 700℃. The higher heating rate was used to conserve resources and was considered a worst-case scenario for achieving uniform melt. Temperature data from the sample boat was recorded and monitored.

Two tests were conducted. In one test the boat was removed when the temperature in the boat reached 200℃ and 375℃. Those temperatures were chosen arbitrarily at points above the melting point of polypropylene, ~130℃. In the second test, the boat was removed when the temperature within it reached 500℃. This temperature was observed to be the point of maximum

production of CO, CO_2, and THC as well as maximum depletion of O_2 in an early analysis.

In all cases, the boat was removed and observed for melt uniformity. Photos were taken at that point if material remained in the boat. These images can be seen below.

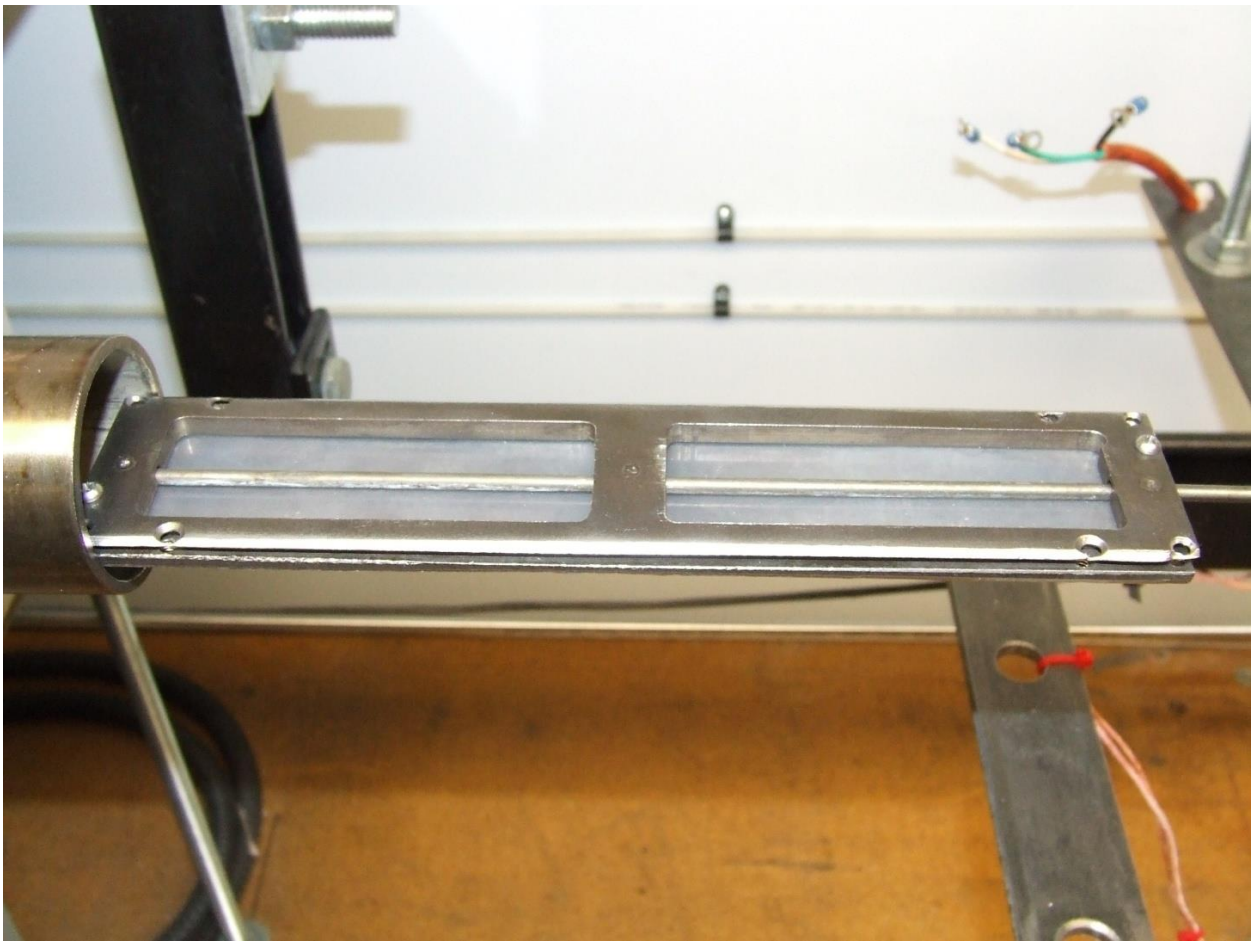

Figure 5-4: Polypropylene Sample Prior to Pyrolysis

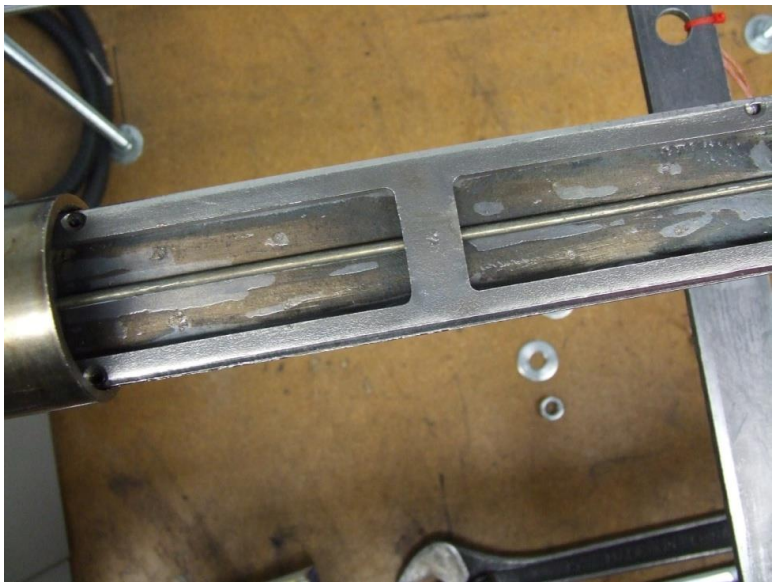

Figure 5-5: Softened Polypropylene After Removal at 200°C

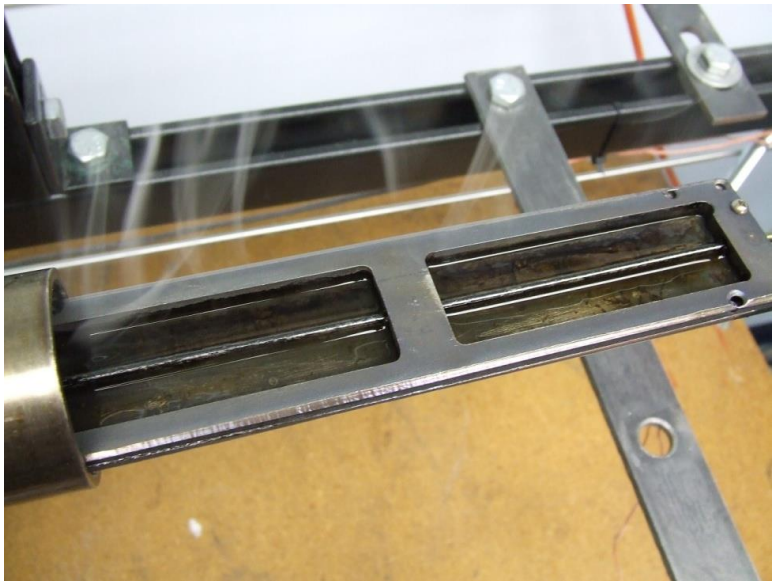

Figure 5-6: Liquified Polypropylene after Removal at 375°C

When the boat was removed at 500°C there was no material left in the boat, so no photograph was taken. The results of the visual check on liquification proved that the material was decomposing uniformly within the boat.

5.1.3 Reactor flow rate consideration

Many factors were considered when selecting the appropriate flow-rate to administer into the reactor during the pyrolysis. The most important of which was the effect of flow on the temperature ramp rate of the reactor. Like the boat temperature characterization procedure, thermocouples were welded at points inside the two windows of the sample boat. The boat was set in the reactor, sealed, and programmed to heat at 3°C/min up to 700°C. Prior to initializing the furnace, a flow rate or air was established at 5, 10, 15, or 25 SLPM.

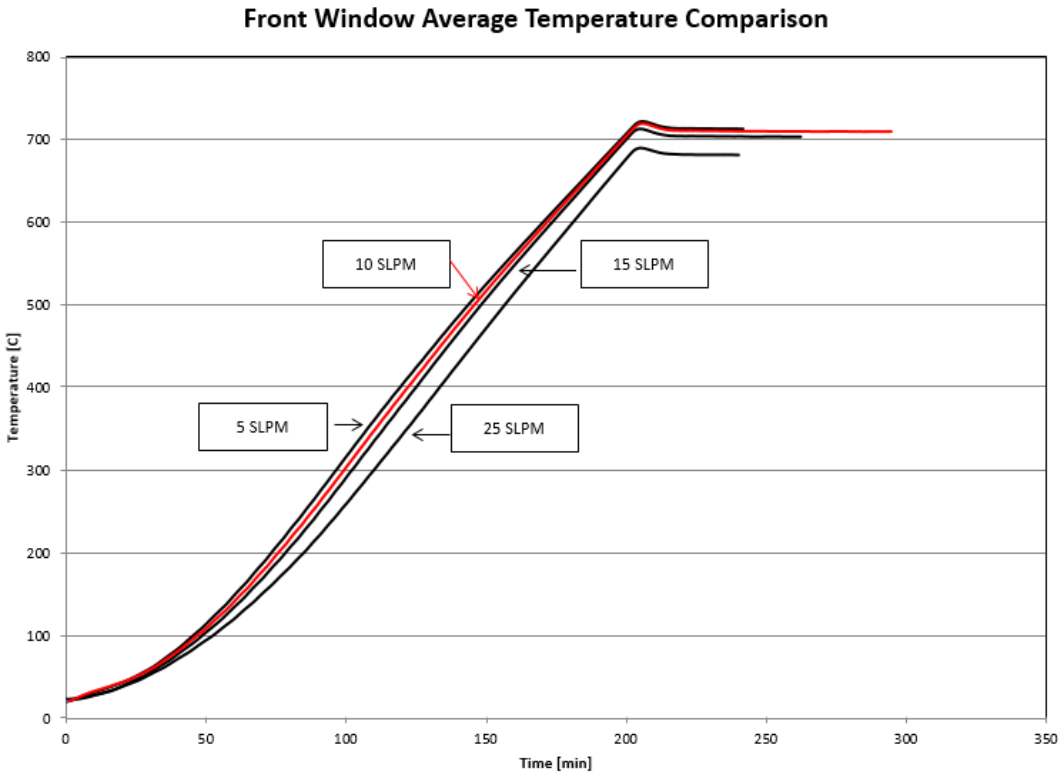

Figure 5-7: Temperature Remping Profiles

The analysis shows that the flowrate does indeed affect the temperature profile of the boat throughout the duration of a test. At 5 SLPM and 25 SLPM the boat seemed to heat up too quickly or too slowly, respectively, and non-linearly. The other main considerations when selecting the flow were dilution effects and final sample volume and pressure. A flowrate of 10 SLPM provided a very linear temperature profile, enough resulting pyrolyzate to meet the requirements of the analysis, and a level of reduced dilution less than that at 15 SLPM.

5.1.4 Boat location consideration

Several tests were conducted to determine the most appropriate location of the sample boat, linearly within the furnace tube, that would reduce the gradient causing effect of the inlet gas stream. Thermocouples were welded to the surfaces of the boat and, in conjunction with the multi-point thermocouple, were used to develop temperature profiles at different distances into the furnace and at different flowrates (5, 10, 15, and 25 SLPM). Flowrates also influenced system pressure and sample collection and thusly factored in to the determination. Figure 5-8, below, provides a view of the sample boat at the determined location within the furnace.

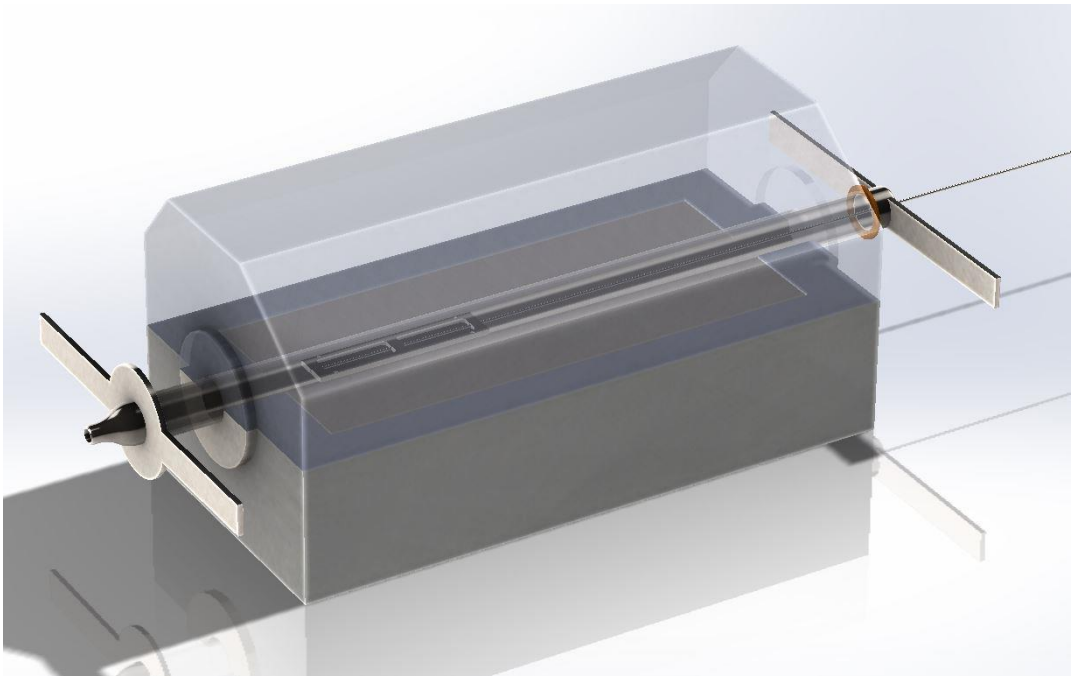

Figure 5-8: Location of Sample Boat Within Tube Furnace

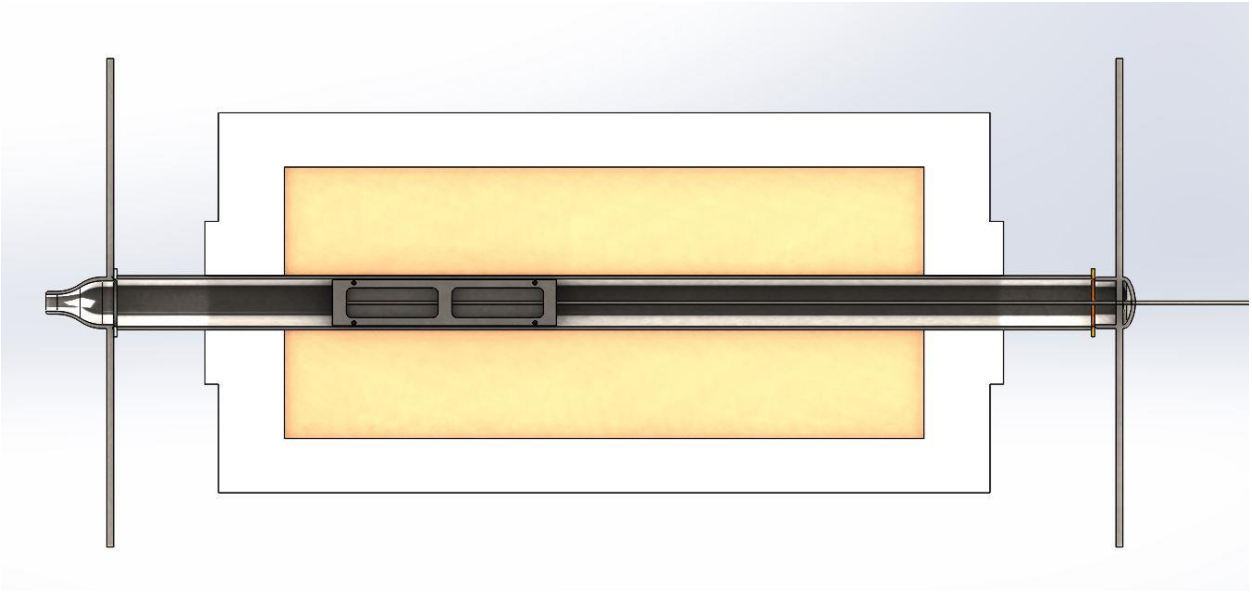

Figure 5-9: Location of Sample Boat – Bird's Eye

5.1.5 Analyzer Time Response

Roughly 20' of tubing separated the pyrolysis reactor from the IR analyzer stack. Due to the distance of separation, characterizing the time response of the analyzers was important to counter-act any delay between the production of the gas in the reactor and the sensing of the gas at the analyzers.

Calibration gases are used to calibrate the CO, CO_2, THC, and O_2 analyzers. The span levels for the calibrations were 90ppm CO, 19% CO_2, 4.5% CH_4, and 20.6% O_2 respectively.

A ¼" stainless steel tube was inserted into the stainless-steel furnace tube, with the outlet

located ¾ of the way down the length of the heated section of the tube. This position would line-up with the center of the sample boat, had the sample boat been loaded into the furnace.

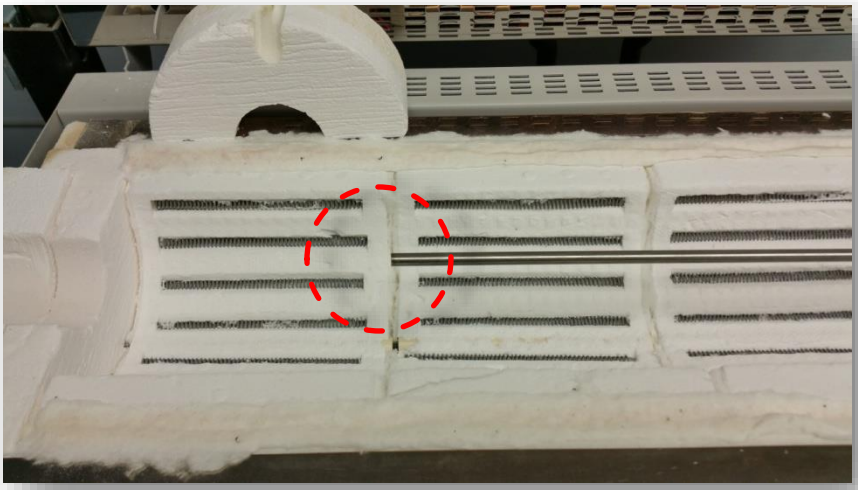

Figure 5-10: Mock-up of Injection Tube Location (w/o Furnace Tube)

Using calibrated rotameters, known concentrations of the calibration gases were injected into the pyrolysis reactor at a total rate equivalent to that of a normal pyrolysis test. Time constants were developed as separate tests were conducted for all 4 calibration gases. At t=0s, the logging of concentration data from the analyzers was initiated. At t=20s, the calibration gases were introduced into the furnace. The gas would flow until a steady state measurement of concentration was reached at the specific gas analyzer.

Three tests were conducted for each analyzer and the concentration data for each was

averaged. d[gas]/dt was calculated for every data point. A threshold rate of change in concentration of 1% was established. A value, τ transport, was calculated and defined as the time necessary to reach a 1% rate of change in the concentration from the initial injection. This represents the time from when the gas is injected into the reactor to when the analyzer reads a value that represents a 1% rate of change in concentration. A second value, τ steady-state, was calculated and defined as the time necessary to reach a 63% rate of change in the concentration from the initial injection. This represents the time from when the gas is injected into the reactor to when the analyzer reads a value that represents a 63% rate of change in concentration. A third value, τ response, is the difference between τ steady-state and τ transport. This represents the time from when the analyzer notices a gas to when that gas has reached a steady-state concentration.

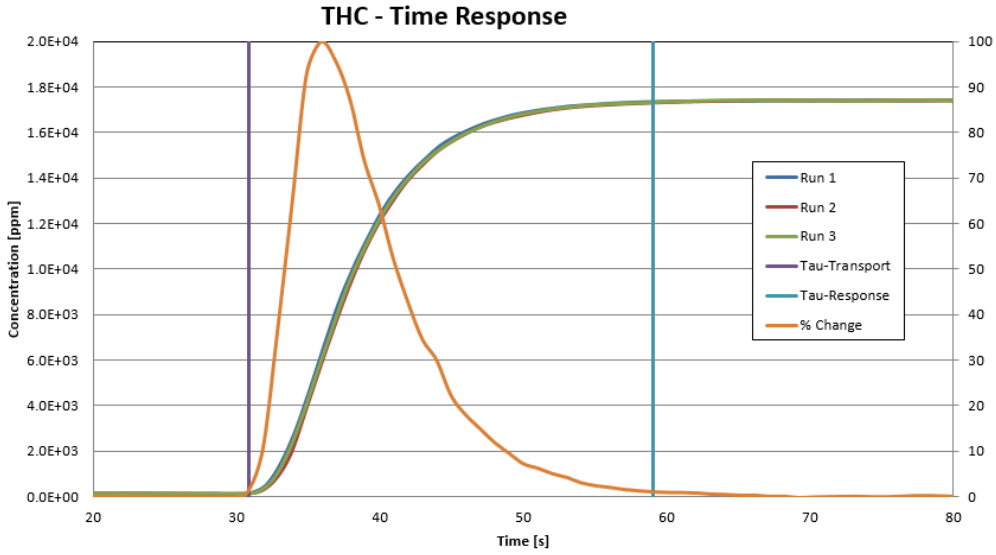

Figure 5-11: The Characterization of Time Constants

Gas	τ_trans [s]	τ_absorption [s]
O_2	10 ± 0.2	2.5 ± 0.5
CO	8.6 ± 0.6	3.5 ± 0.5
CO_2	37.6 ± 0.6	4.0 ± 0.0
THC	7.9 ± 0.2	1.0 ± 0.0

Figure 5-12: Time Constants for 10 SLPM

It takes roughly 10-40 seconds for a gas produced within the reactor to be measured by an appropriate analyzer. Figure 5-12, contains this data. These values are well within the time tolerances of the pyrolysis experiments that are conducted over almost 3 hours.

5.1.6 Concentration Validation

During the same tests used to determine the time delay of the analyzers, the measured concentrations of the gases were compared to the theoretical concentrations to determine the validity of the measurement. Flow of calibration gases were established at 1, 1.5, and 2 SLPM and balanced with nitrogen to make-up a combined 10 SLPM of gas. Using the calibrated flowrates and precise concentrations of the calibration gases, equivalent concentrations were calculated. The table below compares the theoretical values with the measured values.

Gas	Calibration Gas	Flow Rate	Theoretical Concentration	Measured Concentration	Units	1-(MC/TC)
O_2	20.6% O_2, bal. N_2	1.0 SLPM	2.06	2.05	%	0.49%
		1.5 SLPM	3.09	3.01	%	2.59%
		2.0 SLPM	4.12	3.96	%	3.88%
CO	9 % CO, 19% CO_2 bal. N2	1.0 SLPM	0.9	0.91	%	-1.11%
		2.0 SLPM	1.8	1.72	%	4.44%
CO_2	9 % CO, 19% CO_2 bal. N2	1.0 SLPM	1.9	1.91	%	-0.53%
		2.0 SLPM	3.8	3.89	%	-2.37%
THC	4.63% CH_4, bal. N_2	1.0 SLPM	4600	4867	ppm	-5.80%
		2.0 SLPM	9300	9160	ppm	1.51%

Figure 5-13: Comparison of Measure vs Theoretical Concentrations

All the measured concentrations are within 6% of the calculated theoretical concentrations. These values represent the systematic error of the measurements and are within the tolerances of the analysis.

5.2 Plots

5.2.1 0% O_2 – Species Production vs Time

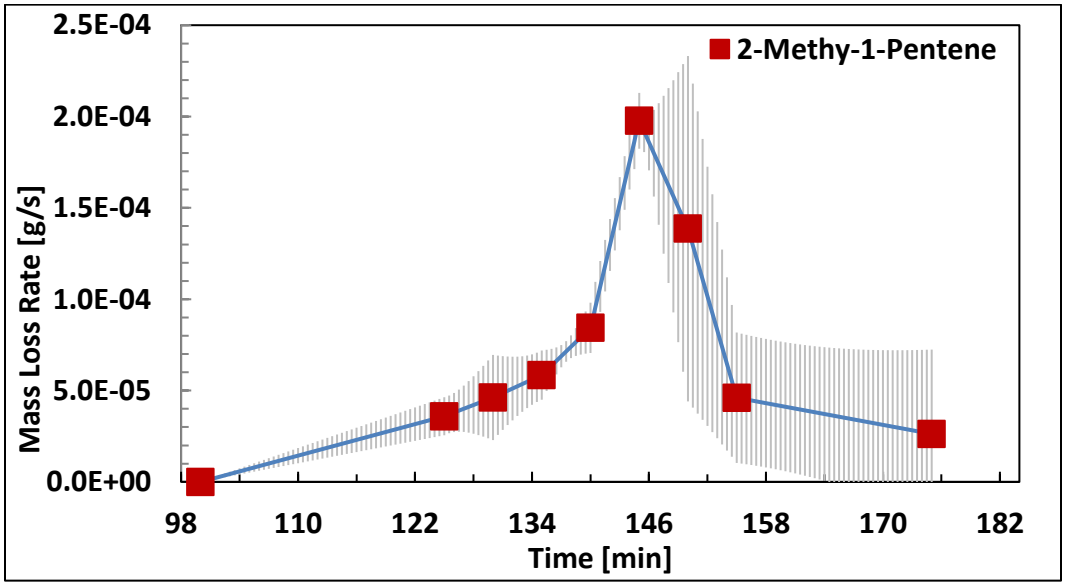

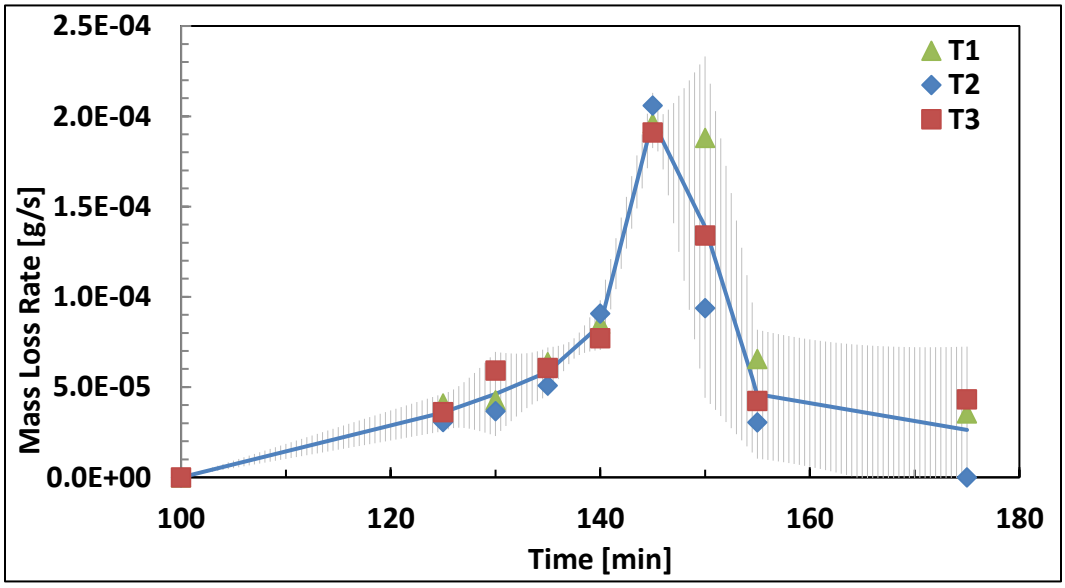

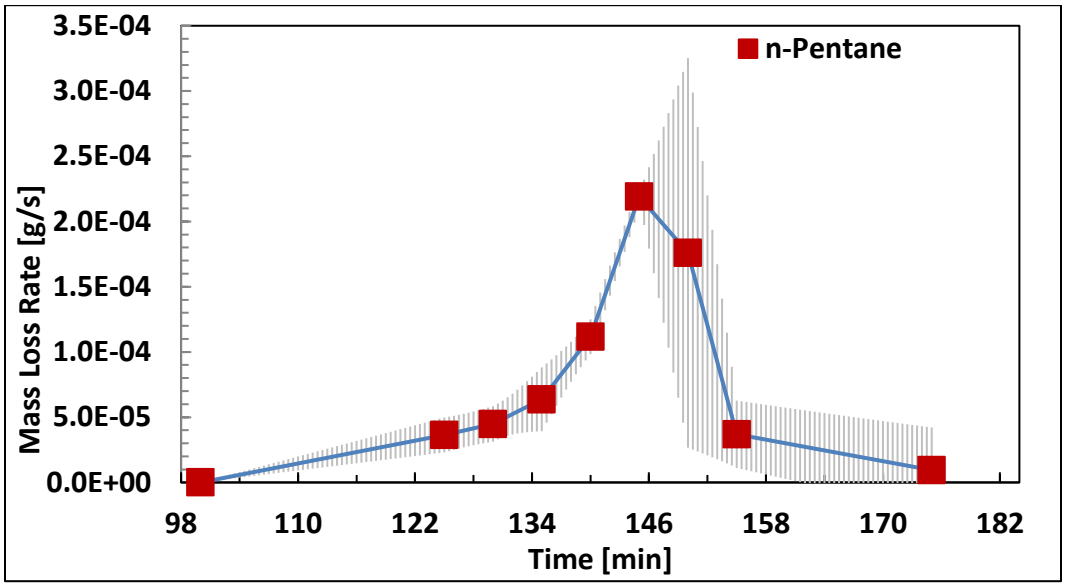
3.5E-04
3.0E-04
2.5E-04
2.0E-04
1.5E-04
1.0E-04
5.0E-05
0.0E+00
Mass Loss Rate [g/s]
n-Pentane
98
110
122
134
146
158
170
182
Time [min]

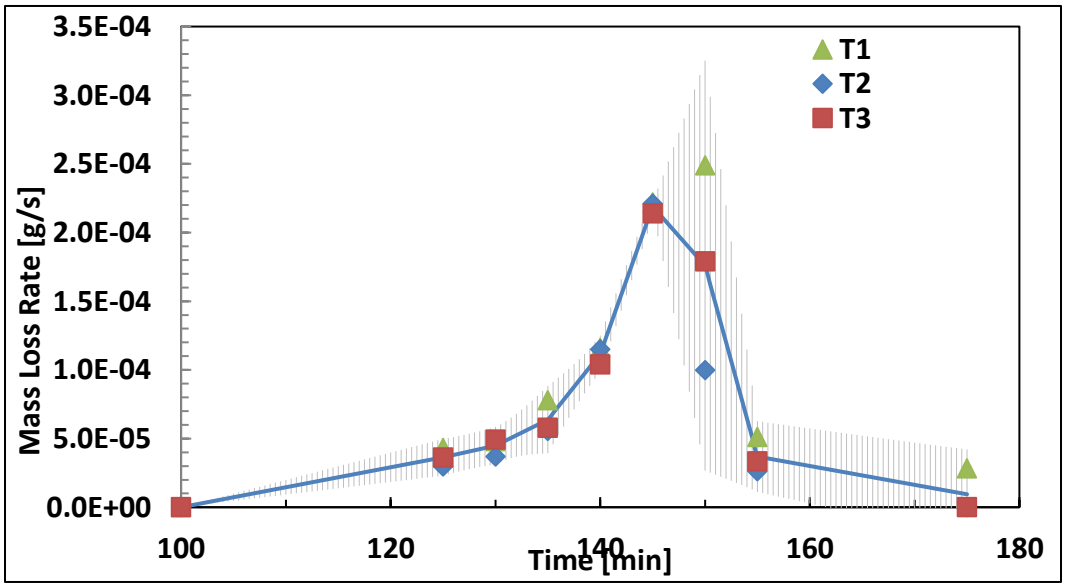
3.5E-04
3.0E-04
2.5E-04
2.0E-04
1.5E-04
1.0E-04
5.0E-05
0.0E+00
Mass Loss Rate [g/s]
T1
T2
T3
100
120
140
160
180
Time [min]

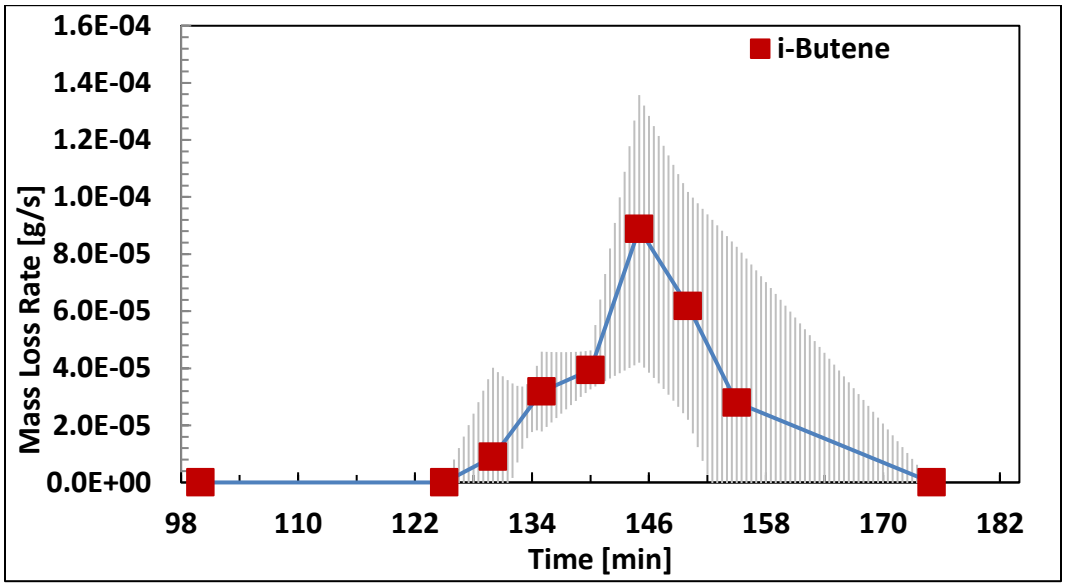
1.6E-04
1.4E-04
1.2E-04
1.0E-04
8.0E-05
6.0E-05
4.0E-05
2.0E-05
0.0E+00
Mass Loss Rate [g/s]
i-Butene
98
110
122
134
146
158
170
182
Time [min]

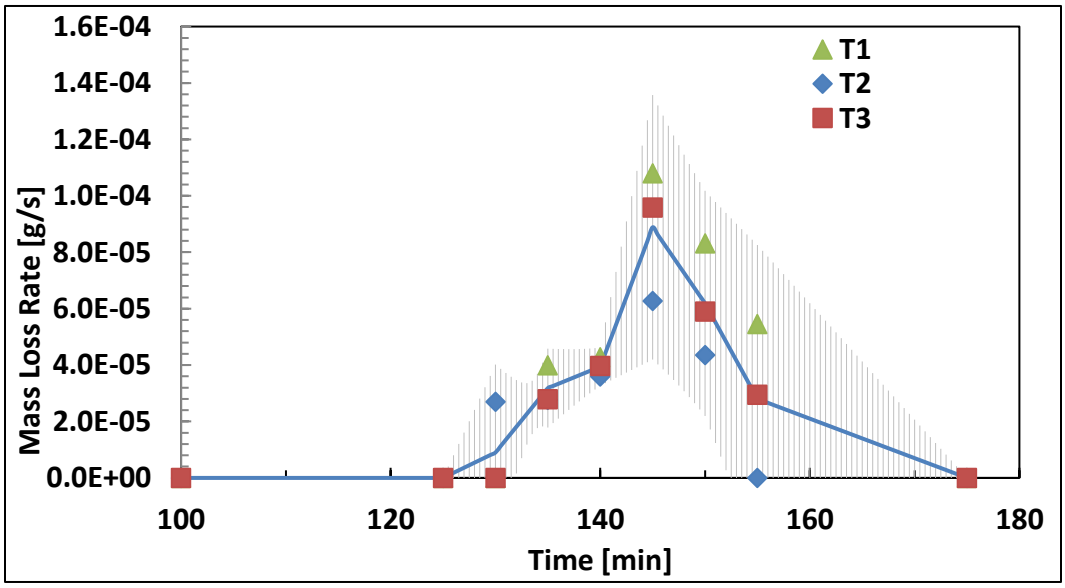
1.6E-04
1.4E-04
1.2E-04
1.0E-04
8.0E-05
6.0E-05
4.0E-05
2.0E-05
0.0E+00
Mass Loss Rate [g/s]
T1
T2
T3
100
120
140
160
180
Time [min]

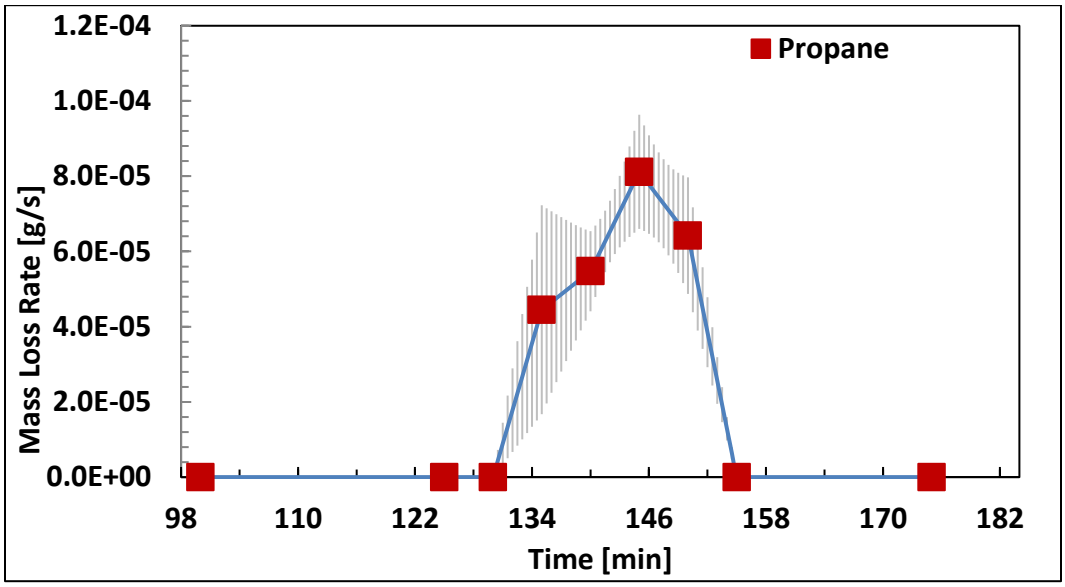
1.2E-04
1.0E-04
8.0E-05
6.0E-05
4.0E-05
2.0E-05
0.0E+00
Mass Loss Rate [g/s]
Propane
98
110
122
134
146
158
170
182
Time [min]

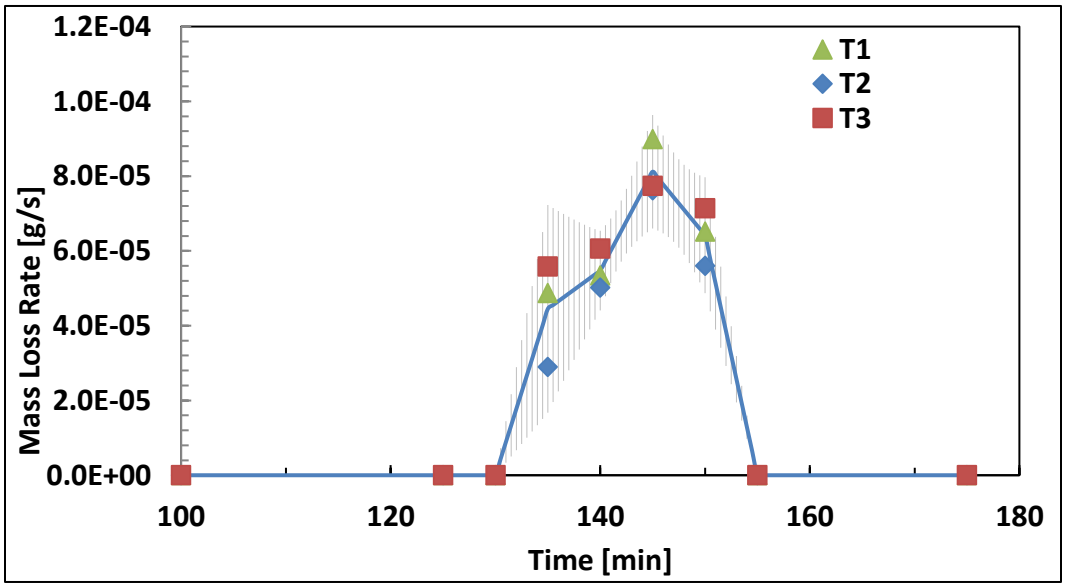
1.2E-04
1.0E-04
8.0E-05
6.0E-05
4.0E-05
2.0E-05
0.0E+00
Mass Loss Rate [g/s]
T1
T2
T3
100
120
140
160
180
Time [min]

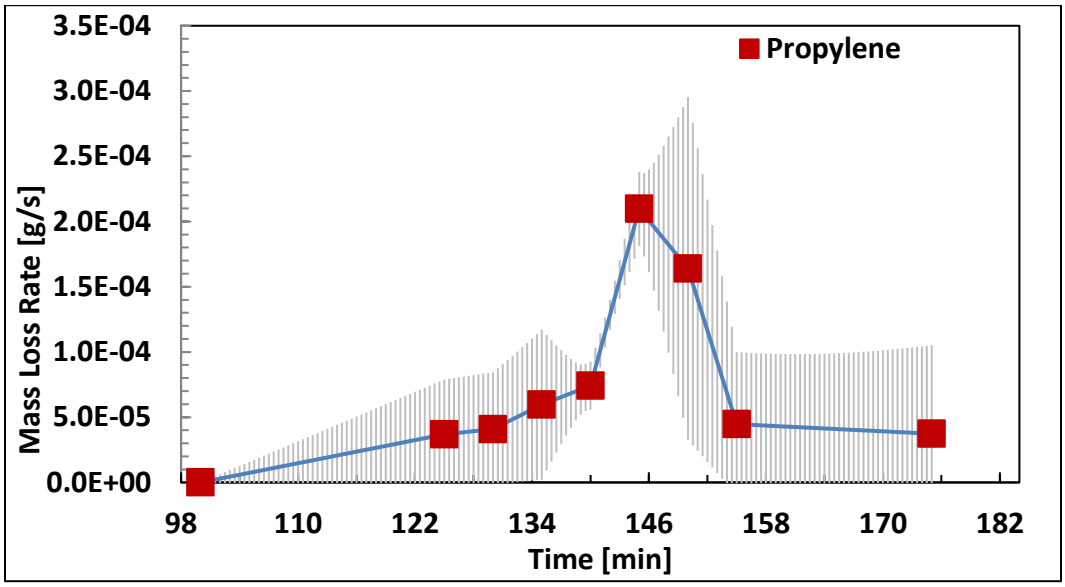
3.5E-04
3.0E-04
2.5E-04
2.0E-04
1.5E-04
1.0E-04
5.0E-05
0.0E+00
Mass Loss Rate [g/s]
Propylene
98
110
122
134
146
158
170
182
Time [min]

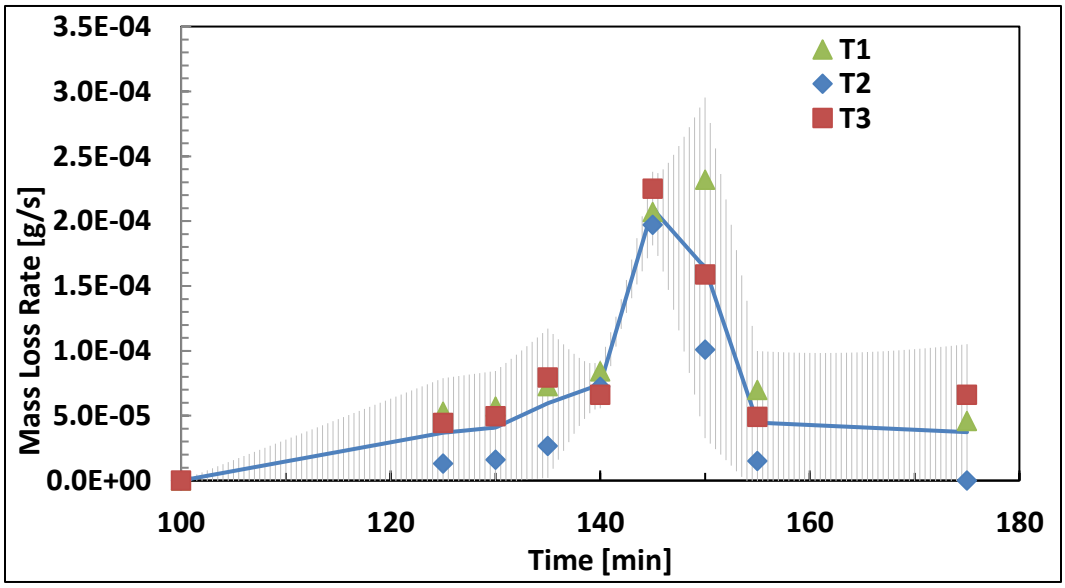
3.5E-04
3.0E-04
2.5E-04
2.0E-04
1.5E-04
1.0E-04
5.0E-05
0.0E+00
Mass Loss Rate [g/s]
T1
T2
T3
100
120
140
160
180
Time [min]

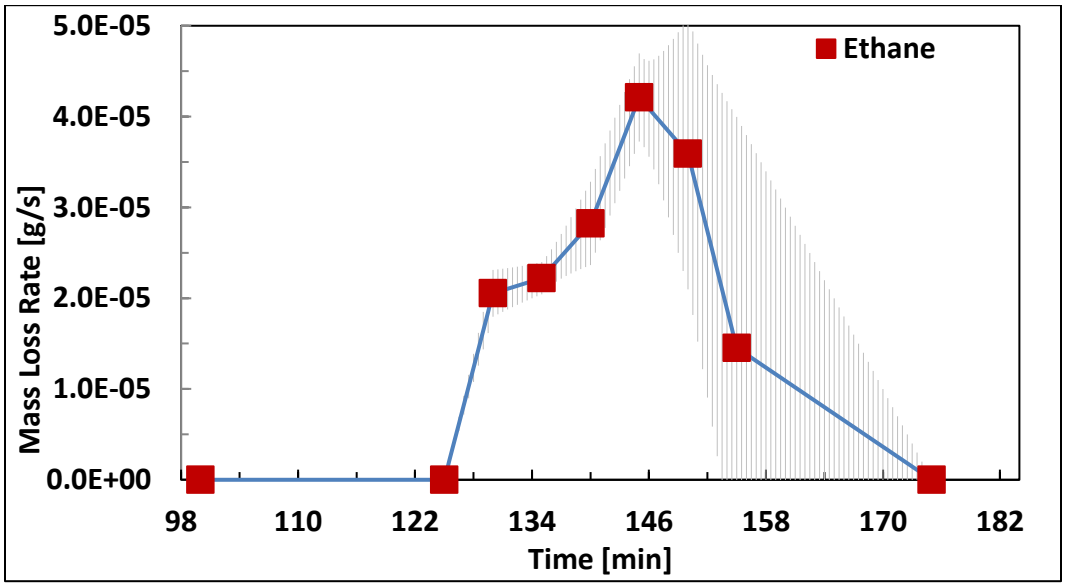
5.0E-05
4.0E-05
3.0E-05
2.0E-05
1.0E-05
0.0E+00
Mass Loss Rate [g/s]
Ethane
98
110
122
134
146
158
170
182
Time [min]

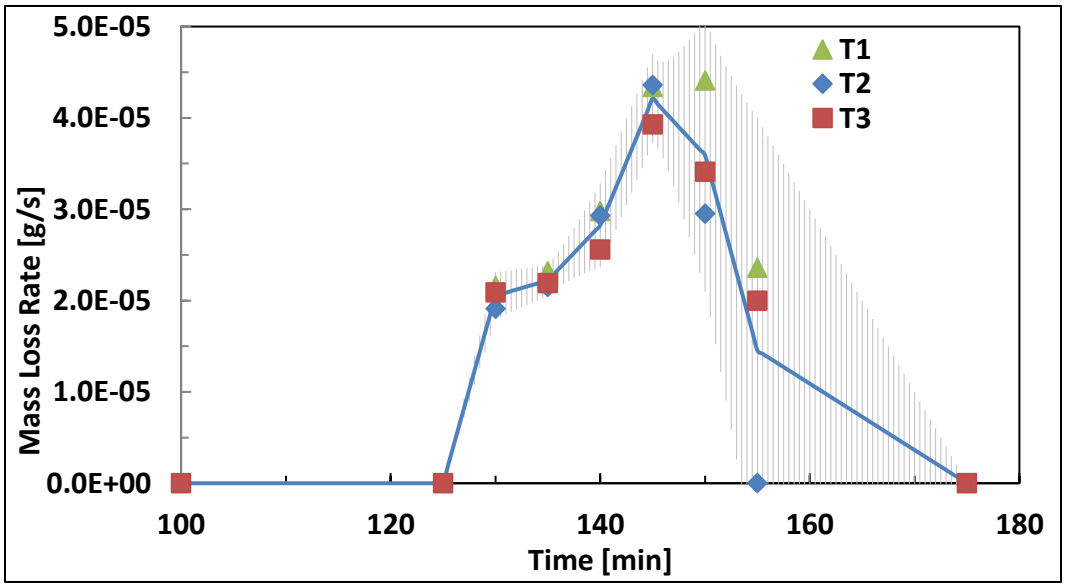
5.0E-05
4.0E-05
3.0E-05
2.0E-05
1.0E-05
0.0E+00
Mass Loss Rate [g/s]
T1
T2
T3
100
120
140
160
180
Time [min]

5.2.2 5% O_2 – Species Production vs Time

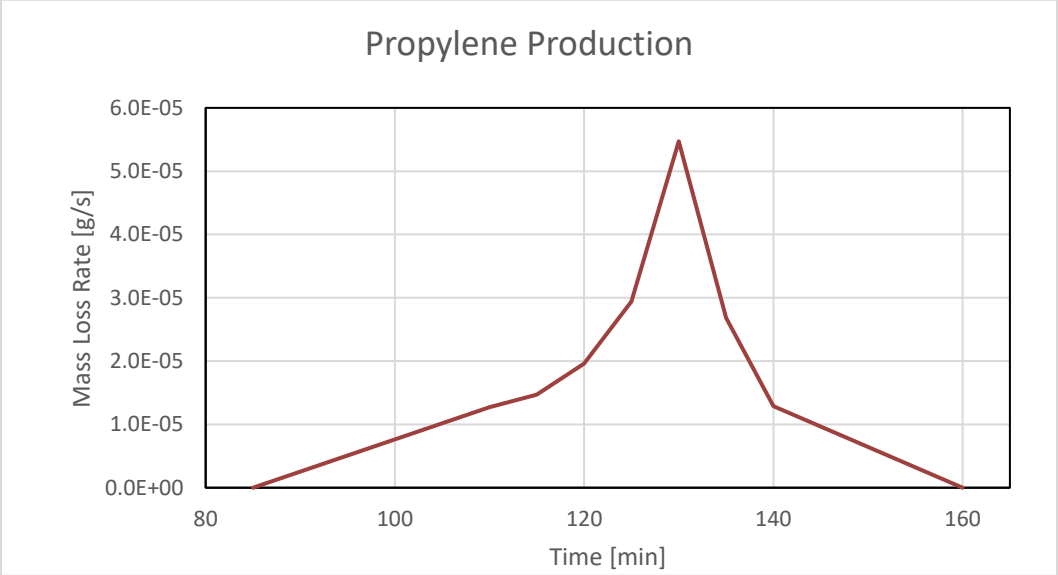

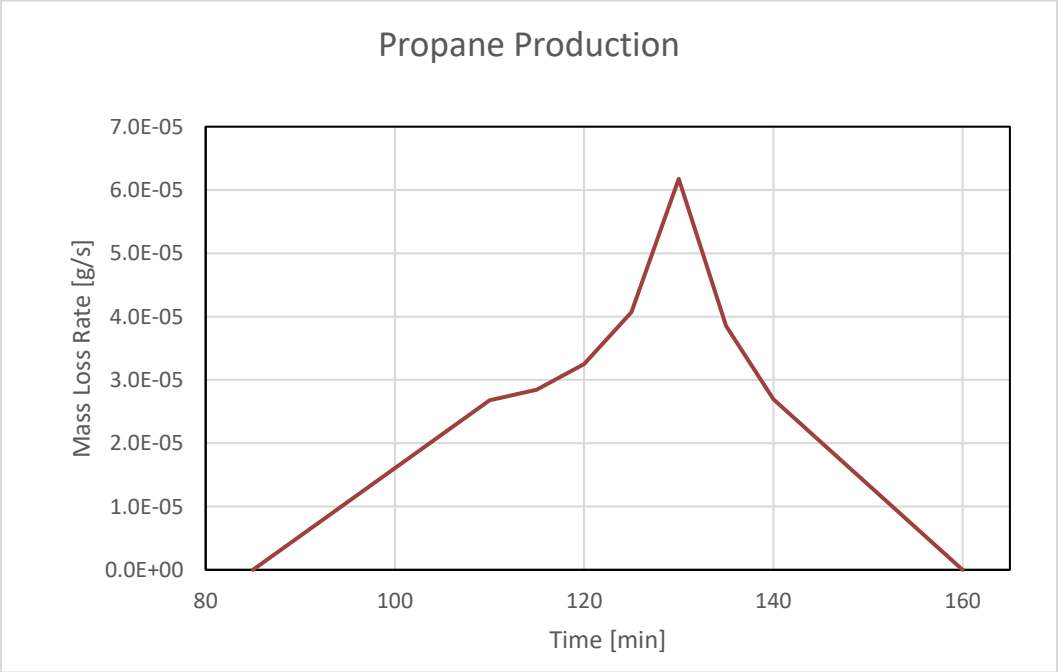

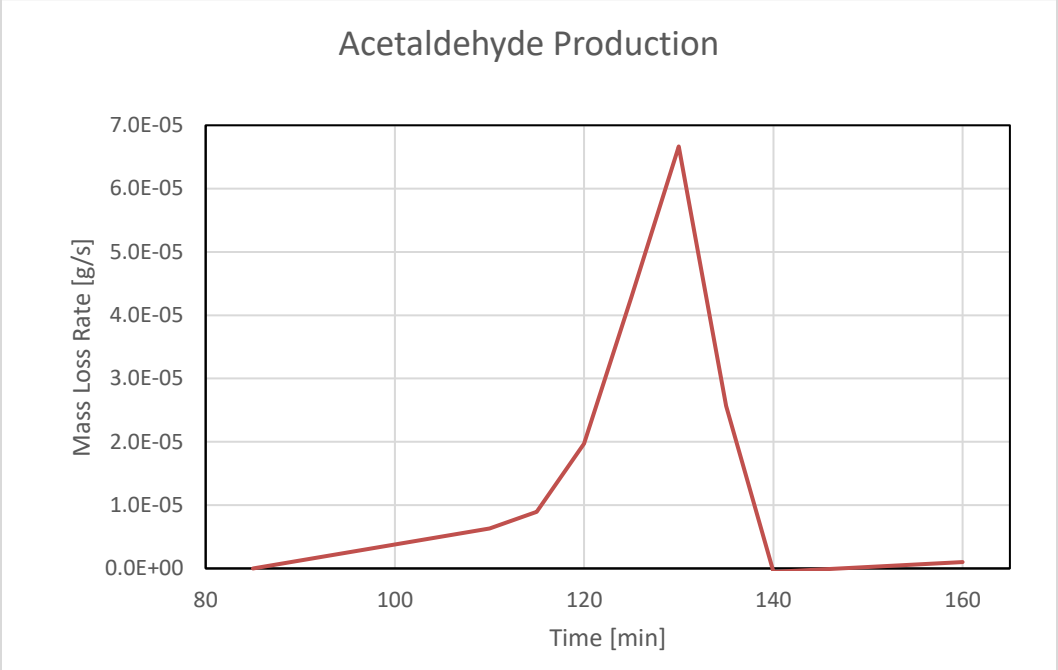
Acetaldehyde Production
Mass Loss Rate [g/s]
7.0E-05
6.0E-05
5.0E-05
4.0E-05
3.0E-05
2.0E-05
1.0E-05
0.0E+00
80
100
120
140
160
Time [min]

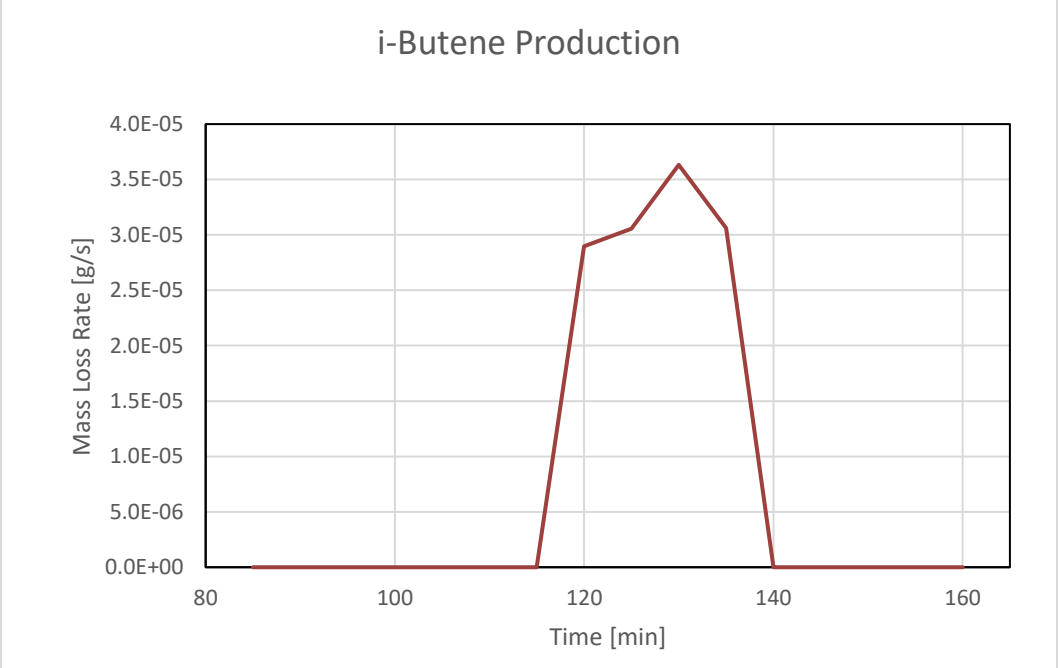
i-Butene Production
Mass Loss Rate [g/s]
4.0E-05
3.5E-05
3.0E-05
2.5E-05
2.0E-05
1.5E-05
1.0E-05
5.0E-06
0.0E+00
80
100
120
140
160
Time [min]

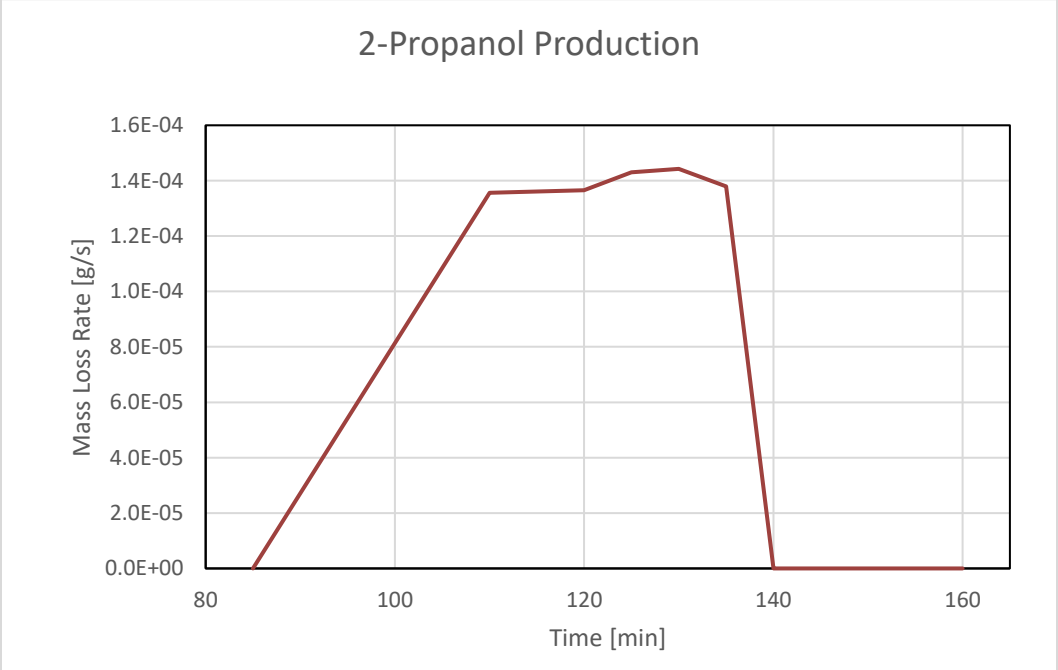
2-Propanol Production
Mass Loss Rate [g/s]
1.6E-04
1.4E-04
1.2E-04
1.0E-04
8.0E-05
6.0E-05
4.0E-05
2.0E-05
0.0E+00
80
100
120
140
160
Time [min]

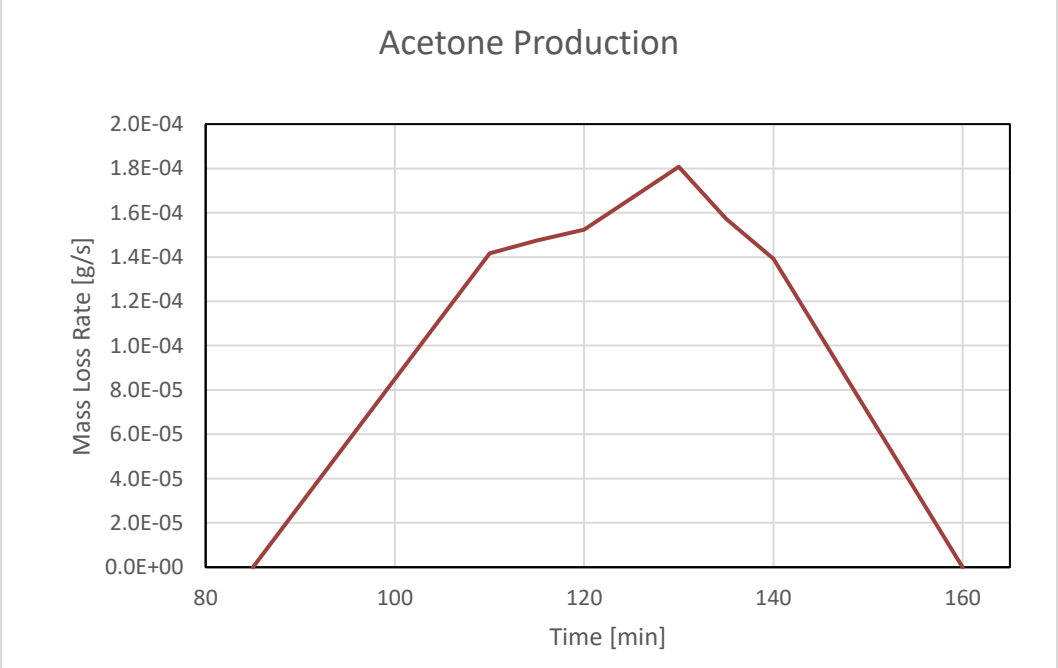
Acetone Production
Mass Loss Rate [g/s]
2.0E-04
1.8E-04
1.6E-04
1.4E-04
1.2E-04
1.0E-04
8.0E-05
6.0E-05
4.0E-05
2.0E-05
0.0E+00
80
100
120
140
160
Time [min]

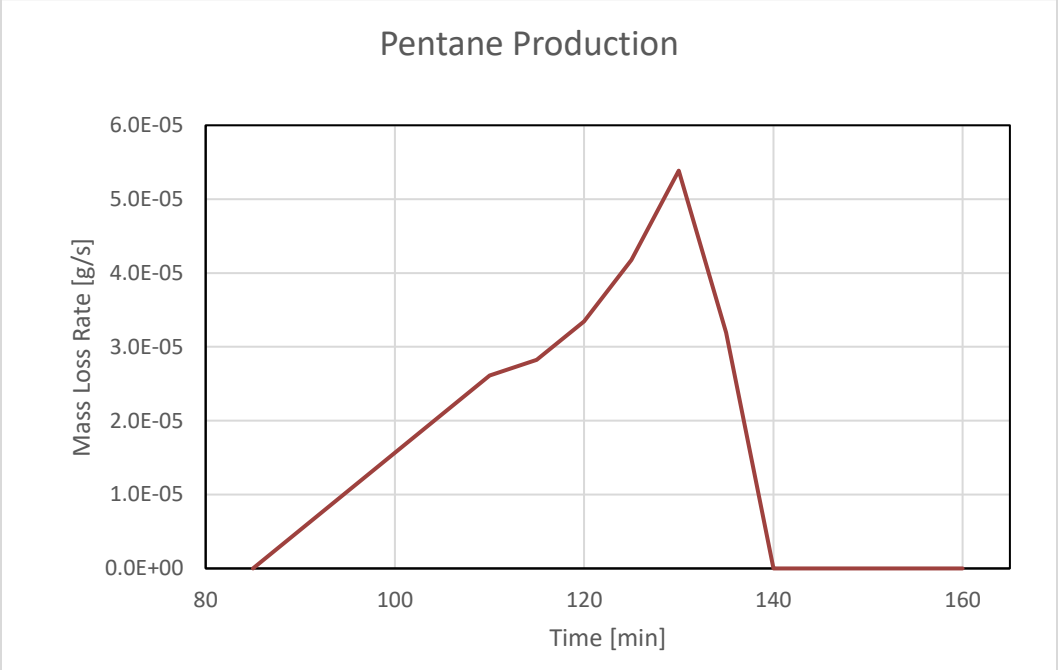
Pentane Production
6.0E-05
5.0E-05
4.0E-05
3.0E-05
2.0E-05
1.0E-05
0.0E+00
Mass Loss Rate [g/s]
80
100
120
140
160
Time [min]

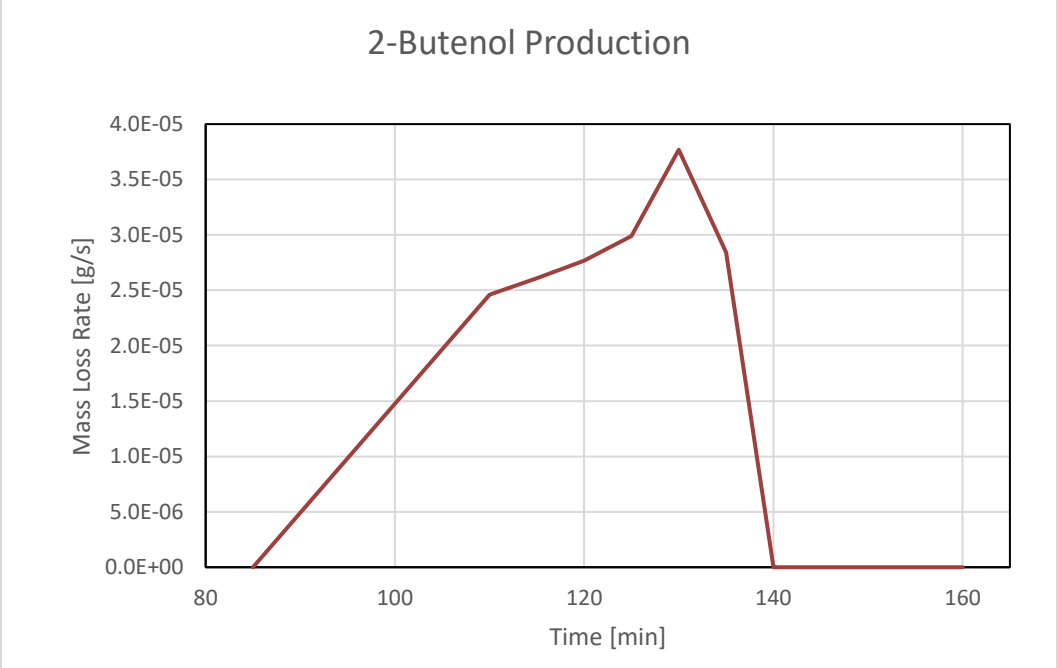
2-Butenol Production
4.0E-05
3.5E-05
3.0E-05
2.5E-05
2.0E-05
1.5E-05
1.0E-05
5.0E-06
0.0E+00
Mass Loss Rate [g/s]
80
100
120
140
160
Time [min]

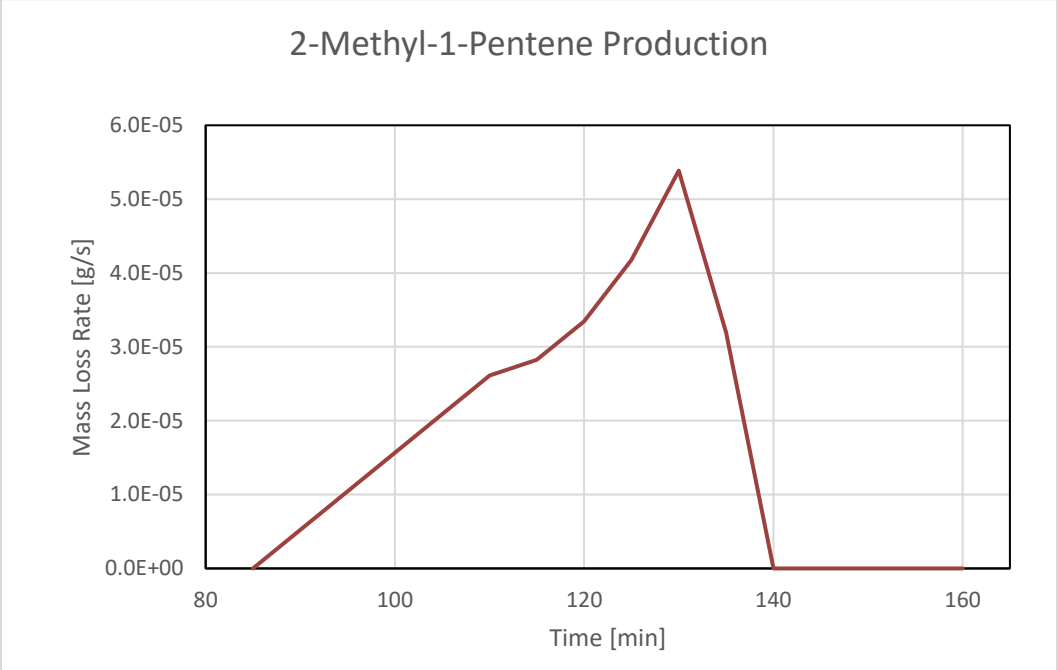
2-Methyl-1-Pentene Production
Mass Loss Rate [g/s]
6.0E-05
5.0E-05
4.0E-05
3.0E-05
2.0E-05
1.0E-05
0.0E+00
80
100
120
140
160
Time [min]

5.2.3 15% O_2 – Species Production vs Time

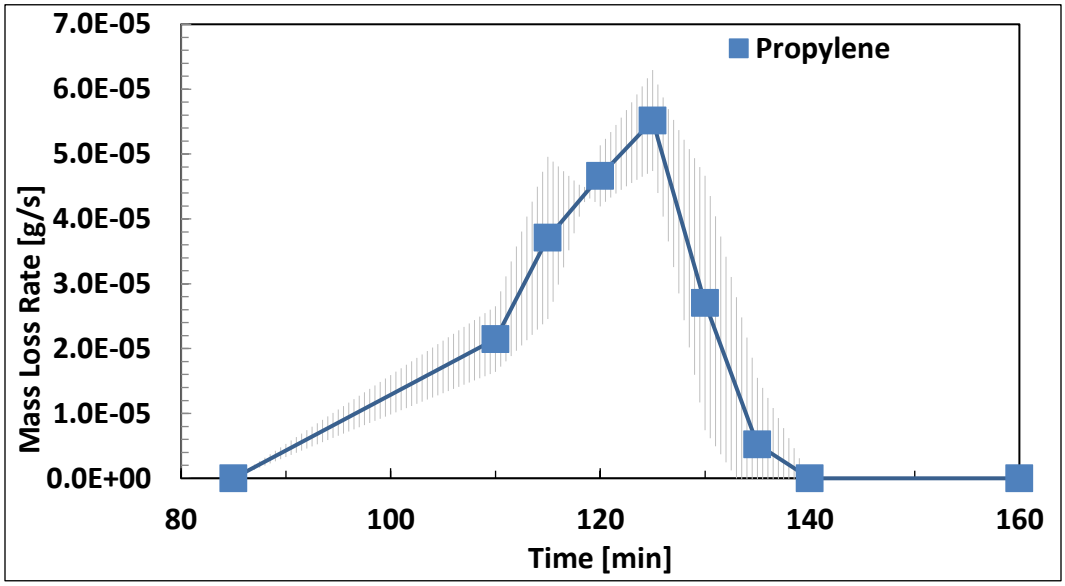

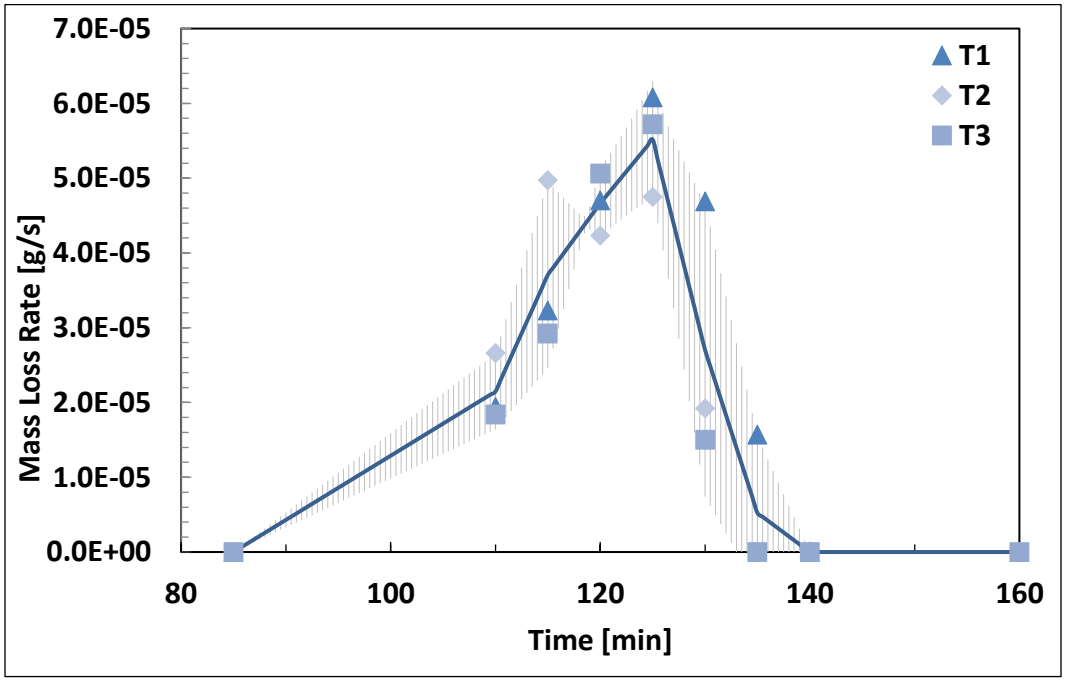

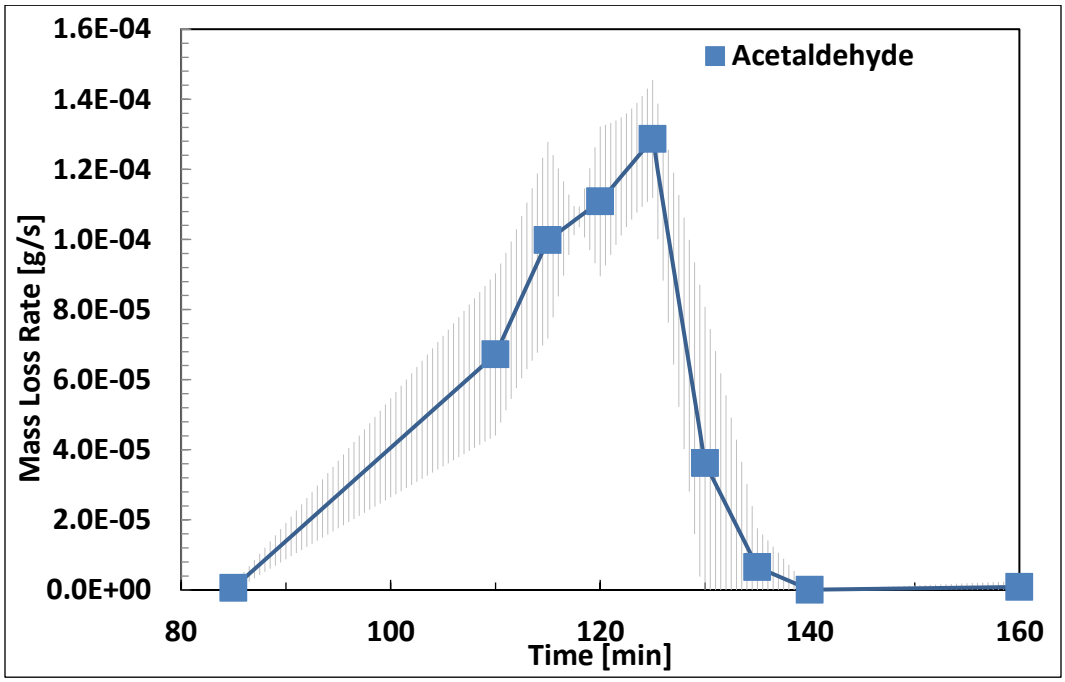
1.6E-04
1.4E-04
1.2E-04
1.0E-04
8.0E-05
6.0E-05
4.0E-05
2.0E-05
0.0E+00
Mass Loss Rate [g/s]
Acetaldehyde
80
100
120
140
160
Time [min]

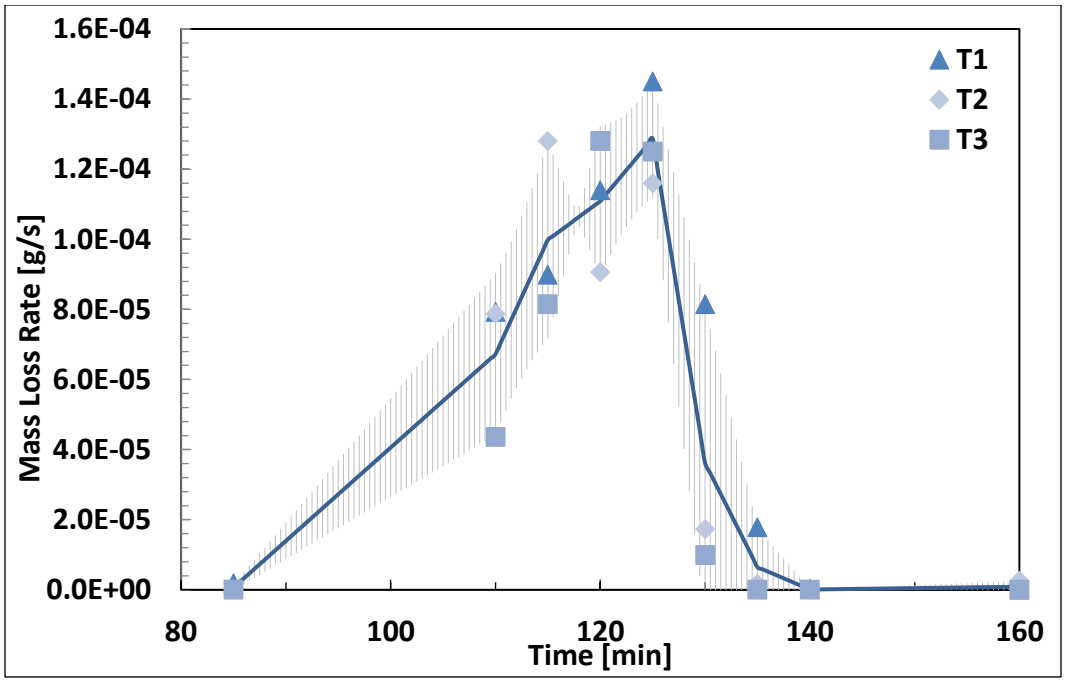
1.6E-04
1.4E-04
1.2E-04
1.0E-04
8.0E-05
6.0E-05
4.0E-05
2.0E-05
0.0E+00
Mass Loss Rate [g/s]
T1
T2
T3
80
100
120
140
160
Time [min]

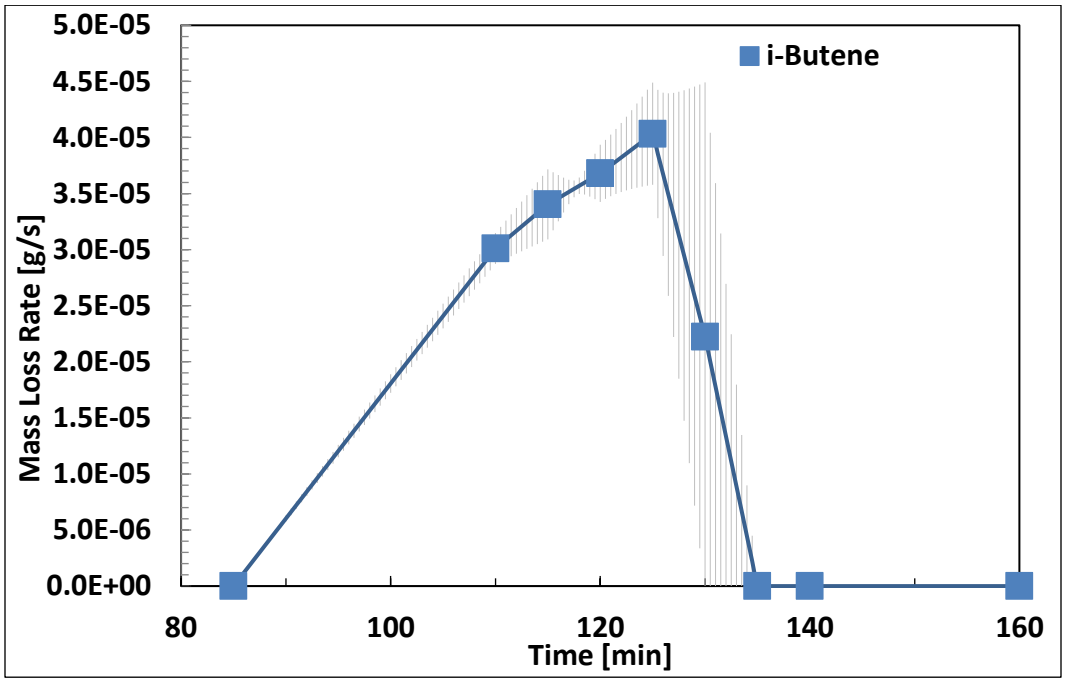
5.0E-05
4.5E-05
4.0E-05
3.5E-05
3.0E-05
2.5E-05
2.0E-05
1.5E-05
1.0E-05
5.0E-06
0.0E+00
Mass Loss Rate [g/s]
i-Butene
80
100
120
140
160
Time [min]

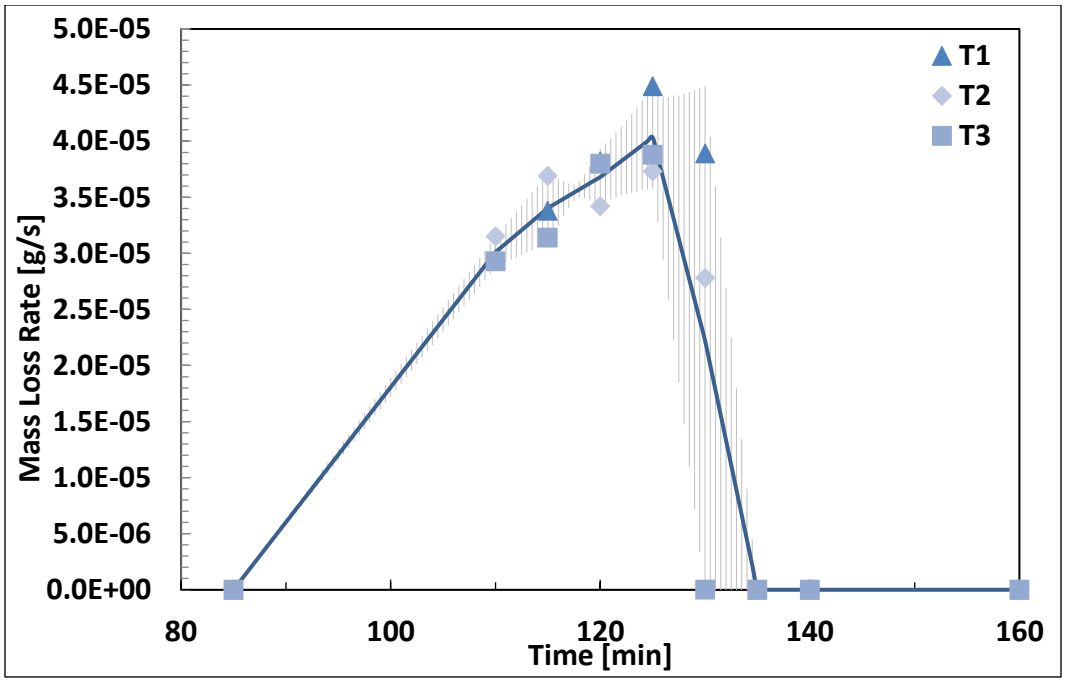
5.0E-05
4.5E-05
4.0E-05
3.5E-05
3.0E-05
2.5E-05
2.0E-05
1.5E-05
1.0E-05
5.0E-06
0.0E+00
Mass Loss Rate [g/s]
T1
T2
T3
80
100
120
140
160
Time [min]

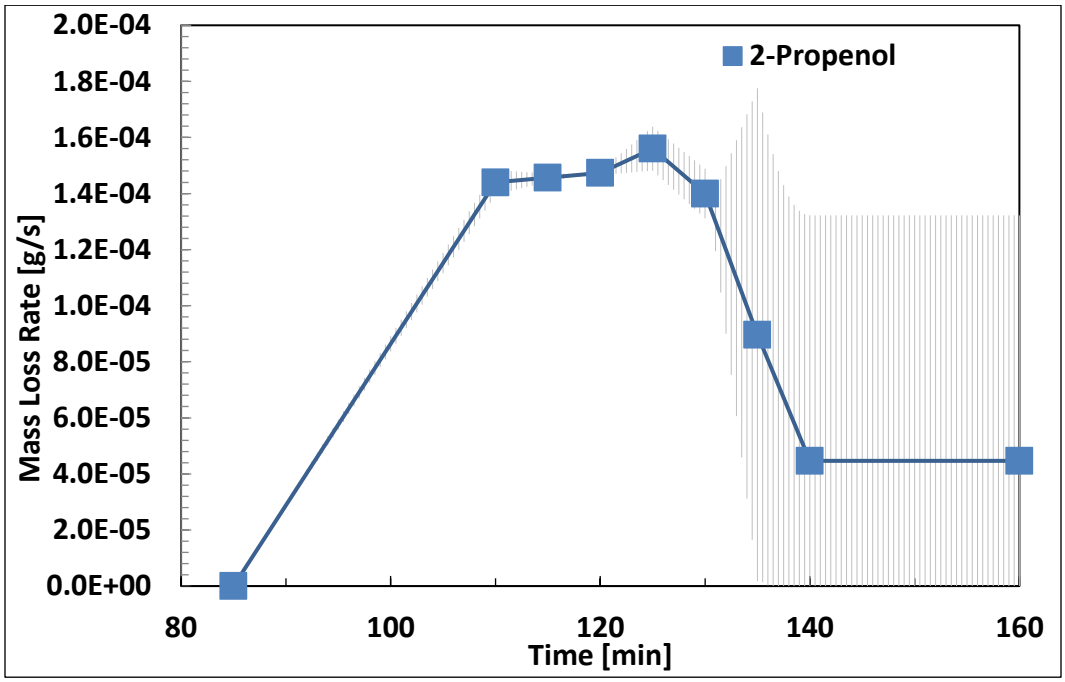
2.0E-04
1.8E-04
1.6E-04
1.4E-04
1.2E-04
1.0E-04
8.0E-05
6.0E-05
4.0E-05
2.0E-05
0.0E+00
Mass Loss Rate [g/s]
2-Propenol
80
100
120
140
160
Time [min]

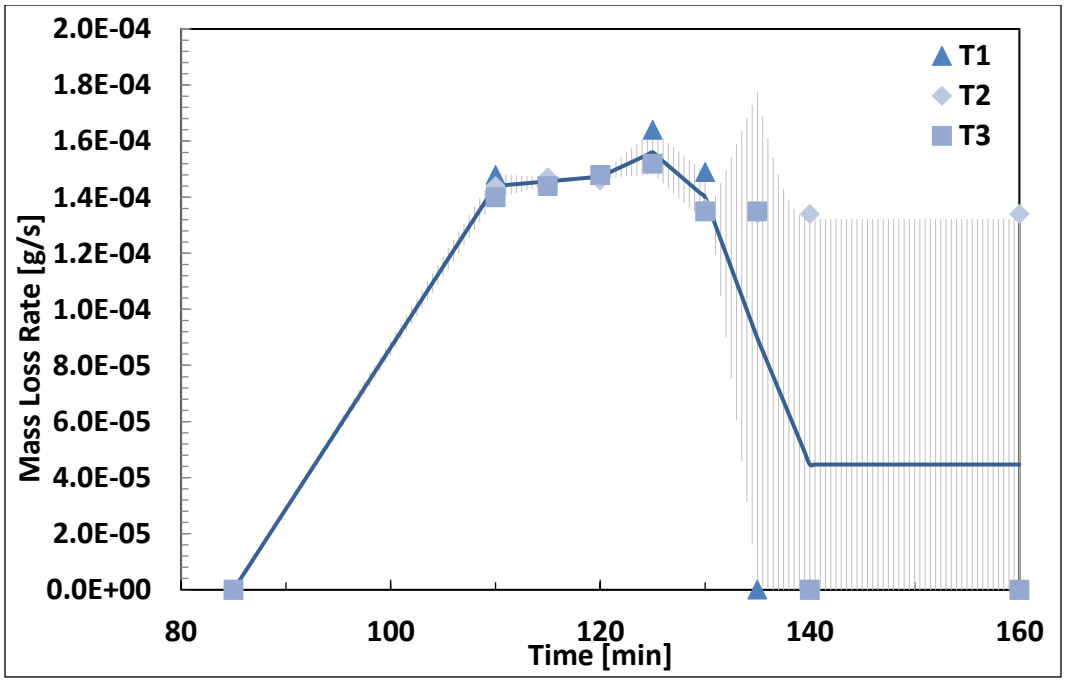
2.0E-04
1.8E-04
1.6E-04
1.4E-04
1.2E-04
1.0E-04
8.0E-05
6.0E-05
4.0E-05
2.0E-05
0.0E+00
Mass Loss Rate [g/s]
T1
T2
T3
80
100
120
140
160
Time [min]

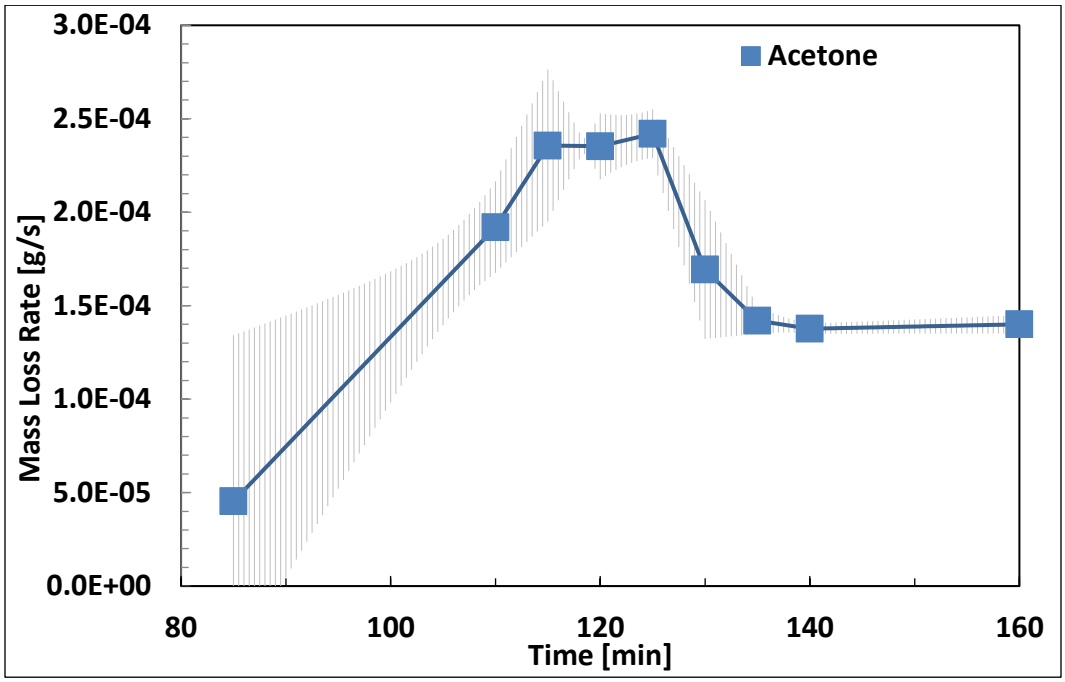
3.0E-04
2.5E-04
2.0E-04
1.5E-04
1.0E-04
5.0E-05
0.0E+00
Mass Loss Rate [g/s]
Acetone
80
100
120
140
160
Time [min]

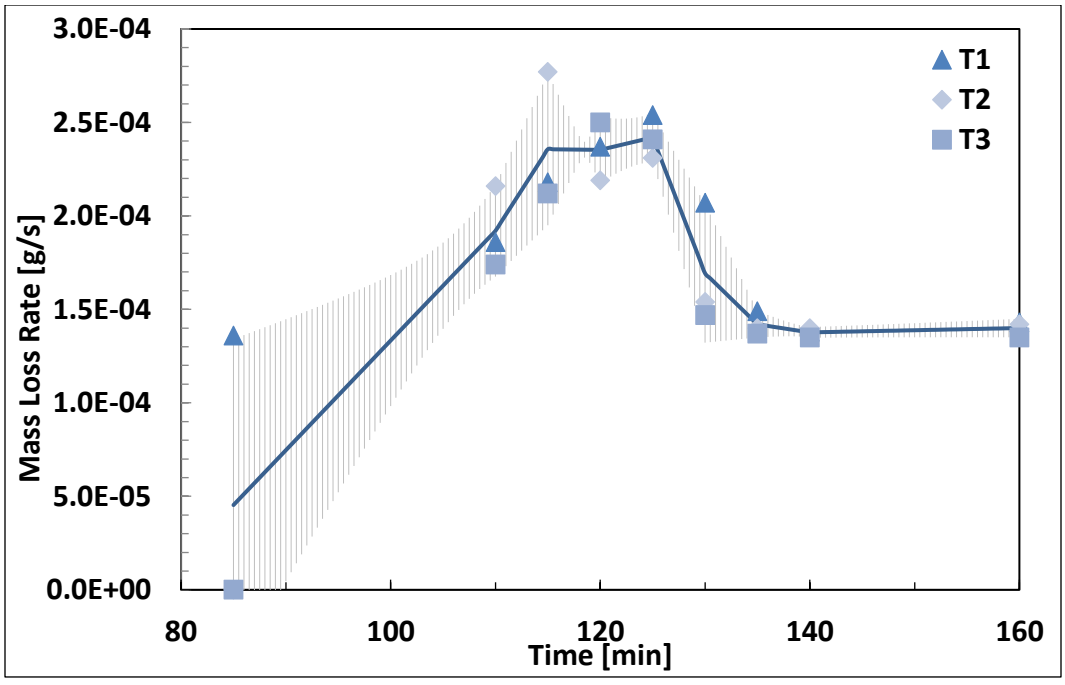
3.0E-04
2.5E-04
2.0E-04
1.5E-04
1.0E-04
5.0E-05
0.0E+00
Mass Loss Rate [g/s]
T1
T2
T3
80
100
120
140
160
Time [min]

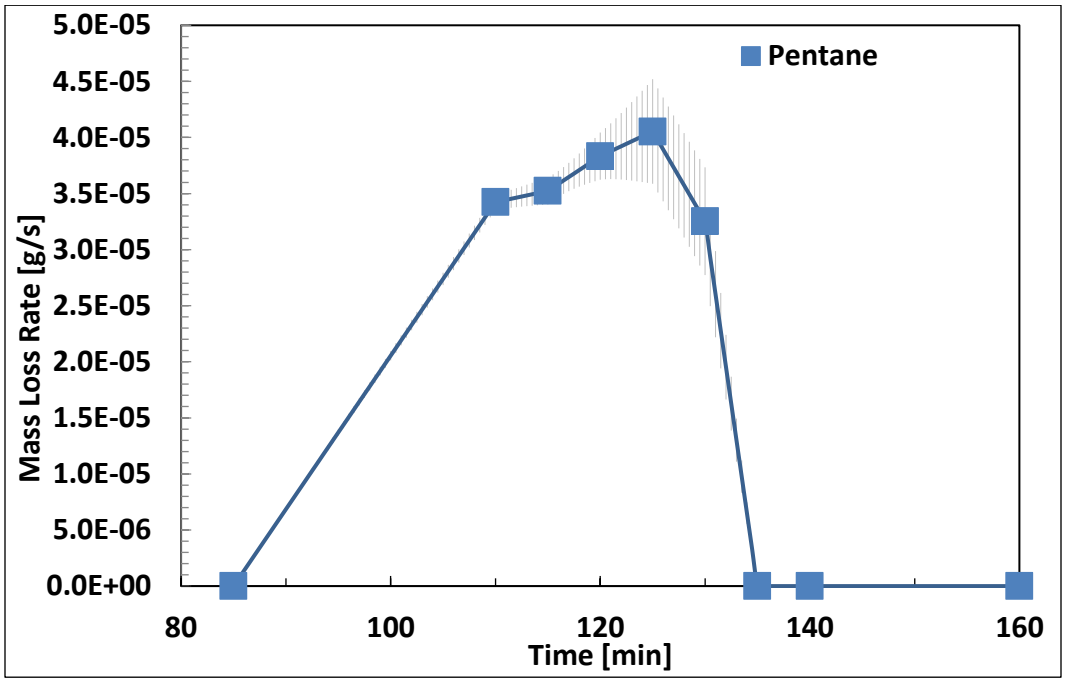
5.0E-05
4.5E-05
4.0E-05
3.5E-05
3.0E-05
2.5E-05
2.0E-05
1.5E-05
1.0E-05
5.0E-06
0.0E+00
Mass Loss Rate [g/s]
Pentane
80
100
120
140
160
Time [min]

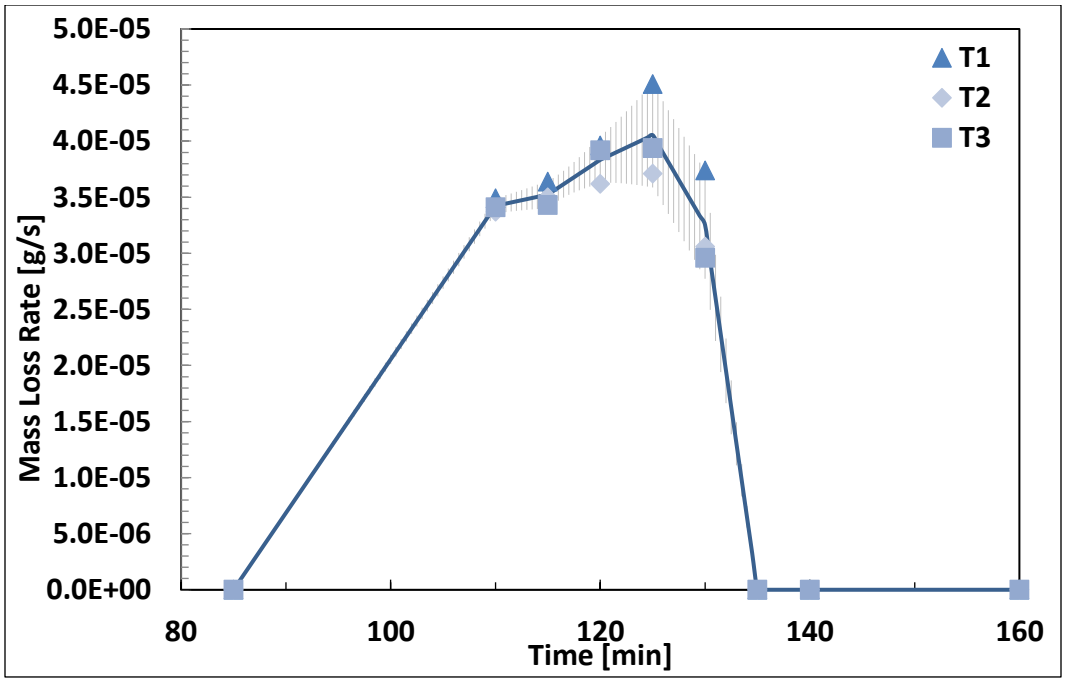
5.0E-05
4.5E-05
4.0E-05
3.5E-05
3.0E-05
2.5E-05
2.0E-05
1.5E-05
1.0E-05
5.0E-06
0.0E+00
Mass Loss Rate [g/s]
T1
T2
T3
80
100
120
140
160
Time [min]

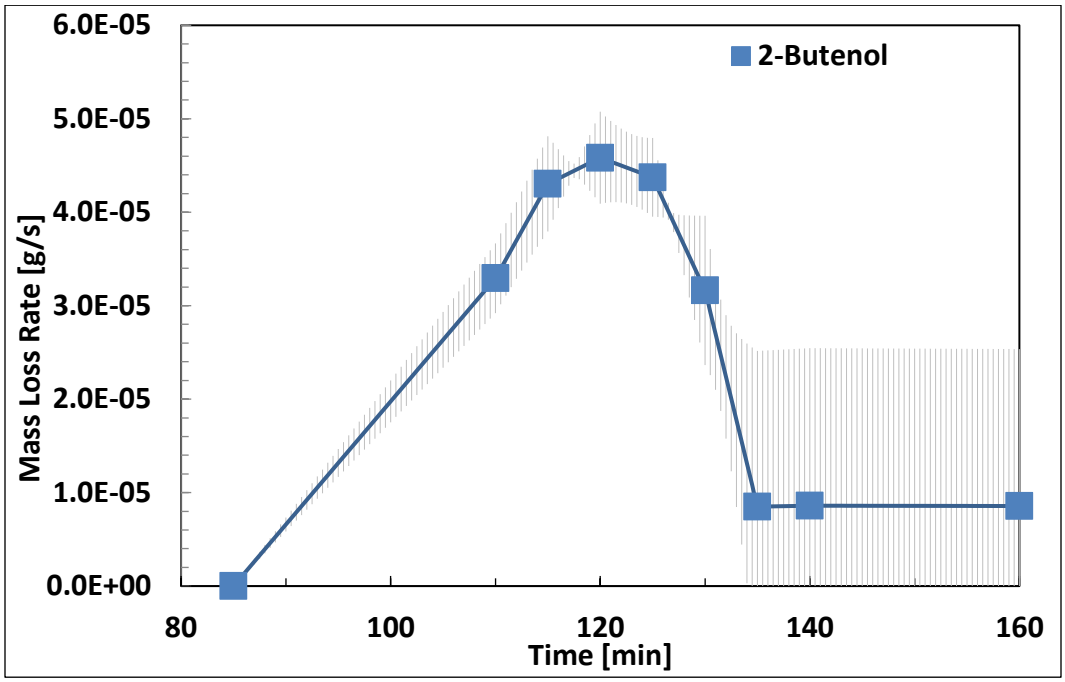
6.0E-05
5.0E-05
4.0E-05
3.0E-05
2.0E-05
1.0E-05
0.0E+00
Mass Loss Rate [g/s]
2-Butenol
80
100
120
140
160
Time [min]

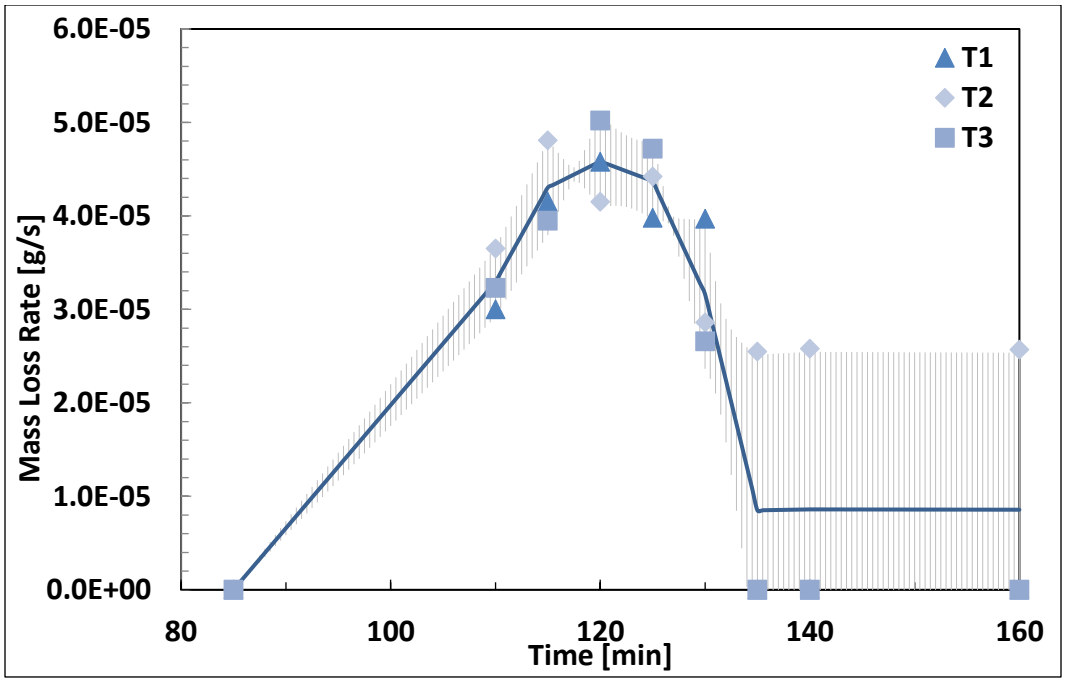
6.0E-05
5.0E-05
4.0E-05
3.0E-05
2.0E-05
1.0E-05
0.0E+00
Mass Loss Rate [g/s]
T1
T2
T3
80
100
120
140
160
Time [min]

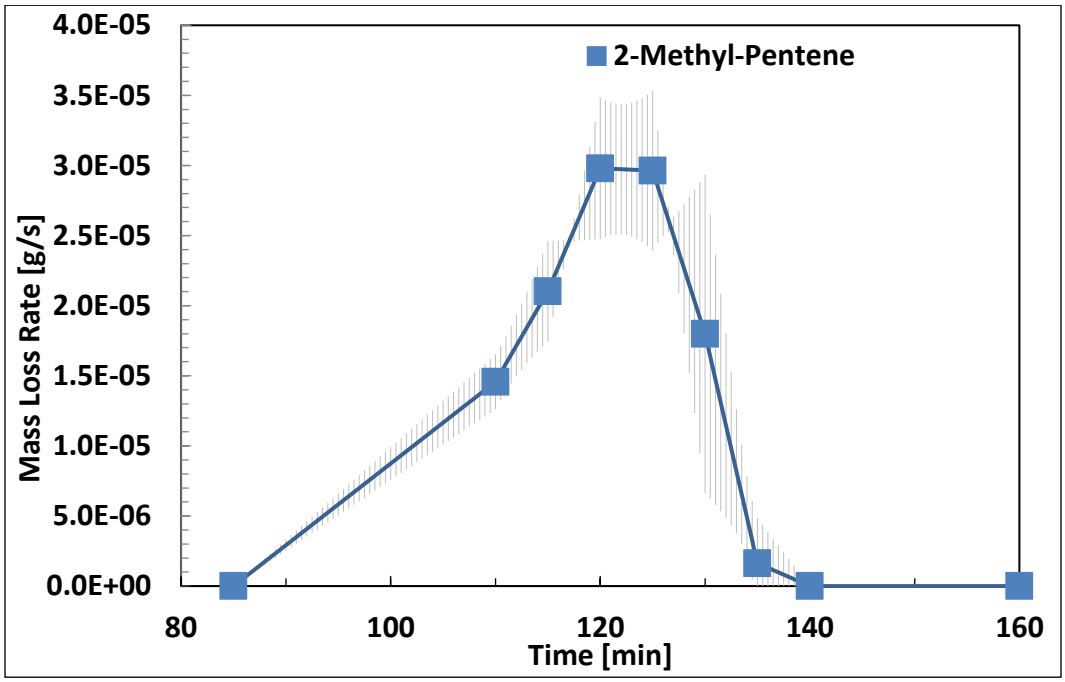
4.0E-05
3.5E-05
3.0E-05
2.5E-05
2.0E-05
1.5E-05
1.0E-05
5.0E-06
0.0E+00
Mass Loss Rate [g/s]
2-Methyl-Pentene
80
100
120
140
160
Time [min]

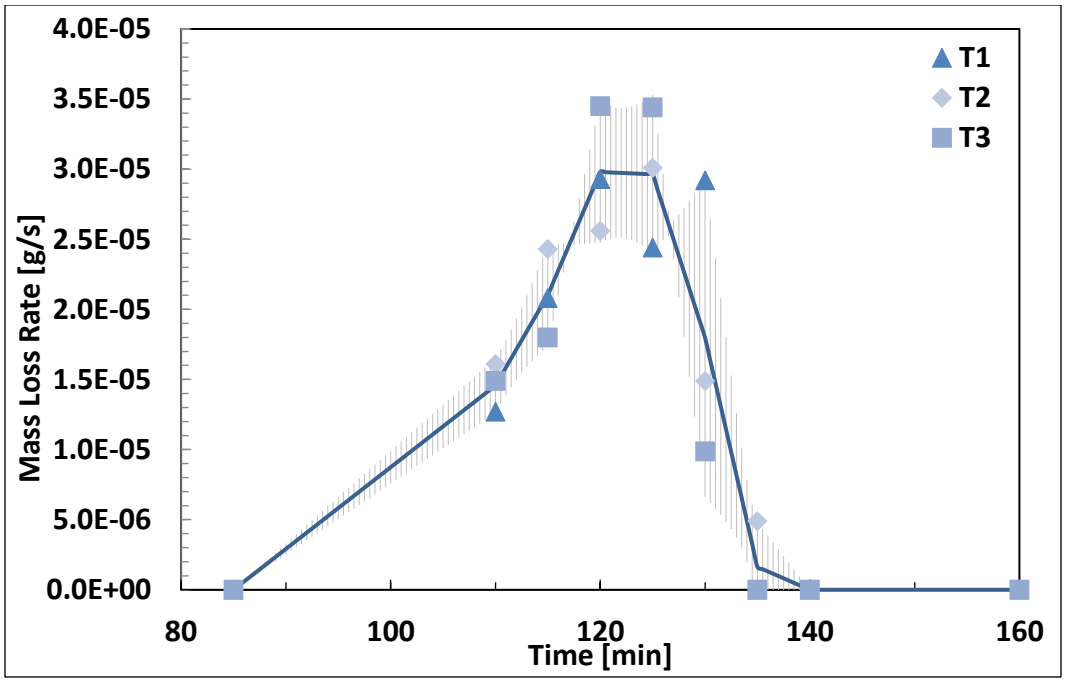
4.0E-05
3.5E-05
3.0E-05
2.5E-05
2.0E-05
1.5E-05
1.0E-05
5.0E-06
0.0E+00
Mass Loss Rate [g/s]
T1
T2
T3
80
100
120
140
160
Time [min]

Chapter 6: References

[1] A. D. McNaught and A. Wilkinson, Eds., Compendium of Chemical Terminology (the "Gold Book"), 2nd ed., Oxford: Blackwell Scientific Publications, 1997.

[2] R. Geyer, J. R. Jambeck and K. L. Law, "Production, Use, and Fate of All Plastics Ever Made," *Science Advances*, vol. 3, no. 7, 2017.

[3] Unites States, Congress, Office of Land and Emergency Management, "Advancing Sustainable Materials Management: 2014 Fact Sheet," 2016.

[4] PlasticsEurope Market Research Group, and Consultic Marketing & Industrieberatung GmbH, "World Plastics Production 1950-2015," Berlin, 2016.

[5] T. e. a. Kashiwagi, "Ignition of Polymers in a Hot Oxidizing Gas," *Combustion Science and Technology,* vol. 8, no. 3, pp. 121-131, 1973.

[6] E. Kiran and J. K. Gillham, "Pyrolysis-Molecular Weight Chromatography: A New on-Line System for Analysis of Polymers. II. Thermal Decomposition of Polyolefins: Polyethylene, Polypropylene, Polyisobutylene," *Journal of Applied Polymer Science,* vol. 20, no. 8, pp. 2045-2068, 1976.

[7] M. Amorim, C. Comel and P. Vermande, "Pyrolysis of Polypropylene," *Journal of Analytical and Applied Pyrolysis,* vol. 4, no. 1, pp. 73-81, 1982.

[8] T. Kashiwagi, "Polymer Combustion and Flammability—Role of the Condensed Phase," *Symposium (International) on Combustion,* vol. 25, no. 1, pp. 1423-1437, 1994.

[9] X. Chen, J. Yu and S. Gui, "Thermal Oxidative Degradation Kinetics of PP and PP/Mg (OH)2 Flame-Retardant Composites," *Journal of Applied Polymer Science,* vol. 103, no. 3, pp. 1978-1984, 2006.

[10] J.-I. Hayashi, N. Takeshi, K. Kusukabe and S. Morooka, "Pyrolysis of Polypropylene in the Presence of Oxygen," *Fuel Processing Technology,* vol. 55, no. 3, pp. 265-275, 1998.

[11] H. Bockhorn, A. Hornung, U. Hornung and D. Schawaller, "Kinetic Study on the Thermal Degradation of Polypropylene and Polyethylene," *Journal of Analytical and Applied Pyrolysis,* vol. 48, no. 2, pp. 93-109, 1999.

[12] L. Ballice and R. Rainer, "Chapter 1: Classification of Volatile Products from the Temperature-Programmed Pyrolysis of Polypropylene (PP), Atactic-Polypropylene (APP) and Thermogravimetrically Derived Kinetics of Pyrolysis," *Chemical Engineering and Processing: Process Intensification,* vol. 41, no. 4, p. 2890296, 2002.

[13] T. Kruse, H.-W. Wong and L. J. Broadbelt, "Mechanistic Modeling of Polymer Pyrolysis: Propylene," *Macromolecules,* vol. 36, no. 25, p. 9594–9607, 2003.

[14] E. Hajekova and M. Bajus, "Chapter 1: Recycling of Low-Density Polyethylene and Polypropylene via Copyrolysis of Polyalkane Oil/Waxes with Naptha: Product Distribution and Coke Formation," *Journal of Analytical and Applied Pyrolysis,* vol. 74, no. 1-2, pp. 270-281, 2005.

[15] L. Sojak, R. Kubinec, H. Jurdakova, E. Hajekova and M. Bajus, "GC-MS of Polyethylene and Polypropylene Thermal Cracking Products," *Petroleum & Coal,* vol. 48, no. 1, pp. 1-14, 2006.

[16] U. Hujuri, A. K. Ghoshal and S. Gumma, "Temperature-Dependent Pyrolytic Product Evolution Profile for Polypropylene," *Journal of Applied Polymer Science,* vol. 119, no. 4, pp. 2318-2325, 2010.

[17] S. S. Park, D. K. Seo, S. H. Lee and J. Hwang, "Study on Pyrolysis Characteristics of Refuse Plastic Fuel Using Lab-Scale Tube Furnace and Thermogravimetric Analysis Reactor," *Journal of Analytical and Applied Pyrolysis,* vol. 97, pp. 29-38, 2012.

[18] X. Jing and H. Wen, "Thermal Cracking of Virgin and Waste Plastics of PP and LDPE in a Semibatch Reactor under Atmospheric Pressure," *Energy & Fuels,* vol. 29, pp. 2289-2298, Apr. 2015.

[19] J. C. Chien and J. K. Kiang, "Pyrolysis and Oxidative Pyrolysis of Polypropylene," *Stabilization and Degradation of Polymers,* pp. 175-197, 1978.

[20] I. Glassman, R. A. Yetter and N. G. Glumac, "Chemical Kinetics," in *Combustion,* Elsevier, 2015, pp. 43-74.